



FACULTY OF ENGINEERING AND SUSTAINABLE DEVELOPMENT  
Department of Computer and Geospatial Sciences

---

# Extracting dendrometric parameters of urban trees using remotely sensed data for quantifying their ecological services in Valls Hage, Sweden

P.G. Chrishan C. Fonseca

2023

Student thesis, Advanced level (Master degree, two years), 30 HE  
Geospatial information science  
Master Programme in Geospatial Information Science

Supervisor: Nancy Joy Lim  
Co-supervisor: Andrew Mercer  
Examiner: Faramarz Nilfouroushan  
Co-examiner: Mohammad Bagherbandi

---



## Abstract

Urban spaces have undergone notable transformations recently, emphasizing the integration of green areas for sustainable city development. Specifically, urban trees offer not just aesthetic appeal but also numerous ecological benefits. Yet, effectively quantifying these benefits demands intricate models. The i-Tree Eco model is prominent in this field, but its reliance on fieldwork for determining diameter at breast height and tree species is a limitation. This research introduces a methodology using airborne laser scanning and four-band orthophoto products from Lantmäteriet, focusing on Valls Hage, Gävle, Sweden. For ground-truthing, 191 trees were measured in the field using the total station. Employing a raster-based watershed segmentation, tree canopies and treetops were delineated, showing a minor overestimation (2.09%) in tree detection against field data. Furthermore, a canopy height model was implemented to identify dendrometric parameters including tree height, canopy-base height, crown light exposure, canopy width and length. A linear regression deduced the diameter at breast height, with a 71.32% R-squared value. Combined with a normalized vegetation index obtained through RGB-NIR orthophotos, a feedforward neural network multilayer perceptron predicted the tree family taxonomic rank with 92.5% accuracy. Implementing these in the i-Tree Eco model, ecological services were quantified, and the main focus was on carbon storage, gross carbon sequestration and avoided runoff. By obtaining average values at various taxonomic levels (i.e., species, genus, family, and order level) deviations were observed up to 15% when comparing the field-measured values and those derived from airborne laser scanning data. Averaging values at the species level resulted in a 30% change from the base value outputs. Notably, letting the i-Tree Eco model estimate parameters other than the diameter at breast height, species, and tree height led to an 80% difference from the base value in avoided runoff. Overall, I concluded that readily available airborne laser scanning data and orthophotos covering Valls Hage can be used to detect individual trees and derive dendrometric parameters at the family taxonomy level. Further work will merit this research by expanding the ground truth dataset to be used in Convolutional Neural Networks for orthophotos and multilayer perceptron for dendrometric parameters. A probability approach can be employed to enhance the accuracy of species estimation of an individual tree. This study highlights the potential of remote sensing data to quantify the ecological services of urban trees, thereby supporting urban planning and development.

**Key words:** Dendrometry, ALS, Watershed delineation, Ecological services, CHM, i-Tree Eco



## **Preface**

In the endeavour to bring this research to fruition, the insightful guidance and unwavering support of Nancy Joy Lim and Andrew Mercer have been paramount. Their profound expertise, coupled with their passion for research, not only steered this study to its intended objective but also instilled in me a deeper appreciation for the scientific process.

I would like to extend my gratitude to Faramarz Nilfouroushan, the examiner, and Mohammad Bagherbandi, the co-examiner. Their meticulous reviews and constructive feedback have significantly elevated the quality of this work.

P.A.M.R. Chandrasiri deserves special recognition for her invaluable guidance and resolute support, which were instrumental in refining this thesis to its present form.

Lastly, I am deeply indebted to my friends and family, particularly my wife M.I.N. Fernando, for their unwavering moral support throughout this academic journey.



# Table of contents

Abstract.....	i
Preface.....	iii
Table of contents .....	v
1 Introduction.....	1
1.1 Background.....	1
1.2 Problem statement.....	3
1.3 Research question and objectives .....	3
1.4 Significance of the study .....	4
2 Literature review.....	5
2.1 Urban forests and ecological services.....	5
2.2 Biomass and carbon storage estimation methods .....	7
2.2.1 Allometric equations.....	9
2.3 i-Tree Eco model .....	10
2.4 Remote sensing for forest inventories.....	12
2.4.1 LiDAR and airborne laser scanning methods .....	13
2.4.2 Analysis of ALS data for urban forest ecological services.....	14
2.4.3 Sampling design for ground truth data collection.....	20
2.4.4 Tree species detection using machine learning.....	22
3 Methodology.....	25
3.1 Study area .....	26
3.2 Data and software.....	26
3.3 Field work.....	27
3.4 Individual crown delineation and tree detection .....	30
3.5 Deriving dendrometric parameters.....	33
3.5.1 Tree heights.....	33
3.5.2 DBH estimation.....	33
3.5.3 Crown light exposure (CLE).....	34
3.5.4 Canopy base height (CBH).....	35
3.6 Species identification .....	35
3.7 Validation of extracted parameters with field data.....	36
3.8 i-Tree Eco modelling.....	37
3.9 i-Tree Eco modelling sensitivity analysis.....	38
4 Results.....	41
4.1 Crown delineation and tree detection.....	41
4.2 Extraction of dendrometric parameters.....	41
4.3 Validation of tree heights, tree count, and tree species prediction .....	43
4.3.1 Field measured heights vs CHM derived heights.....	43
4.3.2 Field measure tree count vs ALS derived tree count .....	44
4.3.3 Field measured tree species vs predicted species .....	45
4.4 i-Tree Eco modelling.....	46

4.5	i-Tree Eco model sensitivity analysis .....	46
5	Discussion .....	51
5.1	Field work.....	51
5.2	Individual tree crown delineation and tree detection.....	52
5.3	Extraction of dendrometric parameters.....	53
5.3.1	Tree heights.....	53
5.3.2	DBH estimation .....	54
5.3.3	CLE calculation .....	54
5.3.4	CBH calculation.....	55
5.4	Species identification .....	55
5.5	i-Tree Eco model sensitivity testing with field acquired and remotely sensed data estimated inputs.....	57
5.6	Future aspects.....	58
6	Conclusions .....	60
	References .....	62
	Appendix A. Species, genus, family, and order of field measured trees .....	1
	Appendix B. Results from MLP model .....	1
	Appendix C. NDVI map.....	1
	Appendix D. Inputs for i-Tree Eco model .....	1

## List of Abbreviations

ALS	Airborne Laser Scanning
CBH	Canopy Base Height
CHM	Canopy Height Model
CLE	Crown Light Exposure
CNN	Convolutional Neural Networks
DBH	Diameter at Breast Height
DSM	Digital Surface Model
DTM	Digital Terrain Model
GIS	Geographic Information Science
GPS	Global Positioning Systems
ITC	Individual tree crowns
LAI	Leaf Area Index
LiDAR	Light Detection and Ranging
MLP	Multi-Layer Perception
RNN	Recurrent Neural Networks
TLS	Terrestrial Laser Scanning
UAV	Unmanned Aerial Vehicle

# 1 Introduction

## 1.1 Background

Urban trees play a pivotal role in enhancing the urban environment and contributing to the overall health and well-being of cities and their inhabitants (United States Digital Services [USDS], 2019). They provide a diverse range of essential ecological services that are integral to creating sustainable and liveable urban landscapes. These services encompass energy conservation, carbon dioxide sequestration, oxygen production, stormwater management, aesthetic enhancement, air pollution mitigation, noise reduction and wildlife habitat provision, among others (McCoy et al., 2022). Hence, the significance of urban trees in enhancing urban ecosystems and elevating the quality of life for urban residents cannot be overstated.

To comprehensively understand the functioning and the ecological services of trees in any given environment, it is crucial to measure and quantify their physical characteristics accurately through the scientific field known as dendrometry. Dendrometry involves measuring and analysing various parameters of trees, including tree height, diameter, volume, biomass, and crown dimensions (Cabo et al., 2018). These parameters can be measured using various techniques such as field measurements, remote sensing, image analysis, etc. (Skovsgaard, 2004 and Cabo et al., 2018). Each method has its own distinct advantages and disadvantages, making the choice of method dependent on the specific research question, scale of analysis, and available resources.

Among the most common dendrometric parameters, tree height holds a significant scientific relevance and is found in numerous fields in estimating important ecological factors like biomass, carbon sequestration, and growth rates (Ostadhashemi et al., 2014). Similarly, tree diameter at breast height (DBH) is another important dendrometric parameter that is extensively employed in ecological and forestry applications such as estimating basal area, volume, and biomass (Pace et al., 2022). Tree volume and biomass are also important dendrometric parameters that provide critical insight into estimating the productivity and carbon sequestration potential of forests. These parameters can be estimated using various methods, including the utilization of allometric equations, biomass expansion factors, and biomass models (Morgenroth & Gomez, 2014). Additionally, crown dimensions, such as crown width, length, and crown projection area, are also important dendrometric parameters that play a vital role in estimating factors like canopy cover and light interception within forest ecosystems (Pace et al., 2022).

Quantifying the ecological services provided by urban trees hold paramount importance for urban planning, policy-making, and sustainable development

initiatives. Accurate assessment and validation of these services enable decision-makers to prioritize and allocate resources efficiently, ensuring the effective management, preservation, and enhancement of urban green spaces. Such assessments provide valuable insights into the multifaceted benefits conferred by urban trees, allowing urban planners and policymakers to make informed choices and develop evidence-based strategies (USDS, 2019). Hence, recognizing and utilizing the ecological services of urban trees are essential for building resilient and prosperous cities for current and future generations.

To quantify ecological services, the i-Tree Eco model can be identified as one of the widely used models providing a robust framework (King and Locke, 2013). However, its implementation typically demands extensive fieldwork involving surveying and physically collecting and measuring tree variables such as tree height, crown diameter, crown density, leaf area, and biomass (USDS, 2019). This traditional approach to data collection is time-consuming, costly, labour-intensive, and logistically challenging, particularly when dealing with large-scale urban areas. For example, the i-Tree project in the United Kingdom, initiated in 2013, is still ongoing due to the extensive fieldwork involved. Similarly, the i-Tree project in Sweden, initiated by the Stockholm University of Agriculture Science (Sveriges lantbruksuniversitet, SLU) in 2017, had to conclude prematurely due to insufficient funds for the required manpower. Consequently, there is a need to explore alternative methods that can achieve the objectives of these kinds of studies while minimizing the reliance on extensive fieldwork.

Recent advancements in remote sensing methods, such as those utilizing airborne laser scanning (ALS) and orthophotos, provide a promising alternative for efficiently acquiring data on urban tree attributes (Lines et al., 2022). ALS, commonly known as light detection and ranging (LiDAR), is a remote sensing technique that employs laser pulses to capture precise and detailed 3D measurements of the Earth's surface, including vegetation. By emitting laser pulses and measuring the time taken for the reflected signal to return, ALS systems can create highly accurate digital elevation models (DEM) and point clouds, capturing the vertical structure of vegetation with exceptional precision (Jaskierniak et al., 2021). According to Lines et al. (2022), this technology enables the extraction of valuable dendrometric parameters, including tree height, crown dimensions, canopy volume, and vegetation density, facilitating a more precise and comprehensive assessment of urban tree characteristics. On the other hand, multispectral orthophotos that capture data in multiple spectral bands, including red (R), green (G), blue (B), and infrared (IR) bands provide another valuable source of information for assessing urban tree characteristics (Ventura et al., 2022). These spectral bands can offer more information about the vegetation allowing for visual identification of tree species, assessment of their health and condition, and

estimation of canopy cover and fragmentation (Guo et al., 2022). The combination of ALS data and multispectral orthophotos presents a powerful and synergistic approach for extracting dendrometric parameters and species information of urban trees (Degericks et al., 2018). By leveraging these remotely sensed data sources, researchers and practitioners can overcome the limitations of traditional field methods and obtain a more comprehensive and accurate information on urban tree characteristics at a larger scale area.

## **1.2 Problem statement**

Accurate assessment and quantification of ecological services provided by urban trees is of utmost importance in understanding their contribution to urban ecosystems and sustainable development. While various models exist to estimate the ecological services of urban trees, many of them require extensive fieldwork to obtain accurate inputs. The fieldwork is time-consuming, expensive, and often impractical for large-scale assessments. However, existing models such as the i-Tree Eco, which aims to quantify urban forest ecosystem services, have faced challenges in terms of the resources and manpower needed to collect the necessary input data. Consequently, there is a need to explore alternative approaches that can leverage remotely sensed data, such as ALS and orthophotos, to derive the required inputs for these models while minimizing the dependence on extensive fieldwork.

On the other hand, the Swedish Cadastral and Land Registration Authority, Lantmäteriet, provides ALS data and multispectral orthophotos covering the entirety of Sweden. Hence, this study aims to develop an approach that optimizes the use of available remotely sensed data provided by Lantmäteriet in extracting required inputs for the i-Tree Eco to quantify the ecological services of urban trees. This approach can help significantly reduce the reliance on fieldwork, saving resources and time, while providing the information needed for decision making, urban planning, and more effective management of urban green spaces.

## **1.3 Research question and objectives**

With a focus on quantifying ecological services using remotely sensed data (ALS data and multispectral orthophotos), this study will try to extract dendrometric parameters, and identify the species type of urban trees in Vallshage, Gävle, that can be used in the i-Tree Eco model to help quantify their ecological services. Furthermore, this study aims to further analyze the sensitivity of the i-Tree Eco model. The main research questions that will be addressed are the following:

1. How can the dendrometric parameters and the species needed to be used as inputs for the I-Tree Eco model be extracted from already available ALS data and RGB-NIR orthophotos in Sweden?
2. How different the species and dendrometric parameters obtained from fieldwork for the i-Tree Eco model compared to those derived from ALS data covering Valls Hage, Sweden?
3. How do the i-Tree Eco model's outputs vary when inputs are replaced with ALS-derived inputs and averaged to the taxonomy ranks, species, family, genus, and order level?

#### **1.4 Significance of the study**

This study holds significant implications for urban planning, environmental management, and decision-making processes related to urban trees. By exploring the potential of ALS data and multispectral orthophotos to extract dendrometric parameters and species information, it can offer a more manageable and cost-effective approach to quantifying the ecological services of urban trees. The findings of this research can assist policymakers, urban planners, and researchers in better understanding the contribution of urban trees to the urban ecosystem, facilitating decision making and sustainable urban development practices.

## **2 Literature review**

Time is an invaluable resource, and maximizing efficiency is important. This study aims to simplify the quantification of ecosystem services provided by urban forests using remotely sensed data, which can be obtained at a lower cost and with minimal labour effort. In this section, a summary of existing literature related to the subject matter is presented.

### **2.1 Urban forests and ecological services**

An urban forest is an area that encompasses the vegetation and associated natural resources present in urban, suburban, and adjacent areas, irrespective of ownership (Moeller, 1977). Recently, Dobbs et al. (2014) broaden the definition, by considering including all trees, shrubs, lawns, and previous soils found in an urban area. Furthermore, it is considered as an integral part of green infrastructure and the broader urban ecosystem (Doick et al., 2016). Therefore, the concept of an urban forest provides a better understanding of the diverse ecological services provided by them, that are crucial for sustainable urban planning and development.

Ecological services, also known as ecosystem services, refer to the benefits that ecosystems provide to humans and the environment (Davies et al., 2017). Here, the main focus is drawn to the ecological services provided by the urban forests or urban trees. Table 1 illustrates a categorical overview of the ecological services associated with urban trees.

Table 1. Ecological services of urban trees.

<b>Regulating</b>	<b>Provision</b>	<b>Cultural</b>	<b>Supporting</b>
Air purification	Woodfuel	Health	Habitats for species/biodiversity
Carbon storage and sequestration	Biological / genetic resources	Nature/ landscape connections	Soil formation
Noise mitigation	Food	Social development/ connection	Nutrient cycling
Storm water regulation		Education/ learning	Water cycling
Temperature regulation		Economy	Oxygen production
Disease / pest regulation		Cultural significance	
Pollination / seed dispersal			
Soil protection			

As a result of the photosynthesis process, trees contribute to minimizing the greenhouse gases in the atmosphere, specifically carbon dioxide, by storing the excessive carbon in their biomass. As the tree grows, the biomass increases and studies state that approximately half of the total dry weight of the tree's biomass is carbon (Nowak et al., 2008). This carbon storage capacity is therefore an important ecological service of trees. To calculate this carbon storage of trees, the DBH, tree height, and canopy size must be measured or estimated. According to McPherson et al. (2005), these measurements are crucial to calculating a tree's total volume of timber or dry mass, which is correlated with how much carbon it can store.

Carbon sequestration is the annual rate of trees, capturing and storing atmospheric carbon dioxide as tree biomass (McPherson et al., 2005). The trees' yearly growth rate (change in biomass) is taken into consideration when quantifying carbon sequestration. It is important to note that these rates are slower in older trees and faster in younger trees (White, 1998). Tree death or decay is not considered in this context.

Rainfall that accumulates and flows over the ground surface is known as stormwater runoff. Urbanized environments consist of a high percentage of impervious surfaces, which highly contribute to runoff. However, trees and forests play a crucial role in mitigating this effect by capturing and storing rainfall in the canopy. This stored water is released into the atmosphere through evapotranspiration (Doick et al., 2016).

Additionally, trees intercept rainfall by reducing both the volume and kinetic energy of rainfall that reaches the ground.

Urban trees have the ability to emit volatile organic compounds, which can contribute to the formation of ozone gas (Chameides et al., 1988). Additionally, trees can intercept airborne particles, thereby, contributing to the reduction of air pollution. Nowak et al. (2006) state that forest canopies can reduce the mixing of air above the canopy and air below the canopy that leads to considerable improvement of the air below the canopy. The highest impact of urban trees on ozone, sulphur dioxide, and nitrogen dioxide is most pronounced during the in-leaf season when trees are actively transpiring water during the daytime. This study has used several computer-modelled equations to model the pollution removal potential of urban trees, carbon monoxide, nitrogen dioxide, ozone, particulate matter less than 10  $\mu\text{m}$  and sulphur dioxide in 55 US cities.

Water transpiration in trees is the loss of water in them due to evaporation. This process is deeply coupled with the global hydrological cycle which is an essential process in maintaining life. Roberts (1987), in his study discusses several models to measure the water status and water loss due to transpiration in trees. Roberts' study focuses on calculating several parameters related to water status including plant water status, relative water content, water potential by thermocouple psychrometry, water potential by pressure equilibration, water status as measured by changes in stem diameter, water status as reflected by changes in leaf temperature, water status as reflected by computer modelling of transpiration, and finally reducing transpiration water loss in trees. These parameters provide insights into the water dynamics within trees and contribute to a better understanding of their role in ecological services.

## **2.2 Biomass and carbon storage estimation methods**

The quantification of biomass and carbon storage in vegetation, particularly trees, and forests, holds great significance. These estimation methods provide essential insights into the amount of organic matter and carbon sequestered within ecosystems. Generally, there are two main categories of methods commonly used: destructive and non-destructive methods (Fonseca et al., 2011). Destructive methods involve the complete or partial destruction of vegetation to obtain precise measurements of biomass and carbon content. This typically includes felling trees, collecting, and separating their components, such as stems, branches, and foliage, and weighing them. Subsequent laboratory analysis is conducted to determine the carbon content of the collected samples (Schettini et al., 2022). Destructive methods yield precise measurements, but can be demanding in terms of labour, and are typically more applicable to smaller sample sizes.

In contrast, non-destructive methods enable biomass and carbon storage estimation without causing permanent damage to the vegetation. These methods offer broader-scale assessments while minimizing disruption. A commonly employed non-destructive approach is the utilization of allometric equations. These equations establish mathematical relationships between easily measurable parameters such as tree diameter, height, or crown size, and biomass or carbon content. By applying these equations to field data, estimates of biomass and carbon storage can be derived. Another non-destructive method is remote sensing, which utilizes satellite or aerial imagery, LiDAR, and hyperspectral data. Remote sensing techniques capture the structural and spectral characteristics of vegetation, allowing large-scale assessments of biomass and carbon storage. By correlating remote sensing data with field measurements, it becomes possible to develop models that estimate biomass and carbon content more accurately (Schettini et al., 2022). The choice of method depends on the research objectives, available resources, and the scale of assessment.

The study conducted by Ostadhashemi et al. (2014) focuses on non-destructive methods for estimating biomass and carbon storage of trees in northern Iran. The authors evaluated several approaches and models to assess their effectiveness. According to their findings, the Jenkins et al. (2003) model and Chojnacky and Jenkins (2010) model yield more accurate results for native species. The Jenkins et al. (2003) model provides a comprehensive set of diameter-based allometric regression equations for estimating total aboveground biomass for trees in the United States, which is a significant development in biomass estimation. This model laid the groundwork for the Chojnacky and Jenkins (2010) technique. They chose equations among around 2,500 available in a refined meta-analysis, focused especially on predicting biomass using just diameter measurements. This improved method provides precise biomass calculations for individual trees as well as specific components such as branches, boles, barks, or leaves, and is applicable to a wide range of North American tree species. On the other hand, the authors stated that the Intergovernmental Panel on Climate Change (IPCC) model demonstrates greater reliability when applied to exotic species. These observations provide valuable insights into the suitability of various models in estimating biomass and carbon storage in specific tree species within the study area.

When estimating biomass and carbon storage in trees, several parameters are commonly employed. One widely used parameter is the DBH, which measures the trunk diameter at a standard height above the ground. The age of the trees is also considered as an important factor (Jithila & Prasad, 2018). These parameters, along with others, have been investigated in various studies to determine the total biomass and carbon storage in different contexts. For instance, Jithila and Prasad (2018) conducted a study in which they randomly selected 610 trees and measured their DBH

and age to quantify the rate of carbon sequestration. They employed allometric equations, such as those proposed by Udayakumar et al. (2016), MacDicken (1977) and Hangarge et al. (2012), and Sheikh et al. (2011), to estimate the above-ground biomass, below-ground biomass, and total biomass, respectively. Carbon storage was determined using the equation proposed by Birdsey (1992), while carbon sequestration was calculated using the equation from Vishnu and Satish (2016). The study reported a linear relationship between DBH and carbon sequestration, where the latter shows a logarithmic increase with the number of trees.

Leaf area and leaf biomass are essential parameters that must be calculated to estimate many forest-based services such as the exchange of energy, light interception, carbon cycling, plant growth, forest productivity, etc. According to Das (2014), the leaf area and leaf biomass can be used for assessing gas exchange, ecosystem modeling, ecophysiological studies (e.g., photosynthetic efficiency, evapotranspiration, atmospheric deposition, biogenic volatile organic emissions, light interception), examining tree growth models, and studying forest nutrient cycling. This study conducted in the Moulvibazar Forest Range in Bangladesh, focused on the dominant tree species *Lagerstroemia speciosa* (L.). The authors have measured leaf area, DBH, and tree height data in order to explore the relationship between leaf area and leaf biomass with DBH and tree height. They have developed 24 models between those parameters and found the 10th and 24th model as the best models that account for more than 96% variation and have lower RMSE.

### **2.2.1 Allometric equations**

An allometric equation is a mathematical formula that relates one biological variable to another. In the context of biomass and carbon storage estimation, allometric equations relate measurable parameters (e.g., tree diameter, height) to the biomass or carbon content of trees or vegetation. These equations are developed through empirical studies that involve collecting field data on various tree characteristics, and measuring biomass or carbon content (Vorster et al., 2020). The parameters used in allometric equations can vary depending on the specific type of vegetation being studied.

Besides, predicting the DBH of trees using allometric equations is a common practice in forestry and ecological research. Allometric equations relate various tree characteristics to DBH, allowing for non-destructive and efficient estimation of DBH, which is an essential parameter for assessing tree growth, volume, and biomass. These equations are particularly useful when direct measurements of DBH are not feasible or when studying large tree populations. The development of allometric equations for DBH prediction involves collecting data from a sample of trees where DBH and other tree characteristics (e.g. height, crown diameter, species) are measured. The

data are then used to build a statistical model that establishes a relationship between the predictor variables (e.g. height, crown diameter) and the response variable (DBH). Various regression techniques, such as multiple linear regression or nonlinear regression, can be employed depending on the complexity of the relationship. Equation 1 illustrates a simplified example of allometric equation using a simple linear regression, to predict the DBH based on tree height.

$$DBH = \beta_0 + \beta_1 \times H \quad [1]$$

Where, H represents tree height in meters (i.e. the predictor variable),  $\beta_0$ , and  $\beta_1$  are coefficients that the regression model estimates to establish the relationship between DBH and H. Various research studies have developed different allometric equations tailored for specific tree species and different forest ecosystems, including urban trees. For instance, allometric equations were developed for urban street tree species in the study of Yoon et al. (2013). In another study conducted by Nowak et al. (2013) to assess the contribution of urban forests to climate change, a set of allometric equations was employed. The study included urban trees from 28 cities and 6 states across the United States.

Nowak (1996) presents a logarithmic regression model to predict the leaf area and leaf biomass from crown parameters. The study was conducted in Chicago, Illinois on 54 deciduous open grown park trees. This study claims that the relationship between the leaf surface area and leaf biomass with the tree crown parameters is more reliable than their relationship with DBH.

Negash et al. (2013) have done a study to develop and assess allometric equations that can be used to estimate the aboveground biomass of *Coffea arabica* plants cultivated within the indigenous agroforestry system. Their developed parameterized square power equation has confirmed the importance of parameterization of allometric equations with site-specific data when possible.

### **2.3 i-Tree Eco model**

i-Tree Eco is a model developed by the United States Department of Agriculture Forest Service primarily focused on urban forests (<http://www.itreetools.org/eco/>). The i-Tree Eco is part of the i-Tree suite, especially focusing on quantifying a variety of ecosystem services provided by urban trees whilst providing valuable insights into their structure and composition (Doick et al., 2016). By utilizing standardized inputs, the model generates a range of outputs related to species or strata, offering insights into the ecosystem services provided by urban trees. The outputs generated by the i-Tree Eco model are diverse and comprehensive. These outputs of the model also procure future management of urban trees in relevance to protection and maintenance aspects. One of the main advantages

of using the i-Tree Eco model is its ability to integrate multiple parameters and generate all the outputs within a single software suite (Nowak, 2008). In comparison to other approaches, where each parameter must be calculated individually, this model can provide an efficient process for assessing and evaluating urban forest benefits.

The model involves using several equations to calculate various aspects of carbon storage and environmental impact related to urban trees. The carbon storage (in kg) is calculated based on the biomass of the trees (in kg) and the carbon content in their tissues. The equation for carbon storage is illustrated by equation 2 (Chow and Rolfe, 1989). The total amount of organic matter (in terms of weight) contained within a tree is referred to as its biomass. This comprises the roots, trunk or stem, branches, leaves or needles, and even the fruits or seeds. It is essentially a measurement of how much a tree weighs minus its water content. The biomass of a tree is estimated based on its tree diameter (DBH) and tree height. The carbon content fraction represents the proportion of carbon in the tree's biomass, which is typically assumed to be around 50% or 0.5.

$$\text{Carbon Storage} = \text{Biomass} \times \text{Carbon Content Fraction} \quad [2]$$

Gross carbon sequestration represents the total amount of carbon dioxide (CO<sub>2</sub>) absorbed and sequestered by urban trees through photosynthesis during a specific time period (e.g. annually). Equation 3 is the general mathematical expression for gross carbon sequestration (Mohammadi et al., 2017). Here, the Net Primary Productivity (NPP) is the difference between the amount of carbon dioxide absorbed through photosynthesis and the amount released through respiration. It represents the net carbon gain by the trees. The carbon fraction is the proportion of carbon in the organic matter produced during photosynthesis, which is estimated to be around 50% (0.5).

$$\text{Gross Carbon Sequestration} = \text{NPP} \times \text{Carbon Fraction} \quad [3]$$

Avoided runoff represents the reduction in stormwater runoff attributed to the presence of trees (equation 4). Here, the precipitation (in mm) is the total amount of rainfall during a specific time period and interception (in mm) is the portion of rainfall that is intercepted and retained by the tree canopy, reducing the amount of water reaching the ground. All values of this equation should be in millimetres (Hirabayashi, 2013).

$$\text{Avoided Runoff} = \text{Precipitation} - \text{Interception} - \text{Retention} \quad [4]$$

Below Table 2 illustrates the required inputs for the i-Tree Eco model when quantifying those ecological services.

Table 2. Essential inputs for the selected ecological services.

Ecosystem Service	Inputs needed for the i-Tree Eco
Carbon storage	Species, DBH, total height, land use, crown width, crown height, % crown missing
Gross carbon sequestration	Species, DBH, total height, land use, CLE, crown health
Avoided run-off	% Tree cover, species, total height, crown base height, crown width, % crown missing

Numerous earlier studies have utilized the i-Tree Eco model to assess the benefits provided by urban trees in different contexts. In the study by Nowak et al. (2013), the researchers utilized the i-Tree Eco model to estimate carbon storage and sequestration by trees in urban and community areas across the United States. It demonstrated the effectiveness of the model in assessing and quantifying the carbon storage and sequestration capabilities of urban forests. Bodnaruk et al. (2020) employed the i-Tree Eco model to assess the ecosystem services provided by different types of urban green spaces. In the study conducted by Derkzen et al. (2015), the researchers utilized the i-Tree Eco model as part of their assessment of urban ecosystem services in Rotterdam, Netherlands, which was aimed to quantify and evaluate the ecosystem services provided by urban green spaces in the city. These studies witness the i-Tree Eco model's versatility and significance in comprehensively assessing and quantifying the wide-ranging benefits of urban trees.

## 2.4 Remote sensing for forest inventories

Forest inventories are assessments of forest resources that can provide valuable information about the structure, composition, and health of forest ecosystems. These inventories consist of both direct and indirect attributes, which are key components of the data collected through remote sensing and field surveys. Tree height, DBH, canopy cover, leaf area index, and species identification are direct attributes, and above-ground biomass, carbon storage, volume of tree components, and biomass allocation are indirect attributes of forest inventories (Lister et al., 2020). Remote sensing has emerged as a valuable tool for conducting forest inventories, offering the potential to gather wide-ranging information on important attributes such as biomass, stem volume, and biodiversity with required accuracies. Remote sensing technologies, such as aerial and satellite imagery, LiDAR, and hyperspectral sensors, enable the collection of data at regional or even global scales (Knoke et al., 2021).

Several studies have also explored the applicability of remote-sensing technologies including terrestrial laser scanning (TLS) in forest assessments (Wiman and Larsson, 2023). The study by Lister et al. (2020) aimed to enhance the efficiency of national forest inventories by integrating remote sensing data, emphasizing the significance of

effective forest management for human well-being and ecosystem health. In the study of Liang et al. (2016), they evaluate the applicability of TLS in forest inventories highlighting the limitations of conventional methods and the advantages of the TLS in measuring parameters like stem volume and biomass components. The integration of various technologies such as Remote Sensing, Airborne Photogrammetry, LiDAR, Geographic Information systems (GIS), Global Positioning Systems (GPS), and conventional geodetic techniques for data acquisition, processing, analysis, and management was discussed by Cristea and Jocea, (2015). Their study demonstrates the applicability and potential capabilities of using TLS and GIS technologies in forest assessments. Despite the advancement in TLS technology, it discusses the disadvantages of TLS, particularly the lack of automation in data processing and the high cost of equipment. Krooks et al. (2014) used quantitative structure modeling and terrestrial laser scanning to produce detailed information on branch-level metrics in Trees. This study has found that the branch size distribution is similar for trees of different heights in similar conditions, and that tree height can be used to estimate branch size distribution in areas with similar growing conditions and topology.

Furthermore, Tiede et al. (2005) provide a method to extract and delineate single trees from small-footprint, high-intensity laser scanning point data in a GIS environment. The authors have developed a local maxima algorithm to identify treetops and then have developed a region-growing algorithm to delineate the respective tree crowns. By comparing with field surveys, the results indicate 72.2% of tree detection for dominant trees and 51% for overall tree detection. Overall, remote sensing technologies have been identified as essential tools in forest inventories, providing efficient and accurate means to assess forest attributes and monitor changes over time.

#### **2.4.1 LiDAR and airborne laser scanning methods**

LiDAR stands for light detection and ranging where it uses the technique of calculating distances based on the time taken for the return of emitted light or pulse using the speed of electromagnetic radiation (GISGeography, 2023). This technique is widely used in various applications including forestry. Three main methods exist, ground based (TLS), air based (ALS), and satellite based (spaceborne). For this study only airborne and terrestrial methods will be discussed. The main advantage of LiDAR, especially airborne and terrestrial LiDAR, is its capability to penetrate through vegetation. Unlike other remote sensing techniques, LiDAR can effectively capture data from the top of the canopy to the ground level (Zolkos et al., 2013). This ability allows LiDAR to provide detailed information about the vertical structure of forests, including the height and density of trees, which is essential for forest assessments.

Airborne laser scanning can effectively be used to extract biophysical variables and for updating forest inventories on a national scale (Pascual et al., 2018). The main two approaches are the single tree method and the area-based method. The single-tree method provides more detailed information on individual trees, allowing for precise assessments of tree-level characteristics. On the other hand, the area-based method is more efficient for large-scale assessments, providing estimates of stand-level attributes across extensive forested regions (Maltamo et al., 2014). However, measured data are usually stored as point clouds consisting of 3D coordinates of laser return locations. Studies on ALS have shown that laser pulse penetration into the canopy causes an underestimation of 0.5 m – 2.0 m, depending on the tree species, canopy shape and structure (Woodget et al., 2007). ALS can minimize time, manpower, and cost, making it an attractive option for forest assessments (Pascual et al., 2018). Hence, despite the limitations, ALS is proven to be a valuable tool for forest inventory and management.

#### **2.4.2 Analysis of ALS data for urban forest ecological services**

ALS data provides a wealth of information that enables researchers and urban planners to quantify and model the ecological services of urban forests effectively. Some of the key parameters that can be extracted from ALS data and are relevant to model ecological services include individual tree and crown, sub-canopy forest structure, tree health, tree diameter and tree height, leaf area index, tree size distribution, tree species classification, above-ground biomass, and basal area and stand volume. Their applicability in studies will be described in the below paragraphs.

##### **2.4.2.1 Individual tree and crown**

Identifying each tree and its crown is a fundamental process that must be performed initially on a LiDAR data set to progress further in deriving other parameters of a tree in addition to its use in ecological services models. The exact identification and delineation of tree canopy borders in natural environments is required for the segmentation of individual tree crowns (ITCs). This operation can be accomplished using a variety of methods, including watershed segmentation, the valley-following algorithm (Gougeon, 1995), local maximum algorithm (Wulder et al., 2000), seed region growth algorithm (Fan et al., 2005), edge detection algorithm (Zhao et al., 2023), cluster analysis (Kaartinen et al., 2012), etc. Among them, the watershed segmentation is widely used, especially when working with remote sensing data (Chen et al., 2006; Schardt et al., 2002). By strategically placing markers within the watershed algorithm, each tree crown is regarded as a separate segment during the segmentation process. In order to make ITC identification easier, watershed segmentation can help distinguish between tree canopies and background (Hanapi et

al., 2019). The approach enables the identification of canopy boundaries by utilizing canopy height models (CHMs) (Wu et al., 2019).

Watershed segmentation, however, has certain drawbacks, one of which is its propensity for over-segmentation because of noise and data abnormalities (Hanapi et al., 2019; Ma et al., 2022). This emphasizes how crucial high-quality data is to guarantee accurate segmentation. The effectiveness of this method for ITC detection has been used in numerous investigations. For accurate ITC segmentation using LiDAR data, Yang et al. (2020) suggested a unique approach that combines the watershed algorithm and 3D spatial distribution analysis. The method relies on the identification of tree crowns based on their convexity and the highest point, followed by segmentation based on watersheds and 3D refinement.

Similarly, Wu et al. (2019) evaluated various segmentation techniques while focusing on estimating canopy cover using UAV-based LiDAR data. Approaches based on individual tree segmentation, CHM, and statistical models were investigated. The point cloud segmentation method, ITC segmentation, and watershed techniques were shown to be the most accurate. To monitor the state of the forest, Dous and Farah (2010) conducted a study to extract individual trees using CHM. For ITC segmentation and local maximum function of individual tree detection, they employed a watershed algorithm there. A marker-controlled segmentation technique that confines the watershed algorithm to a set of markers, in this case, treetops, increased the accuracy of this method. Three different window widths were tested, and the findings obtained showed that the number of trees had R-squared values of 0.84, 0.76, and 0.78. With an overall RMSE of 3.4% and a correlation coefficient of 0.88, the study concluded that the approaches were reasonably accurate when compared to actual data.

The study by Jaskierniak et al. (2021) presents an individual tree crown delineation algorithm, which uses a bottom-up approach. This algorithm has been tested on a LiDAR data set with a mean point density of 1,485 points per meter with 39 flight sites over a mixed species eucalypt forest, along with 2,790 field measurements. They have used kernel densities to stratify various understory vegetation profiles and watershed clustering procedures on point density measures for overstorey vegetation. Afterwards, a principal component analysis was done to merge the sliced clusters into trunks, branches, and canopy clumps. Finally, a voxel connectivity procedure had been performed to cluster the biomass segments into overstorey trees. According to the authors the individual tree and crown delineation algorithm has a mean F score of 0.91 and an 85% true positive tree representation with respect to the field measurements.

Another study by Sačkov et al. (2019) presents a comparison of two tree detection methods: the multisource based method executed in reFlex software, and the raster-based method implemented in OPALS software used to estimate forest stand and ecological variables from airborne LiDAR data in central European forests. It compared the estimated variables from the ALS data against four stands of ground reference data, each covering an area of 7.5 ha and within an overall area of 64 ha. The authors have derived the individual tree location and height using the raster method, tree species group into broadleaves and conifers using a combination of the canopy height model and the intensity raster having a pixel size of 1 m, tree diameter using nonlinear regression models, tree volume, forest stand and ecological variables. The study concludes that both software methods showed an overall performance rate between 52% to 64% compared to field collected data, with statistical significance ( $p$ -value  $< 0.05$ ).

In addition, Hu et al. (2014) have developed a framework that makes use of the finely detailed vertical structures found in high-density LiDAR data to improve the delineation of individual tree crowns. Finding treetops for marker-controlled watershed segmentation was the major goal of the multi-scale ITC delineation, which was constructed on a number of main processes. A tree crown was thought to resemble a half-ellipsoid or cone shape when viewed through a CHM. Two plots were chosen for the study from the study region. 74% of the mixed wood treetops in Plot 1 and 72% of the deciduous trees in Plot 2 were accurately defined when the findings were compared to a manually segmented CHM. These findings imply that the approach yields satisfactory results, particularly when compared with manual interpretation.

#### 2.4.2.2 Sub-canopy forest structure

The sub-canopy structure is a key parameter that can be derived from ALS data in forest inventory studies. It refers to the detailed and three-dimensional arrangement of vegetation components and features within lower layers of the forest, beneath the main canopy layer (Goodwin and Coops, 2016). In the study of Jarron et al. (2020), the researchers used ALS data to estimate a subcanopy forest of 48,000 ha dominated by coniferous trees in Canada. The ALS point density was 23 per square meter. The authors have distinguished the sub-canopy from the main canopy using the Lorey's mean height (i.e., a metric used in forestry and ecology to estimate the average height of trees within a stand or vegetation layer) as a threshold where the value below 70% was considered as sub-canopy. For calibration, 28 ground plots had been used with stepwise regression for predicting height, structure and cover based metrics. The R-squared values in cross-validating tree volume, basal area and number of sub-canopy trees are 0.88, 0.68 and 0.55, respectively.

#### 2.4.2.3 Tree health

In quantifying the ecological services of urban forests, tree health plays an important role. A dead or sick tree may not provide the required benefit and can lead to false statistics if identified as healthy. Due to unfavorable conditions, healthy trees may become unhealthy and continuous monitoring must be performed on them for more accurate estimations. ALS technology provides detailed information about the vertical structure and health of individual trees within a forest stand. The study by Degericks et al. (2018) presents a workflow to monitor the defoliation and discoloration of broadleaved trees. This study is based on a combination of hyperspectral imagery and LiDAR data. The authors have first delineated the trees using object-based tree detection and segmentation algorithms upon the LiDAR data. The average accuracy is 91%. They have then used partial least squares regression models to estimate the chlorophyll content and the leaf area index of trees using the average canopy spectrum with R-squared values of 0.77 and 0.66, respectively. The study further suggests the laser penetration metrics from the LiDAR data to be used for leaf area index calculations. In conclusion, the authors claim that in comparison to detecting healthy and unhealthy trees using remotely sensed data with the visual assessment, results proven to be 93% and 71% accurate respectively.

#### 2.4.2.4 Tree diameter and tree height

ALS technology provides high-resolution point cloud data, which enables the measurement of individual tree attributes, such as DBH and tree height. The tree diameter at breast height is a fundamental parameter for the i-Tree Eco model and the tree height data improves overall accuracy and the reliability of the i-Tree Eco outputs. The study by Corte et al. (2020) provides an automated approach for measuring individual tree DBH and height using a UAV-lidar system called GatorEye. In this study, a total of 63 trees were used as ground truth data with their DBH, height and position measure in the field. The correlation coefficients between field measurements and their corresponding LiDAR derived parameters are 0.77 and 0.91 and RMSE are 3.46 cm and 1.51 cm for DBH and tree height. These findings highlight the effectiveness and usability of this technique in deriving the tree DBH and height.

#### 2.4.2.5 Leaf area index (LAI)

LAI is another important parameter that can be derived from ALS data. It is a key biophysical variable that quantifies the total area of leaves per unit ground area in a forest or vegetation canopy. The study by Wang et al. (2020) reviews the capabilities of LiDAR technology in estimating the LAI, validating and other impact factors regarding the LAI. The authors state that LAI is mainly estimated from the methods correlation between the gap fraction (laser penetration matrices from LiDAR) and the contact frequency and from regression models developed using biophysical

parameters of trees such as canopy height and foliage density estimated from LiDAR. The authors further state that in such cases usually field data is collected through destructive sampling for validation purposes. Liang et al. (2016), investigated the assessment of LAI in boreal forests utilizing both ALS and TLS techniques and then compared LAI values estimated from both ALS and TLS data. The findings revealed that ALS data yielded highly precise LAI estimates, demonstrating a strong correlation coefficient of 0.89 when compared to the measurements taken in the field.

#### 2.4.2.6 Tree size distribution

Forest systems are always threatened by development projects, global changes, and other threats hence the changes must be monitored rapidly. Remote sensing techniques such as LiDAR technologies have made it possible to detect such changes on a global scale. Identifying tree size distributions over time is one way of quantifying forest changes. The utilization of ALS data allows for the extraction of tree size distribution within forest areas. Taubert et al. (2021) utilized the vertical LiDAR profile (not a point cloud) to estimate the tree size distribution, which provides information about the number and size of trees within different size classes. The study uses a tree-leaf matrix to calculate this and fit it to the observed leaf area density profile using the LiDAR data. The study has been performed on rain forests of Panama for spatial scales ranging from 0.004 ha to 50 ha. Results indicate that a higher accuracy is obtained for scales over 1 ha with a RMSE of 77.6 trees per hectare. Basal area estimations prove to be accurate at one hectare scale and have a RMSE of 4.7 trees per hectare and a bias of 0.8 square meters per hectare but are not accurate for smaller scales.

#### 2.4.2.7 Tree species classification

LiDAR technology has enabled capturing trees in three-dimensional point clouds increasing the capability of object extraction and identification with an improved accuracy than passive remote sensing techniques. This process involves analyzing the characteristics of the ALS point cloud, such as the intensity, height, shape, and number of returns, to classify individual trees into specific species categories. The study by Michałowska et al. (2021) reviews various studies which have LiDAR scanned data to determine tree species on several tree types. In total, 44 publications have been reviewed in this study. Based on the evaluation, the authors state that the tree parameters extracted from the full waveform of the LiDAR data have led to the highest overall accuracy. Regarding machine learning algorithms to identify species, the authors conclude that the random forest and support vector machine classifiers provide the best results in discriminating tree species.

#### 2.4.2.8 Above ground biomass (AGB)

In quantifying the ecosystem services of trees, AGB is a major parameter that must be estimated first. AGB refers to the total weight of living vegetation above the ground surface and is an important metric for quantifying carbon storage and understanding forest ecosystem dynamics. The study by Saarela et al. (2020) presents a hierarchical model-based inference approach for estimating AGB and associated uncertainties in central Sweden. This study area covered a vast region of 5,005 km<sup>2</sup> and the model generated high-resolution AGB maps with pixel values ranging from 9 to 447 mg/ha. The study found that the RMSE values for the AGB maps ranged from 10 and 162 mg/ha. Further, the authors identified that 75% of the mean square error in the maps is because of the uncertainties from the tree-level models. It has been found that the relative uncertainty is considerably high when the predicted quantity is small. Hence, careful consideration of such uncertainties is essential in interpreting and utilizing the AGB maps for forest management and carbon accounting purposes.

In the study by Billenberg (2023), AGB of two different tree species was calculated using TLS in Valls Hage, Gävle, and the findings were compared with actual field measurements. The SimpleForest tool in the Computree software was used to analyse the data from TLS, and the Quantitative Structure Model (QSM) and Wood Density were used to determine AGB. With an RMSE of 154 kg (0.997%) to 189 kg (0.990%), the comparison of the TLS-derived AGB estimates and the field validation revealed nearly perfect agreement. TLS shows promise for reliable AGB estimation despite data processing constraints and offers opportunity for improving future allometric models.

Lin (2023) has used the random forest approach in her study to estimate aboveground biomass (AGB) in Southern Sweden using Google Earth Engine (GEE) and data from Sentinel-1, Sentinel-2, and LiDAR. Model 1 looked at AGB changes from 2016 to 2021, whereas Model 2 focused on Hultsfred municipality and emphasized canopy height. Combining SAR polarization, multispectral bands, and vegetation indices improved AGB estimate, with certain spectral bands and radar backscatter values being most important. The resulting R-squared of Model 1 ranged from 0.33 to 0.74, with the greatest -squared of 0.91 achieved in the group where all variables were used with the canopy height in Model 2. The study demonstrates the value of combining various remote sensing data sources for monitoring.

#### 2.4.2.9 Basal area and stand volume.

Basa area refers to the cross-sectional area of a tree stem at breast height, usually expressed in square meters per hectare. Stand volume, on the other hand, is the total volume of wood in a forest stand, typically measured in m<sup>3</sup>/ha. To estimate wood and biomass quantities in a forest sample, basal area, and stand volume must be

determined first. They play an important role in forest management. The study by Zhao et al. (2020) provides a method to automatically segment forest stands. They have chosen Qilian Mountains in China as their study area. The Bysh method has been used to extract the forest parameters at the stand level. Their results indicate that the limited region growing method based on the gradient best suits the particular study area. The R squared value for mean height is 0.744 (RMSE 5.24%), for average diameter at breast height is 0.720 (RMSE 28.57%), for the basal area is 0.562 (RMSE 19.93%), and for stand volume is 0.696 (RMSE 17.66%).

### **2.4.3 Sampling design for ground truth data collection**

Generally, ALS-based data collection approaches for forest or tree inventory aim to reduce time and cost compared to traditional methods. However, it is not practical to conduct ground truthing for the entire population due to logistic constraints. Therefore, sample plots must be generated to represent the tree attributes that will be extracted by the ALS model accurately and scientifically (Koprivica 2017). The estimations made from the samples can be extrapolated to the entire population.

In defining the population, choosing the sampling frame, plot configuration and sampling design are the most important steps. The sampling frame points out all probable sample units, sampling design explains how a subset of sample units are selected which best represent the population, and plot configuration describes attributes such as size, shape, and components of the field map. Fixed area plots are recommended for this project as no tree attributes is focused, but a variety of attributes are to be collected with ancillary data. Fixed-area plots favor this situation. The two main sampling designs are subjective sampling and probability sampling. In subjective sampling, the professional opinion is considered when selecting sample units, whilst in probability sampling objective methods are implemented depending on the probabilities of choosing entities from a population (McRoberts et al., 2002). In systematic sampling, fixed grids with regular grids are assigned as plots. This will increase the average distance between plots leading to decreased spatial correlation between measurements and improving the statistical efficiency (Hayes, 2022). This approach is suggested for inexperienced decision makers in sampling.

#### **2.4.3.1 Stratified sampling**

Stratified sampling is a sampling technique commonly used in research and surveying to improve the accuracy and representativeness of the sample when the population exhibits variability or heterogeneity. In this method, the population is first divided into non-overlapping subgroups called strata based on certain characteristics or attributes shared by the elements within each stratum. These characteristics can be geographic location, land cover type, forest type, age class, or any other relevant criteria. The key steps in stratified sampling are defining strata, sample size allocation,

random sampling with strata, and estimation and aggregation (Schreuder et al., 1993). According to Köhl & Magnussen (2016), this method favors avoiding bias based on the estimator. Overall, this approach provides a statistically robust and effective method for conducting forest inventories and other sampling-based studies. The study by McRoberts et al. (2002) used landcover classification maps to design strata in differentiating aggregated forests and non-forest classes.

The sample size is another important factor that must be considered if the size is inadequate the uncertainty may increase and if it is oversized the cost and time may increase. Maltamo et al. (2011) evaluated different plot selection techniques for training forest inventories derived from ALS data. The authors employed four plot selection strategies for a total of 201 plots, including random selection, random selection within pre-stratification according to forest type, systematic selection of plots from south to north based on geographical location, and selection of plots based on properties of the ALS data. The results indicated that the accuracy decreased when the number of training plots was reduced. The researchers also stated that the systematic selection of plots for training data performed well even with fewer than 100 plots. However, they concluded that their results were not conclusive, highlighting the need for further research in this area.

On the other hand, Næsset (2004) in his study utilized 116 georeferenced field sample plots to estimate various parameters such as mean tree height, dominant height, mean diameter, stem number, basal area, and timber volume in a forest area. The plot distribution was conducted using a systematic approach with regular grid cells each having a size of 232.9 m<sup>2</sup>. These 116 plots were divided into three predefined strata based on their age class and site quality. The study revealed that the precision of the estimations was degraded when the plots within a stratum were dominated by a combination of deciduous and coniferous trees, as well as when there were combinations of coniferous and deciduous trees inside stands. This finding emphasizes the significance of proper stratification to maintain precision in forest inventory assessments. By carefully designing strata to ensure a more homogeneous distribution of tree species and forest types, the accuracy and reliability of the estimations can be improved. Koprivica (2017) provided a detailed explanation of how stratified sampling can be used in forest inventories and its advantage over other sampling methods. The efficiency of using systematic stratified sampling is compared against the systematic simple sampling method. Eleven stands of beech-high forests were used as the test bed. The findings of the study suggest that when the inventory units of a forest inventory are larger than a stand, stratified systematic sampling, where the sample plots are allocated proportionally, should be practiced. Additionally, the author emphasizes that systematic samples generally yield better estimations compared to random sampling.

Furthermore, Ramezan et al. (2019) conducted a study to evaluate sampling and cross-validation techniques for machine learning classifications. They examined various sampling methods, including simple random, proportional stratified random, disproportional stratified random, and deliberative sampling. The results indicated that the highest classification accuracy was achieved with stratified-statistical-based sampling methods, where random samples were combined with stratification strategies. These approaches enhance the accuracy and reliability of machine learning classifications, making them a valuable tool in forest inventory assessments. Overall, stratified sampling has proven to be a valuable and effective technique in forest inventories.

#### **2.4.4 Tree species detection using machine learning**

Tree species detection using machine learning has emerged as a transformative field that bridges the domains of computer science and environmental sciences. With an increasing need for efficient and reliable methods of species identification, this research area presents a significant opportunity to revolutionize traditional ecological practices. The integration of machine learning algorithms and remote sensing technologies has enabled researchers to harness large-scale datasets comprising satellite imagery, aerial photographs, LiDAR data, and UAV-based surveys. These diverse data sources offer valuable spectral, spatial, and textural information, enabling the development of sophisticated models capable of distinguishing tree species with high accuracy and precision (Cetin and Yastikli, 2022). Through the automation of species identification, this approach holds immense potential in advancing biodiversity conservation efforts, facilitating evidence-based forest management, and contributing to a deeper understanding of ecological dynamics. Moreover, the continuous advancements in machine learning techniques, including deep learning models and ensemble methods, offer a plethora of possibilities to enhance the performance and scalability of tree species detection systems (Seidel et al., 2021). As researchers endeavor to refine and validate these models, addressing challenges related to data quality, class imbalance, and transferability across geographic regions remains a key focus. Marrs and Ni-Meister (2019) conducted a study to accurately classify tree species by combining LiDAR and hyperspectral data with machine learning techniques.

In the context of tree species detection, multi-layer perception (MLP) plays a significant role, especially when dealing with structured data. MLP is a type of artificial neural network that is commonly used for modeling and predicting outcomes in tabular data, where the input features are structured in a table format with rows and columns. Unlike other neural network architectures, such as convolutional neural networks (CNNs) or recurrent neural networks (RNNs) MLP does not assume any

specific probability density functions for the input data. Guo et al. (2022) have done an individual tree species classification based on CNNs and remote sensing images. In the study of Magalhaes et al. (2022), they developed a tree growth app to model individual tree growth using RNNs. Likewise, there are various literature regarding forestry related studies using different machine learning techniques. Among them, researchers have successfully used MLP in combination with remote sensing and field-collected attributes to classify tree species (Sumsion et al., 2019; Chen et al., 2021). By feeding relevant features to the hidden layers of the MLP, the model can learn complex patterns and associations among attributes to discriminate different tree species. The flexibility of MLP allows researchers to customize the architecture by adjusting the number of hidden layers and neurons to suit the complexity of the problem at hand.

One advantage of MLP is its transparency and interpretability. Unlike deep learning models, MLP provides insights into the learned representations and feature importance, which can aid ecologists in understanding the decision-making process of the model and validating the relevance of certain attributes in tree species identification. In MLP, various activation functions and loss functions are utilized to enable the model to learn and make predictions effectively (Sumsion et al., 2019). Among them, the Hyperbolic Tangent (equation 5) activation function prevents vanishing gradient issues, capturing complex data patterns (Sumayli, 2022). For multi-class classification, Softmax (equation 6) ensures proper probability distribution, aiding accurate class assignments. Cross-entropy (equation 7) loss measures prediction accuracy, driving model optimization (Bodhwani et al., 2019). Combining these functions, MLP becomes a powerful tool for tasks like image recognition and natural language processing.

$$\tanh(x) = (e^x - e^{-x}) / (e^x + e^{-x}) \quad [5]$$

Where,  $x$  is the input value to the activation function and  $e$  is the base of the natural logarithm, approximately equal to 2.71828.

$$\sigma(\vec{z})_i = \frac{e^{z_i}}{\sum_{j=1}^K e^{z_j}} \quad [6]$$

Where,  $\sigma$  is softmax,  $\vec{z}$  is input vector,  $K$  is number of classes in the multi-class classifier,  $e^{z_i}$  is standard exponential function for the input vector and  $e^{z_j}$  is standard exponential function for the output vector.

$$L(\hat{y}, y) = -\sum (y_i * \log(\hat{y}_i)) \quad [7]$$

Where,  $\hat{y}_i$  represents the predicted probability for class  $i$ , and  $y_i$  is the true label for class  $i$ , which is 1 for the correct class and 0 for all other classes.

Apart from these functions, there are various functions used in the MLP model such as sigmoid (logistic) function (Yilmaz and Poli, 2022), rectified linear unit (ReLU) (Jahan et al., 2023), Leaky ReLU (Lakhdari and Saeed, 2022), Exponential linear unit (Kim et al., 2020), etc. The goals of the study and the characteristics of the available dataset will determine which activation function is chosen. Making the appropriate decision can improve the model's capacity to recognize patterns and make predictions.

### 3 Methodology

This chapter describes the geographic coverage of the study, the data and software used, and in detail the study workflow. The overall workflow followed in this study was developed based on the review in Chapter 2 and an abstract illustration of that is indicated in Figure 1. The process started with the field measurements, and then individual tree detection, crown delineation, deriving dendrometric parameters, a validation part and finally a sensitivity analysis.

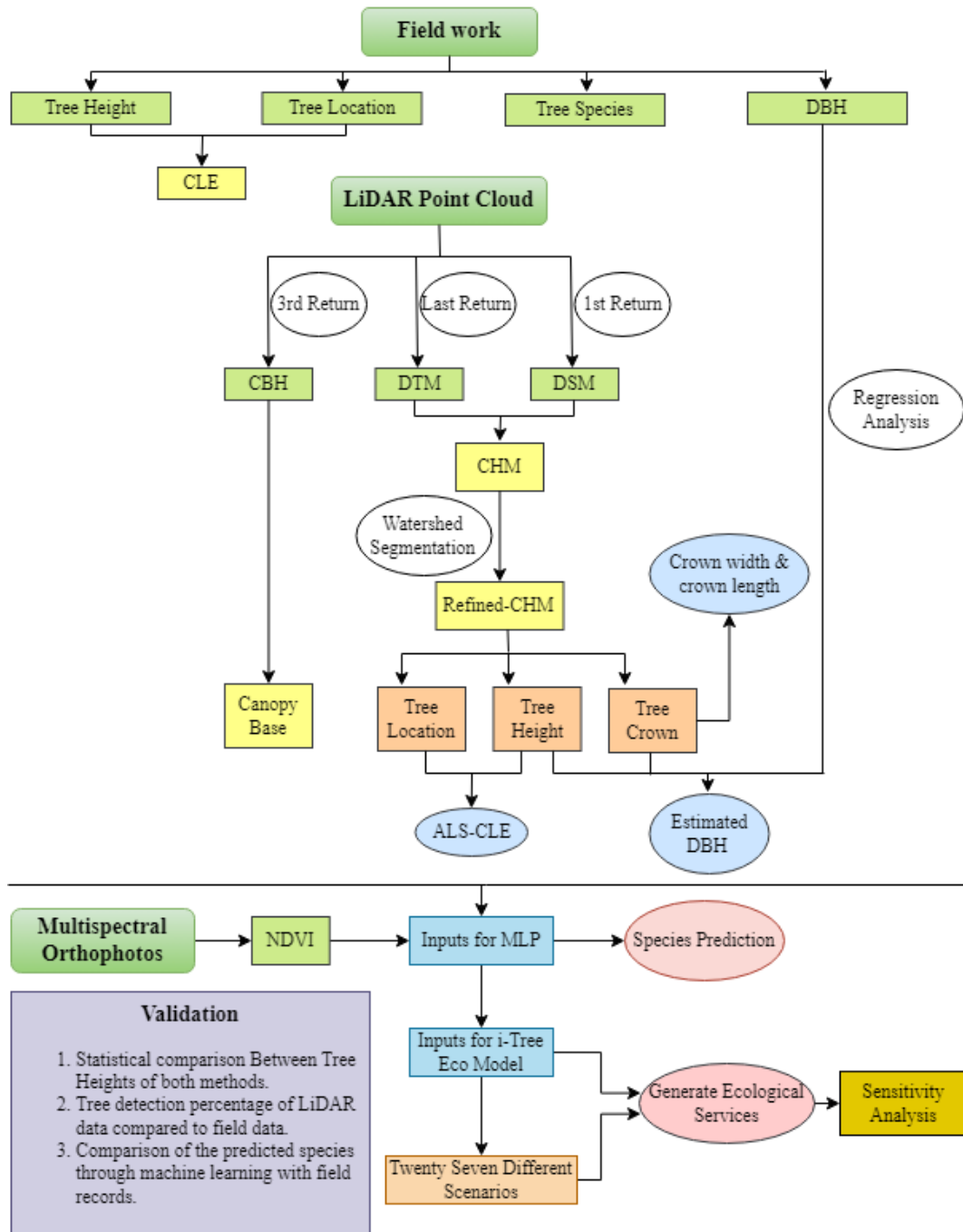


Figure 1. The flowchart of the research methodology.

### 3.1 Study area

The study area is Valls Hage, a beautiful forest botanical park covering approximately 10 ha, situated in the city of Gävle, Sweden (see Figure 2). The location is approximately 60.6777° N, 17.1115° E. This picturesque area boasts an impressive diversity of over 200 different tree species including aspen (*Populus tremula*) and birch (*Betula bendula*), making it a fascinating location for ecological studies (Gunnarsson & Lorentzon, 2017). For the specific research area, we focused on randomly selected four circular plots of Valls Hage.

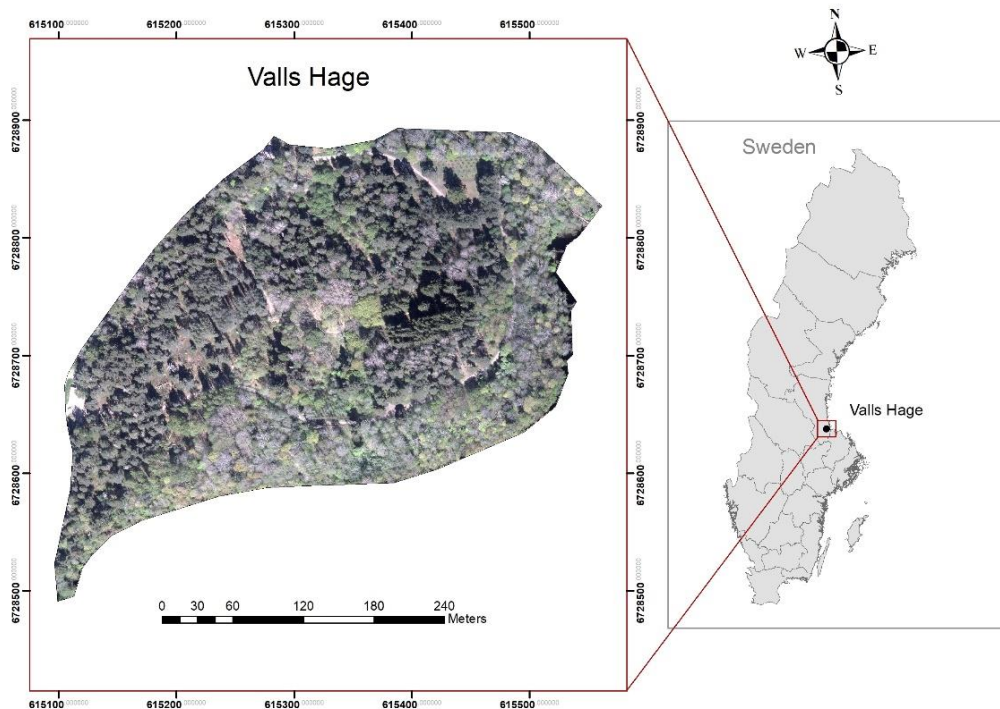


Figure 2. A map of the study area visualized in true color composition using RGB NIR orthophotos produced by Lantmäteriet.

### 3.2 Data and software

Several types of data were utilized for this study, along with specific software tools for analyzing and processing. The whole data set of the study was extracted in two ways as described in earlier chapters: field data and ALS data. Field measured data encompassing various dendrometric parameters such as tree heights, DBH played an important role in gathering on-site information about the trees in the study area. These field-measured data provided ground truth data that served as a reference for validating and calibrating the remotely sensed data. The materials used for field data collection included a GS14 GNSS receiver, a Leica FlexLine TS09 instrument, and a tape measure to obtain the required physical measurements.

In addition to field measured data, ALS data from Lantmäteriet were utilized to capture detailed information about tree height, canopy volume, and spatial arrangement of urban trees. Furthermore, RGB NIR multispectral orthophotos (with red [R], Blue [B], green [G], and infrared [IR] bands) acquired from Lantmäteriet were also used in this study. The orthophotos offered crucial visual information aiding in tree species identification. Table 3 illustrates a clear description of these data.

Table 3. Remote sensing data source used in the study.

Data	Date/Year of the acquisition	Spatial resolution	Format	Source
ALS	01.03.2018	0.5-1 point/m <sup>2</sup>	.laz	Swedish National Survey, Lantmäteriet
Orthophotos	17.05.2019	0.16 m	geotiff	Swedish National Survey, Lantmäteriet

There was various software used to process and analyze the collected data. ArcGIS ArcMap version 10.7 (reference) and QGIS Desktop version 3.18.1 (2021) were employed for geospatial analysis and map production. To process the ALS data, LAStools version 1.3 (2021), which is an extension for QGIS software was utilized. For statistical analysis, Minitab version 19 (2021) was employed. This software package provided the necessary tools for data analysis, hypothesis testing, and correlation analysis. The SPSS-IBM Statistics version 24 (2021) was used to predict the species type of trees utilizing its neural network multilayer perceptron.

### 3.3 Field work

Field work played a crucial role in this study as it aimed to provide essential ground truth data for validation and calibration of the collected information. The fieldwork of the study was carried out over four days (08 March 2021, 23 March 2021, 06 April 2021, and 08 April 2021). Firstly, four circular plots were randomly selected within the study area, each with an approximate radius of 25 meters (see Figure 3, the plots were named as 1, 2, 3, and 4). The decision to use circular plots was influenced by the findings of Paudel et al., (2019), which suggested that circular plots offer the most reliable and accurate results in similar studies.

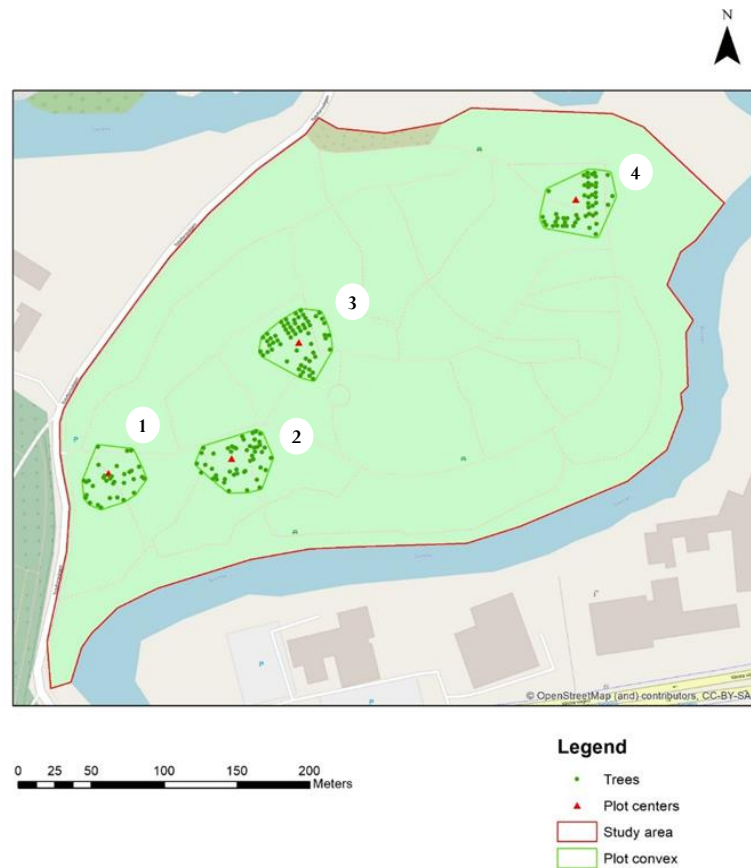


Figure 3. The field measured trees inside four plots of the study area.

Four main plot centers were selected for the survey zone based on their intervisibility with at least two control sites and their ability to cover at least 50 trees in their direct line of sight. The GNSS-RTK technique, as described by HMK (2021), was employed, with corrections obtained from SWEPOS (Stoew et al., 2001) to determine the precise locations of the plot centers. A Leica GS14 GNSS receiver was employed for this task. To ensure precise observations, data recording was done when the 3D accuracy was within a threshold of 1 cm and each observation was carefully carried out during a 15-minute period. This approach proved to be effective in avoiding the need for a traverse in establishing the control network and subsequent adjustment computations. The station coordinates obtained through SWEPOS corrections were considered sufficiently accurate to meet the requirements of this study.

To gather vital data for input requirements, locations of trees were measured using the Leica TS15 total station. The total station was set up on each of these plot centers after the coordinates for each were determined by GNSS-RTK method. The total station established over a know point using another known point as a backlight point. The positions of each tree were then precisely determined by measuring them with a prism pole. Throughout the field work the accuracies were maintained according to the HMK standards.

In addition, as described by Magarik et al. (2020), the circumference measurements of each tree were recorded in meters using a tape measure from a standardized height above the ground (i.e., 1.3 m). Then it was divided by pi (3.1415) to obtain DBH. Tree heights were obtained in meters by using the trigonometric method (Van et al., 2010) and employing non-prism (reflector less) observation type (Mohammed, 2021). Here, the distances from the highest to the lowest point of each individual tree within each plot were measured with an accuracy of 2 mm + 2 ppm (Leica geosystems, 2015).

In this study, to accurately determine the species of the measured trees, a systematic approach was taken by capturing photographs of the tree barks. These photographs were then cross-referenced with the extensive database provided by Pl@ntNet, which is accessible at <https://identify.plantnet.org/>. This database utilizes a RESTful JSON-based application programming interface that can determine tree species. The system employs a convolution neural network, which applies the SoftMax algorithm to generate classification match scores for the input images (August et al., 2020). The species list and corresponding images with classification match scores are presented as output, with the highest scores indicating the closest match to the input photograph (see Figure 4). This step was crucial as tree species identification is a fundamental input required by the i-Tree Eco model. Given the unavailability of professionals with expertise in tree identification for this field work, the Pl@ntNet database and algorithm were utilized to identify the tree species.

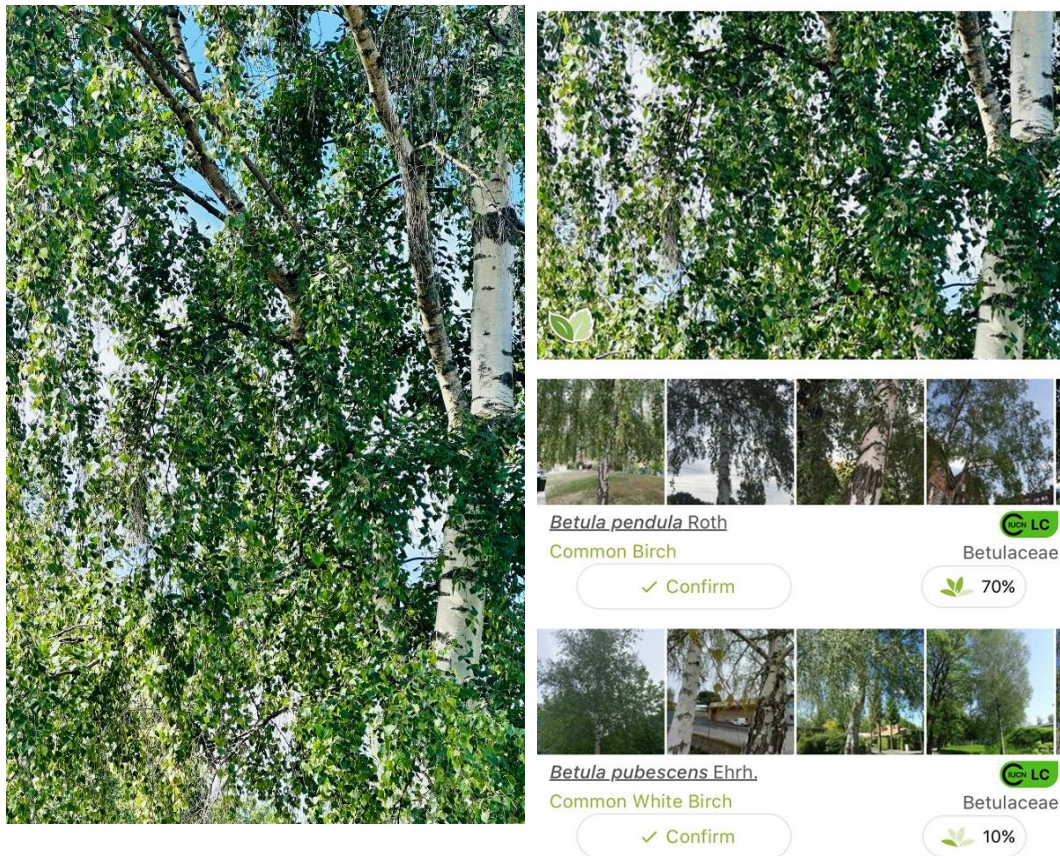


Figure 4. Tree species identification through PI@ntNeT app.

### 3.4 Individual crown delineation and tree detection

The process of individual crown delineation and tree detection from the LiDAR data involved several steps. To begin with the process, the ALS data underwent an examination using the LASinfor tool within LAStools plugin within the QGIS platform, and a metadata description of the data was obtained (Karna et al., 2020). Subsequently, that file was cross-checked with the metadata file provided by Lantmäteriet to ensure the absence of any discrepancies or differences.

Next, the ALS data was clipped to the study area of interest. To ensure the quality of the point cloud data, a visual inspection was performed to detect any potential noise points. Then the clipped point cloud underwent noise removal (De Petris et al., 2020) and overlapping tile removal (Pelc-Mieczkowska et al., 2018) using the built-in algorithms of LAStools in QGIS. By removing noise points, the elevation models were less susceptible to distortions caused by erroneous data, resulting in a more precise representation of the terrain. Rectifying flight misalignment further contributed to improving the accuracy of the elevation model, as it minimized the potential errors caused by misregistered data between flight lines. Additionally, the built-in pit-free algorithm in LAStools was employed to prevent the creation of unnecessary voids after interpolation (Khosravipour et al., 2013). After implementing these techniques,

the ALS data was used to generate the digital surface models (DSM) and digital terrain models (DTM).

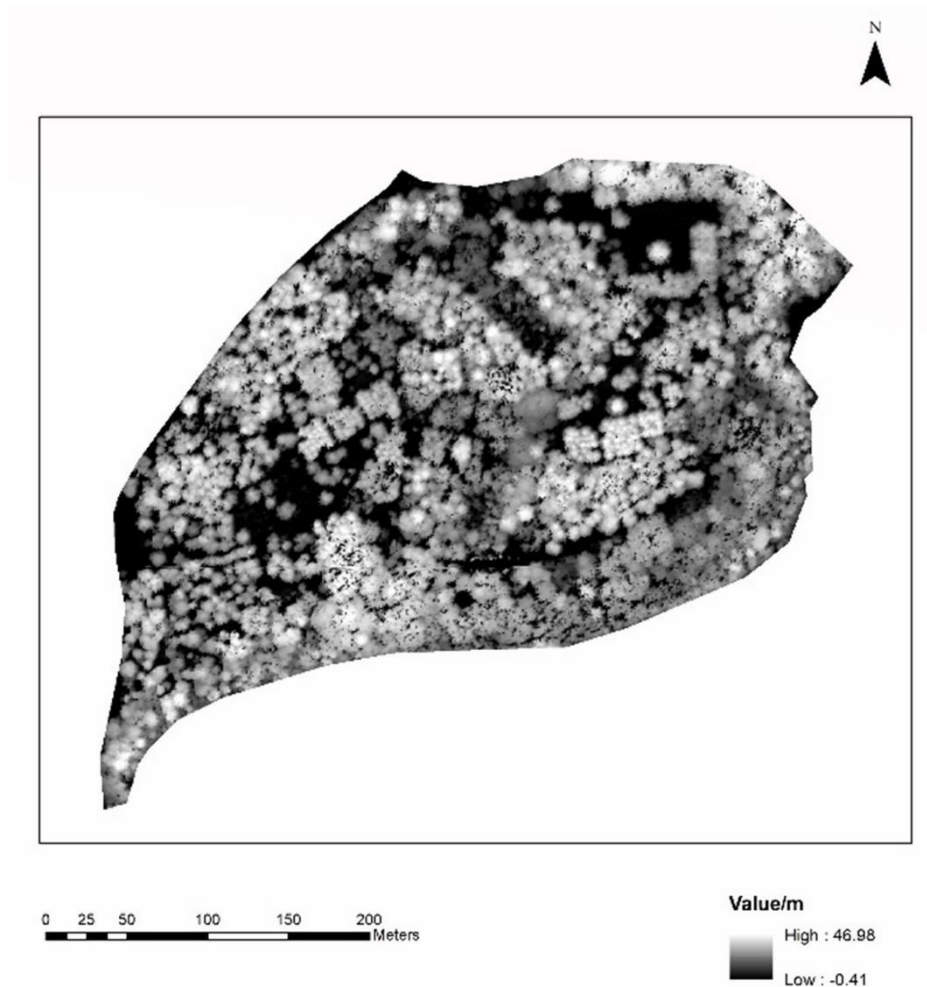


*Figure 5. Canopy base height model derived from ALS technique in the study area.*

The DSM was produced by extracting the first return of the LiDAR point cloud (Sharma et al., 2021). This DSM represented the surface closest to the LiDAR pulse transponder and had a spatial resolution of 0.1 m. Similarly, the DTM was created by extracting the last return of the LiDAR point cloud, representing the ground surface (Sharma et al., 2021). Both DSM and DTM were generated using the LAStools in QGIS. The canopy height model (CHM) was then derived by subtracting the DTM from the DSM (Mielcarek et al., 2018) (see Figure 5). Negative CHM values were filtered out as tree heights cannot be negative.

To further refine the CHM, a mean filter (Tanhuanpää et al., 2016) of 10 m radius was applied in QGIS to reduce height variation and minimize speckle-like noise. A Gaussian filter (Zhan et al., 2011) with a standard deviation of 5, and a search radius of 10 m was further applied to the filtered CHM to help smooth the variation and to filter out additional noise. Its rotational symmetry was particularly advantageous for

enhancing tree crown separation based on crown shape, given the prevalence of coniferous tree species.

Individual tree crowns (ITCs) were delineated from the refined CHM using the watershed segmentation algorithm provided in the SAGA toolbox (Goldbergs et al., 2018). This raster-based technique utilized local maxima of the CHM as seeds for tree locations, with the bounding areas of these seeds considered as tree canopies (Jaskierniak et al., 2021). The reason for using this raster-based technique was that in comparison with other methods this is quite fast, computationally less heavy and provides acceptable results for most cases.

Once the segmentation process provided detailed tree canopies, the next step involved filtering out trees that did not meet the specified criteria for this study. Based on the defined criteria for trees in the existing literature, as well as the field-collected data on the most prevalent tree species, trees with heights of less than 4 m, and trees with crown diameter with a size smaller than 1 m were removed from further analysis (Gschwantner et al., 2009). By conducting this filtering step after segmentation, the study ensured that all heights from the CHM were initially considered for canopy extraction, allowing for a more complete representation of the forested area. Otherwise, it may negatively affect the CHM if this filtering is done before the segmentation since the model will understand that there is no tree. Thus, trees that matched the criteria were retained, while the rest were removed and not included in the analysis.

Thereafter, the delineated ITCs underwent a smoothing process using the PAEK (Polynomial Approximation with Exponential Kernel) algorithm provided in ArcMap (Malabanan et al., 2016). The application of PAEK technique offered several advantages over other smoothing methods. Firstly, it preserves the original shape and structure of the tree crowns during the smoothing process by avoiding excessive smoothing that could potentially lead to the loss of important details in crown delineation. Secondly, it effectively filters out noise and outliers in the ALS data, resulting in cleaner and more reliable crown delineation. Lastly, by incorporating spatial weighting through the exponential kernel, it leverages the local context to produce smoother and more natural-looking crown boundaries.

After the smoothing process, the tree crowns were then combined with the field-measured tree location file (point file) using the spatial join tool in ArcMap. Since the field-measured trees lacked physically measured tree crowns, this process allowed us to integrate the smoothed ALS-generated crowns with the field-measured trees, providing each tree with its own canopy dimensions. Then, the minimum bounding boxes were generated to determine the maximum width and length of each tree's canopy. This provides valuable information about the overall extent of the tree

crowns. Additionally, the square root of the crown area was calculated to estimate the width and length of the canopy in the North-South and East-West direction. These dimensions were essential inputs required by the i-Tree Eco model.

### **3.5 Deriving dendrometric parameters**

In this study, the focus was primarily on deriving tree parameters from ALS data, The methods employed for generating these three dendrometric parameters are detailed and described in the following paragraphs.

#### **3.5.1 Tree heights**

The refined CHM, which was described in Section 3.4, was used to obtain tree heights. Values from the CHM, matching the location of the field measured trees were extracted, and used as ALS derived tree heights in the later steps. The derived CHM was in a raster format, while the field-measured trees were stored in a point layer.

#### **3.5.2 DBH estimation**

DBH is one of the fundamental inputs for the i-Tree Eco model. In this study, DBHs were estimated for trees that derived from ALS data using a linear regression model (equation 8). This decision was taken because the available ALS data was not dense enough to model the DBH. To identify the most suitable regression model for DBH estimation, several models were evaluated including linear, cubic, and quadratic using crown diameters and tree heights (field measured tree heights and/or CHM derived tree heights). Here, average values for these parameters were aggregated based on the taxonomical order, specifically species, genus, family, and order level and then tested each parameter with different regression models individually. Then checked how each parameter fits with the linear, cubic, and quadratic regression models. The primary objective was to determine the model with the highest R-squared value, indicating the best fit. After the analysis, it was found that the linear regression model, using average values from the family taxonomy rank for tree DBHs and CHM tree heights, demonstrated statistical acceptability with an impressive R-squared value of 71.32% (see Figure 6).

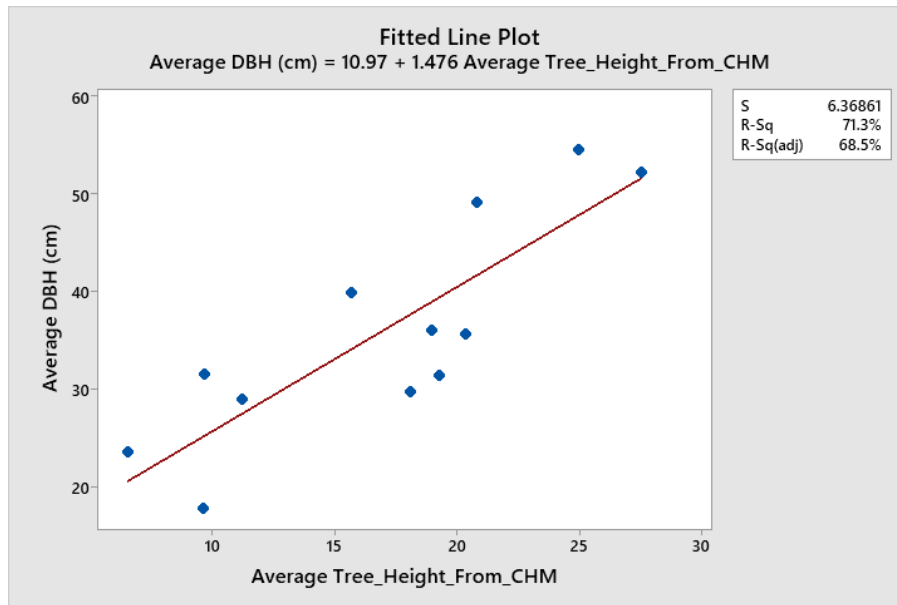


Figure 6. The scatter plot between average DBH and average CHM derived tree height. The red line indicates the best fitted line between the two variables.

$$Avg\ DBH = (1.476 \times Avg\ TH) + 10.97 \text{ [8]}$$

Where, Avg DBH is the DBH value that is averaged based on the family taxonomy and Avg TH is the tree height derived from CHM value that is averaged based on the family taxonomy.

Additionally, the validity of the assumption that the residuals conform a normal distribution was ensured by conducting a normality test, resulting in a p-value of 0.15 (where the confidence level was 95%). With the linear regression model displaying the highest R-squared value compared to other combinations, established this relationship (equation 08) was employed to predict the DBH of all LiDAR-derived trees within the study area. To ensure the accuracy of the predictions, any tree CHM heights that fell outside the minimum and maximum height range specified in the model (Cimburova et al., 2020) were excluded from the analysis. This step was essential as predictions will only be limited to interpolation rather than extrapolation.

### 3.5.3 Crown light exposure (CLE)

The crown light exposure (CLE) is one of the input parameters for the i-Tree Eco model. It was determined by considering the individual tree height and the distance to the nearest tree from the respective tree as they are the main two contributing factors for CLE. Firstly, the tree heights of the whole data set were inspected and the minimal and the maximal tree heights throughout the whole sample were identified. Then the difference between those minimum and the maximum tree height was linearly stretched between 1 and 100 and each tree was assigned a new normalized value proportional to its height. Secondly, the distances between each tree to its

closest tree were listed out and ordered from minimal to maximal. Then the difference between the minimum and maximum was linearly stretched between 1 and 100 and each tree was assigned a new normalized value. Subsequently, these two newly assigned values (tree height and distance to the nearest tree) were added together and interpolated between 1 and 5 proportionally (Osada 2012).

#### 3.5.4 Canopy base height (CBH)

The canopy base height was calculated using a DEM derived from the third return of the ALS data (Holmgren et al., 2004). The CBH was then generated by subtracting the DEM derived from the third return from the DSM (from the first return) for crown base heights (CBH). This method was chosen because the second return came up with many negative values after the DEM from the third return was reduced. DEMs derived from returns four, five, and six, were too sparse. Hence the difference was almost equal to the tree heights.

### 3.6 Species identification

In order to predict the species through machine learning, several field measured parameters and ALS derived parameters were used in MLP. The Normalized Vegetation Index (NDVI) is calculated for each tree location using the RGB and NIR orthophoto product with a resolution of 0.16 m provided by Lantmateriet (see Appendix C). This index is commonly used to assess vegetation health and density, calculated based on the contrast between visible red and near-infrared light reflected by vegetation (equation 9). Then the required data for the task was prepared by arranging a table including variables, tree height, DBH, height to crown base, crown area and NDVI for both datasets where the species is known, and the species is unknown (ALS derived trees).

$$NDVI = (NIR - Red) / (NIR + Red) [9]$$

The collected variables and tree information were used as inputs for a neural network model called Multilayer Perceptron (MLP) implemented in the SPSS IBM software. The MLP model was trained to predict the tree species based on the provided inputs. MLP was chosen over other types of neural networks (such as convolutional neural networks and recurrent neural networks) because it performs better on tabular datasets and does not assume underlying probability density functions. The process was repeated separately to predict tree genus, family, and order in each run. Among the predicted tree attributes, the family-level prediction yielded better results. Therefore, the MLP model was primarily used to predict the family of ALS-derived trees. Here an assumption was made that the whole data set belongs to only the two most common families Betulaceae (Birch) and Pinaceae (Pine). This was done since the trees belonging to other families were too small in number and the MLP couldn't

predict any outputs for them. Table 4 illustrates the network information of species prediction.

Table 4. Network information of MLP model.

Network Information			
Input Layer	Covariates	1	NDVI
		2	CBH
		3	Tree height_From_CHM
		4	Crown_Area
		5	DBH (cm)
	Number of Units excluding the bias unit		5
Rescaling Method for Covariates		Standardized	
Hidden Layer(s)	Number of Hidden Layers		1
	Number of Units in Hidden Layer 1a		3
	Activation Function		Hyperbolic tangent
Output Layer	Dependent Variables	1	Code
	Number of Units		2
	Activation Function		Softmax
	Error Function		Cross-entropy

### 3.7 Validation of extracted parameters with field data

The validation part was carried out in three distinct stages. Firstly, the tree heights derived from ALS data were compared with the tree heights measured in the field. This step allowed us to assess the accuracy and reliability of the ALS-derived tree heights. Initially, a Kolmogorov-Smirnova test (Corrao et al., 2022) was conducted to check the difference between the two tree height datasets following a normal distribution. This test was essential as the paired t-test relies on the assumption that the difference between the paired observations adheres to a normal distribution, ensuring the robustness of the validation process. To validate this comparison, a paired t-test was performed to determine if the field measured tree heights could be effectively replaced with the CHM heights (Mielcarek et al., 2018).

Secondly, a comparison between the number of trees detected through the ALS data and the number of trees measured in the field was made for each plot individually. This was done through ArcMap using a visual inspection (see Figure 7). This was continued for all four plots individually. This comparison aimed to verify the capability of individual tree detection from the ALS data, ensuring that the technology effectively identified trees within the study area.

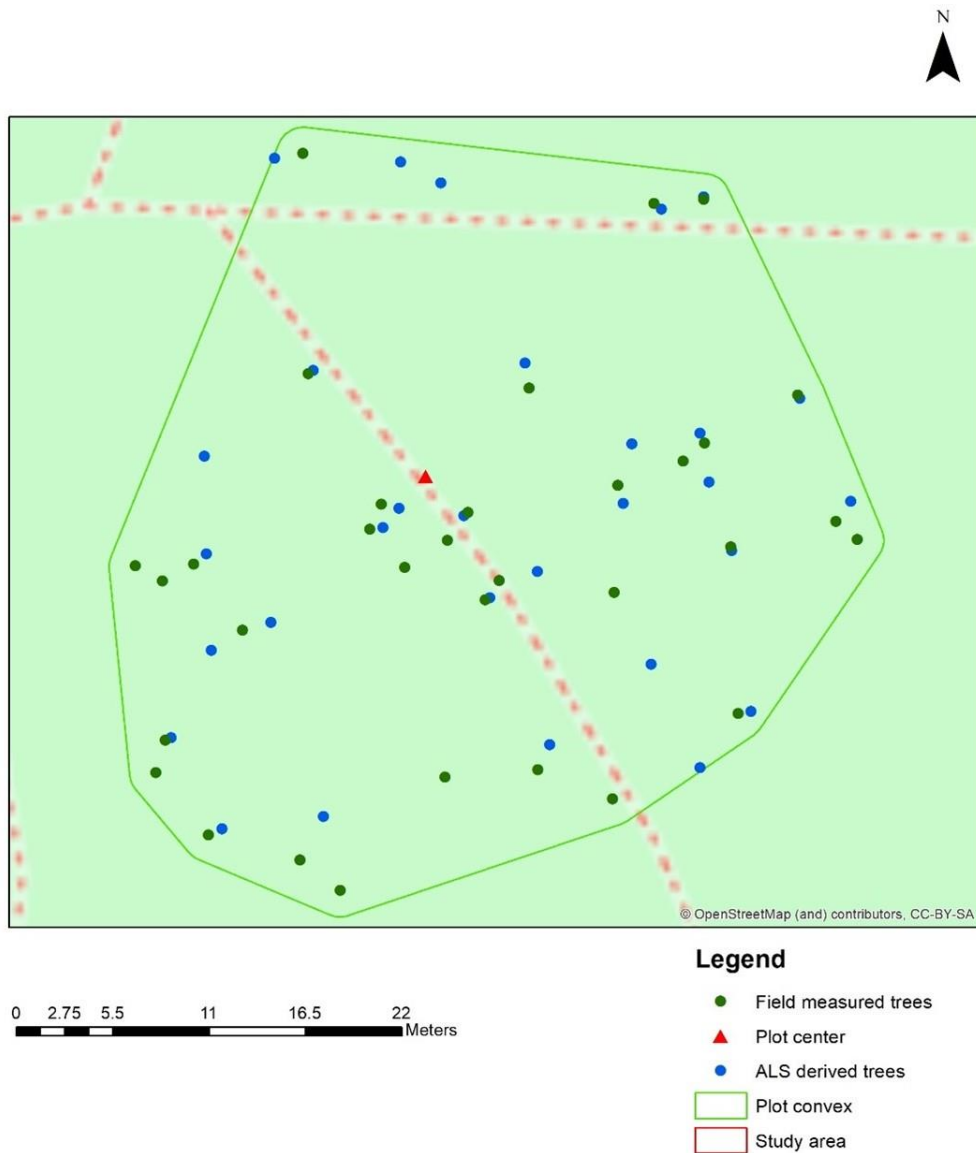


Figure 7. ALS derived trees and field measured trees in plot 1.

Lastly, the results of the species detection performed through machine learning were compared with the field records. The process was delivered a summary report and based on that this validation was done. This crucial step enabled us to evaluate the accuracy of the machine learning algorithm in correctly identifying tree species, providing valuable insights into the effectiveness of our methodology. See case processing summary.

### 3.8 i-Tree Eco modelling

The utilization of the i-Tree Eco model requires specific inputs to be provided for analysis. These inputs include tree locations in the WGS84 coordinate system, tree heights in meters, DBH in centimeters, the number of crowns, tree species, crown area, crown length in both East-West and North-South directions, crown light

exposure, tree height to live top, canopy base height, percentage of crown missing, distance to the nearest building, and the horizontal angle to the nearest building. Additionally, the land use of the area of interest must be specified. Once these inputs are fed into the model, it yields a range of valuable outputs, including carbon storage, annual carbon sequestration, hydrology effects, oxygen production, volatile organic compounds (VOC) emissions, ultraviolet (UV) effects, allergy indexes, transpiration, evaporation, water intercepted, and avoided runoff. For the purposes of this study, our main focus will be on the i-Tree Eco results related to carbon storage, gross carbon sequestration, and avoided runoff.

### 3.9 i-Tree Eco modelling sensitivity analysis

A sensitivity analysis was conducted to observe how the outputs of the i-Tree Eco model changed when the input values derived from ALS are altered. This was performed to determine the feasibility of utilizing published average values in place of field measurements as inputs for the i-Tree Eco model. One of the fundamental inputs for the i-Tree Eco model is the DBH. There are various published documents and other sources where average DBH of trees in species, genus, family, or order level are available (Kubiske, 2013; Kindermann et al., 2018; Roberge, 2022 & Monumental trees, 2023). Hence, based on this sensitivity analysis, we can comment on the direct usability of available data for determining ecosystem services through i-Tree Eco model instead of costly and time-consuming field work. Mainly, 26 scenarios were used in this purpose, and they can be further categorized into eight. They are clearly illustrated by the following table (see Table 5). Here one assumption was made that all the trees were in perfect health hence no tree dies back with 0% of crown missing.

For scenario 1 (reference values), all raw inputs were used without any alteration (i.e. field measured tree locations in latitude and longitude format belonging to WGS1984 coordinate system; tree height from the CHM in meters; canopy base height (CBH) from the third return of the LiDAR point cloud in meters; field measured DBH (cm); species determined from Pl@ntNet; and, ranked CLE). The obtained values for three ecological services (Carbon Storage(ton); Gross Carbon Sequestration (ton/yr); and, avoided runoff (m<sup>3</sup>/yr) were used to compare the values obtained by rest of the 26 different scenarios.

Table 5. Scenarios employed in the sensitivity analysis.

Category	Scenario Number	Scenario Description
1	II	Species-wise DBH values were averaged and used as inputs.

Here, all the inputs for the i-Tree Eco were same as the inputs used to generate the reference values except for the DBH. DBHs were replaced according to four different scenarios.	III	Genus-wise DBH values were averaged and used as inputs.
	IV	Familywise DBH values were averaged and used as inputs.
	V	Order-wise DBH values were averaged and used as inputs.
2  Here, the DBH input for the i-Tree Eco were same as the input used to generate the reference values whilst all the other inputs were averaged according to four different scenarios.	VI	Species-wise canopy width, length, tree height, and CBH values were averaged individually and used as inputs.
	VII	Genus-wise canopy width, length, tree height, and CBH values were averaged individually and used as inputs.
	VIII	Family-wise canopy width, length, tree height, and CBH values were averaged individually and used as inputs.
	IX	Order-wise canopy width, length, tree height, and CBH values were averaged individually and used as inputs.
3  Here, all the inputs for the i-Tree Eco were averaged according to four different scenarios.	X	Species-wise DBH, canopy width, length, tree height, and CBH were averaged individually and used as inputs.
	XI	Genus-wise DBH, canopy width, length, tree height, and CBH were averaged individually and used as inputs.
	XII	Family-wise DBH, canopy width, length, tree height, and CBH were averaged individually and used as inputs.
	XIII	Order-wise DBH, canopy width, length, tree height, and CBH were averaged individually and used as inputs.
4  Here all the inputs for the i-Tree Eco were same as the inputs used to generate the reference values excepts for the tree species. Species were replaced according to four different scenarios.	XIV	Each tree's species name was replaced with the most common species name within its respective Genus.
	XV	Each tree's species name was replaced with the most common species name within its respective Family.
	XVI	Each tree's species name was replaced with the most common species name within its respective Order.

5  Here, all the inputs for the i-Tree Eco were same as the inputs used to generate the reference values excepts for the tree heights. Field measured tree heights were used and replaced according to four different scenarios. Canopy dimensions and CBH were not used for i-Tree Eco inputs.	XVII	The field-measured tree heights were used.
	XVIII	Species-wise field-measured tree heights were averaged and used as inputs.
	XIX	Genus-wise field-measured tree heights were averaged and used as inputs.
	XX	Family-wise field-measured tree heights were averaged and used as inputs.
	XXI	Order-wise field-measured tree heights were averaged and used as inputs.
6  Here, the original parameters were re generated using average CHM tree height value according to four different scenarios. Canopy dimensions and CBH were not used for i-Tree Eco inputs.	XXII	Species-wise CHM-derived tree heights were averaged and used as inputs.
	XXIII	Genus-wise CHM-derived tree heights were averaged and used as inputs.
	XXIV	Family-wise CHM-derived tree heights were averaged and used as inputs.
	XXV	Order-wise CHM-derived tree heights were averaged and used as inputs.
	XXVI	The CHM-derived tree heights were used.
7  This is the most important scenario, as the results are generated from the input tree species predicted from the MLP and all the other parameters are estimated from the ALS data.	XXVII	ALS derived trees with MLP predicted species

After generating the ecological services according to the above 26 scenarios, they were compared based on respective reference values obtained from scenario 1.

## 4 Results

This chapter presents the results obtained through the methodology from the individual tree detection using the ALS data to the i-Tree Eco modelling. Then the findings of the sensitivity analysis are also reported. The comparison between the results obtained from remote sensing methods and the field data are included under the validation part.

### 4.1 Crown delineation and tree detection

The first result of the ALS data was obtained from the step of individual tree detection and crown delineation. The ALS derived trees were obtained in the whole study area first and then they were extracted to each plot individually to continue with the further steps (see Figure 8).

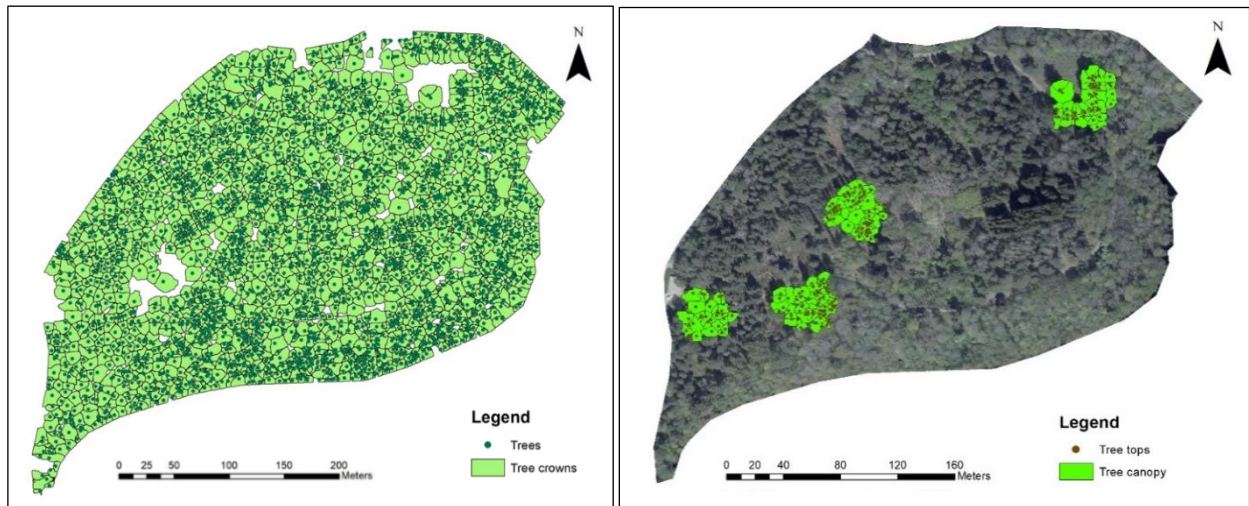


Figure 8. Left side (a) shows the crown belongs to the whole study area and right side (b) shows the crowns belong to individual plots.

### 4.2 Extraction of dendrometric parameters

To serve as the inputs for the i-Tree Eco model, tree heights, DBH, CLE, CBH, and other crown parameters were extracted from both field data and ALS data. Table D1 (Appendix D) illustrates the input parameters derived from field data while Table D2 (Appendix D) illustrates the input parameters derived from ALS data. In Table D2 (Appendix D), the MLP prediction column illustrates the family level species prediction results where 1 represents Betulaceae (birch) and 2 represents Pinaceae (pine). Since the i-Tree Eco model does not allow to enter family names, the predicted results of family names were replaced with the respective most common species. Then they were assigned to each tree carefully. Despite the parameters shown in these two tables, which are required to calculate the carbon storage, gross carbon sequestration and avoided runoff, there were other mandatory inputs as well. They are as height to live top, percent missing, distance and angle to the nearest building,

and land use. For this study the height to live top was assumed same as the tree height and the percent missing was taken as zero. Normally, the height to live top means the Distance and angle to the nearest building for each tree was calculated using ArcMap. As these parameters are not used in estimating the ecological services discussed in this study, they will not be further explained. Species identification using machine learning.

As described under the methodology, the species prediction was done according to the assumption: the whole dataset belongs to only the two most common families Betulaceae and Pinaceae. Table 6 illustrates the case processing summary of the tree prediction through the MLP technique for the whole dataset. Before the test, there were 154 ALS-derived trees in total. The neural network has automatically divided the whole dataset into two samples as training and testing, with percentages of 74% and 26% respectively.

Table 6. Case processing summary of MLP model.

Case Processing Summary			
		N	Percent
Sample	Training	114	74.0%
	Testing	40	26.0%
Valid		154	100.0%

Based on the model summary (see Table 7), the training sample obtained 12.3% of incorrect predictions while the testing sample obtained 7.5% of incorrect predictions. The obtained cross entropy error for the training sample and the testing sample were 34.186 and 7.795 respectively. Cross entropy error indicates the overall dissimilarity between the predicted probabilities and the true class labels in the multi-class classification task. A lower cross-entropy value signifies better model performance, as it implies that the model's predictions are closer to the ground truth (Jarabo-Amores, 2013). Usually the cross-entropy value ranges from 0 to infinity and the minimum cross entropy error depends on the specific problem, dataset, and number of classes.

Table 8 shows the importance of the independent variables on the tree prediction. Based on this table, the most important variable in the MLP was the CBH (0.344 / 34.4%), while the least important was the DBH (0.135/ 13.5%).

Table 7. Model summary of MLP model.

Model Summary		
Training	Cross Entropy Error	34.186
	Percent Incorrect Predictions	12.3%
	Stopping Rule Used	1 consecutive step(s) with no decrease in errora
	Training Time	0:00:00.02
Testing	Cross Entropy Error	7.795
	Percent Incorrect Predictions	7.5%

Table 8. Independent variable importance in MLP model.

Variable	Importance	Normalized Importance
CBH	0.344	100.0%
Crown Area	0.192	55.7%
NDVI	0.176	51.2%
Tree_Height_From_CHM	0.153	44.4%
DBH (cm)	0.135	39.2%

### 4.3 Validation of tree heights, tree count, and tree species prediction

The validation part was conducted in three steps and the respective results will be displayed and described in detail under the subheadings below.

#### 4.3.1 Field measured heights vs CHM derived heights

Firstly, a scatter plot was obtained between the field measured tree heights and CHM derived tree heights. The scatter plot in Figure 9 indicates a positive relationship between CHM derived tree heights (X) and measured tree heights (Y). The R-squared value of 0.202 suggests that 20.2% of the variability in Y can be explained by X. Hence, this does not indicate a better fit since the R-squared is lower than 50%.

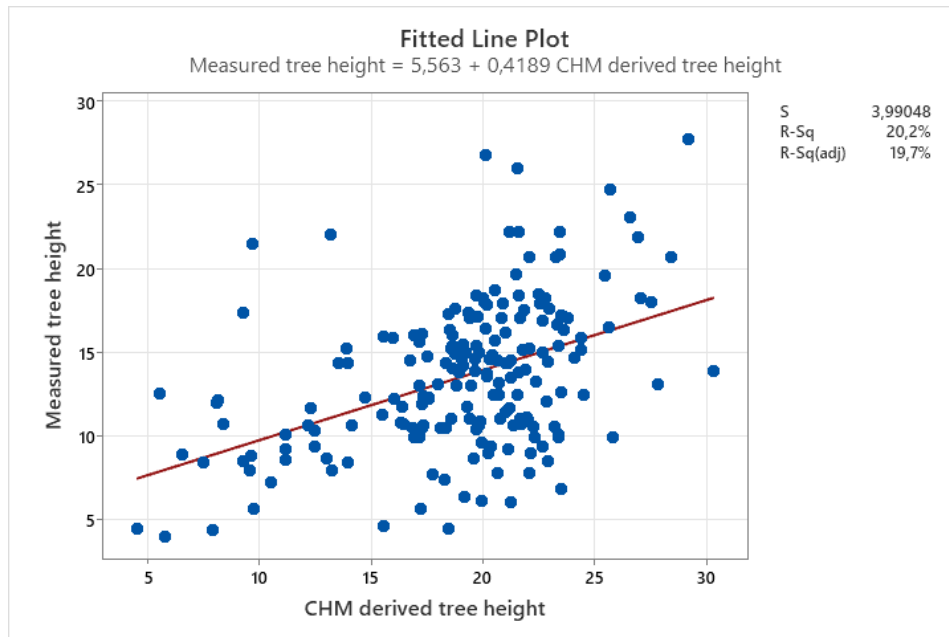


Figure 9. The scatter plot of field measured tree height vs ALS derived tree heights. The red line indicates the best fitted line between the two variables.

Then a paired T-test was performed between field derived tree heights and ALS derived tree heights to check whether the field measured tree heights can be replaced with ALS derived tree heights. A total number of 191 trees were used for this test. The null hypothesis was set as there is no significant difference between field measured tree heights and ALS-derived tree heights. According to the results, the obtained p-value is 0.000 which is less than the significance interval (0.05) indicating a significant difference in the field measured tree heights and the CHM derived tree heights. On the other hand, the negative and large T-value (-15.74) confirms the rejection of the null hypothesis.

#### 4.3.2 Field measure tree count vs ALS derived tree count

In this study, a side-by-side comparison was conducted between tree counts obtained using two different methods. Table 9 presents the results of this comparison. Specifically, within Plot 3, the ALS data method was able to accurately derive the tree count, achieving a 100% match with the field measured trees. However, the results were little varied in other plots. In plot 2, the ALS derived count exceeded the field measured tree counts (126.09%), while both plot 1 and plot 4 experienced a slight reduction in the ALS derived tree counts compared to the field measurements. For these two latter plots, the ALS derived accuracy were 90.91% and 93.88% respectively. Overall, there is a 2.09% over estimation of ALS-derived trees compared to filed measured trees.

Table 9. Field measured tree count vs ALS derived tree count for four plots shown in figure 3.

Plot Number	Filed measured trees	ALS derived trees	Percentage %
1	33	30	90.91
2	48	58	126.09
3	61	61	100.00
4	49	46	93.88

#### 4.3.3 Field measured tree species vs predicted species

This comparison is derived from one of the final results of tree prediction conducted through a machine learning process using the MLP model. Through the model autonomously cross-checked the prediction results of both training and testing samples with the respective field-observed species, and validation was performed based on that. Table 10 illustrates the prediction accuracies of the model.

Table 10. Tree family prediction accuracies.

Sample	Observed	Predicted		
		Betulaceae	Pinaceae	Percent Correct
Training	Betulaceae	20	7	74.1%
	Pinaceae	7	80	92.0%
Testing	Betulaceae	8	2	80.0%
	Pinaceae	1	29	96.7%

The training sample consisted of 27 Betulaceae trees and 87 Pinaceae trees. The MLP correctly identified 20 Betulaceae trees but misclassified 7 as Pinaceae. Additionally, 80 Pinaceae trees were accurately predicted, with 7 misclassified as Betulaceae. Consequently, the prediction accuracies for Betulaceae and Pinaceae within the training sample were 74.1% and 92%, respectively.

Moving to the testing sample, which comprised 10 Betulaceae trees and 30 Pinaceae trees, the trained model was applied. The MLP accurately classified 8 Betulaceae trees but erred in predicting 2 Betulaceae trees as Pinaceae. Moreover, 29 Pinaceae trees were correctly identified, with only 1 misclassified as Betulaceae. Therefore, the prediction accuracies for Betulaceae and Pinaceae within the testing sample stood at 80% and 96.7%, respectively.

This examination sheds light on the efficacy of the MLP algorithm in differentiating between Betulaceae and Pinaceae trees, highlighting the precise and systematic approach taken in predicting tree species based on the provided samples.

#### 4.4 i-Tree Eco modelling

In this step, the i-Tree eco model was employed to calculate the reference values (scenario 1) for various ecological services, using the original input parameters without any modifications. It must be noted that, these resulting reference values from the i-Tree Eco also comes with uncertainties. For carbon storage, the relative standard error is 17.7% in urban areas, for carbon sequestration, the relative standard error is 19.9% in urban areas (i-Tree tools, 2006), and the uncertainty in avoided runoff depends on the weather precipitation data (i-Tree Eco user's manual, 2017). While the model provided a wide array of ecological services, our focus was narrowed to three specific ones. These were carefully selected to align with the purpose of the study and are detailed in Table 11. These outputs from the i-Tree Eco model are specific to the time when the field data were measured and the ALS and orthophotos were captured. Results from more recently acquired inputs for the i-Tree Eco can be different. According to the table, the total carbon storage capacity within all four plots was found to be 63.19 tons. This value represents the accumulated carbon within tree biomass, illustrating the integral role of the vegetation in trapping and containing carbon dioxide from the atmosphere. Next, the gross carbon sequestration was obtained as 1.4 tons on an annual basis. Finally, the model estimated an avoided runoff of 71.27 cubic meters per year. These findings provide a quantifiable measure of the ecological services rendered by the study area (four circular plots), underscoring the multifaceted environmental benefits provided by the urban trees. These results may serve as an essential reference for the sensitivity analysis of this study.

Table 11. Ecological services derived via i-Tree Eco modelling.

Ecological service	Amount
Carbon Storage (ton)	63.19
Gross Carbon Sequestration (ton/yr)	1.41
Avoided runoff (m <sup>3</sup> /yr)	71.27

#### 4.5 i-Tree Eco model sensitivity analysis

The last part of the study was the sensitivity analysis. For this purpose, 26 scenarios (Section 3.9, Table 5) were applied to the i-Tree Eco model. The ecological services obtained through those scenarios were cross-checked with the reference values (scenario 1) scenario wise. The comparison is shown in Table 12 below. Here, the differences were obtained by reducing the scenario values from the respective reference values. A positive percentage in the difference means that the value of the scenario is less than the reference, while a negative percentage means the value of the scenario is greater than the reference. Based on Table 12 and Figure 10, the maximum

deviation compared to the reference values can be seen in avoided runoff (more than 81%) for scenarios from XXII to XXVI. A significant deviation can also be observed in gross carbon sequestration and avoided runoff (around 30% and around 20%, respectively) for scenarios from XVII to XXI.

Table 12. Results obtained through sensitivity analysis.

Scenarios from Table 5	Carbon Storage (ton)	Gross Carbon Sequestration (ton/yr)	Avoided runoff (m <sup>3</sup> /yr)
Reference Values (Scenario I)	63.19	1.41	71.27
Scenario II	57.19	1.44	70.65
Difference	6	-0.03	0.62
Percentage %	9.50	-2.13	0.87
Scenario III	54.8	1.48	70.3
Difference	8.39	-0.07	0.97
Percentage %	13.28	-4.96	1.36
Scenario IV	55.27	1.45	70.08
Difference	7.92	-0.04	1.19
Percentage %	12.53	-2.84	1.67
Scenario V	54.22	1.49	70.26
Difference	8.97	-0.08	1.01
Percentage %	14.20	-5.67	1.42
Scenario VI	63.31	1.5	69.97
Difference	-0.12	-0.09	1.3
Percentage %	-0.19	-6.38	1.82
Scenario VII	63.26	1.53	70.02
Difference	-0.07	-0.12	1.25
Percentage %	-0.11	-8.51	1.75
Scenario VIII	63.53	1.55	70.26
Difference	-0.34	-0.14	1.01
Percentage %	-0.54	-9.93	1.42

Scenario IX	63.58	1.62	70.71
Difference	-0.39	-0.21	0.56
Percentage %	-0.62	-14.89	0.79
Scenario X	57.22	1.47	70.39
Difference	5.97	-0.06	0.88
Percentage %	9.45	-4.26	1.23
Scenario XI	54.81	1.52	70.54
Difference	8.38	-0.11	0.73
Percentage %	13.26	-7.80	1.02
Scenario XII	55.5	1.52	70.55
Difference	7.69	-0.11	0.72
Percentage %	12.17	-7.80	1.01
Scenario XIII	54.51	1.59	71.23
Difference	8.68	-0.18	0.04
Percentage %	13.74	-12.77	0.06
Scenario XIV	67.74	1.73	69.84
Difference	-4.55	-0.32	1.43
Percentage %	-7.20	-22.70	2.01
Scenario XV	70.16	1.81	70.76
Difference	-6.97	-0.4	0.51
Percentage %	-11.03	-28.37	0.72
Scenario XVI	73.31	1.79	70.89
Difference	-10.12	-0.38	0.38
Percentage %	-16.02	-26.95	0.53
Scenario XVII	62.82	1.97	107.29
Difference	0.37	-0.56	-36.02
Percentage %	0.59	-39.72	-50.54
Scenario XVIII	62.88	2.2	107.83
Difference	0.31	-0.79	-36.56
Percentage %	0.49	-56.03	-51.30

Scenario XIX	62.76	2.21	108.05
Difference	0.43	-0.80	-36.78
Percentage %	0.68	-56.74	-51.61
Scenario XX	62.69	2.22	107.95
Difference	0.5	-0.81	-36.68
Percentage %	0.79	-57.45	-51.47
Scenario XXI	62.74	2.28	107.88
Difference	0.45	-0.87	-36.61
Percentage %	0.71	-61.70	-51.37
Scenario XXII	64.04	1.5	129.43
Difference	-0.85	-0.09	-58.16
Percentage %	-1.35	-6.38	-81.61
Scenario XXIII	63.98	1.53	129.49
Difference	-0.79	-0.12	-58.22
Percentage %	-1.25	-8.51	-81.69
Scenario XXIV	64.25	1.55	129.54
Difference	-1.06	-0.14	-58.27
Percentage %	-1.68	-9.93	-81.76
Scenario XXV	64.29	1.62	129.55
Difference	-1.1	-0.21	-58.28
Percentage %	-1.74	-14.89	-81.77
Scenario XXVI	63.92	1.41	129.46
Difference	-0.73	0	-58.19
Percentage %	-1.16	0.00	-81.65
Scenario XXVII	59.53	1.72	65.16
Difference	3.66	-0.31	6.11
Percentage %	5.79	-21.99	8.57

Furthermore, Figure 10 provides a graphical representation of the changes across different scenarios, displaying the percentage variations in comparison of their respective reference values. This visualization offers an overview of the relative shifts in values and helps to identify the most suitable scenarios.

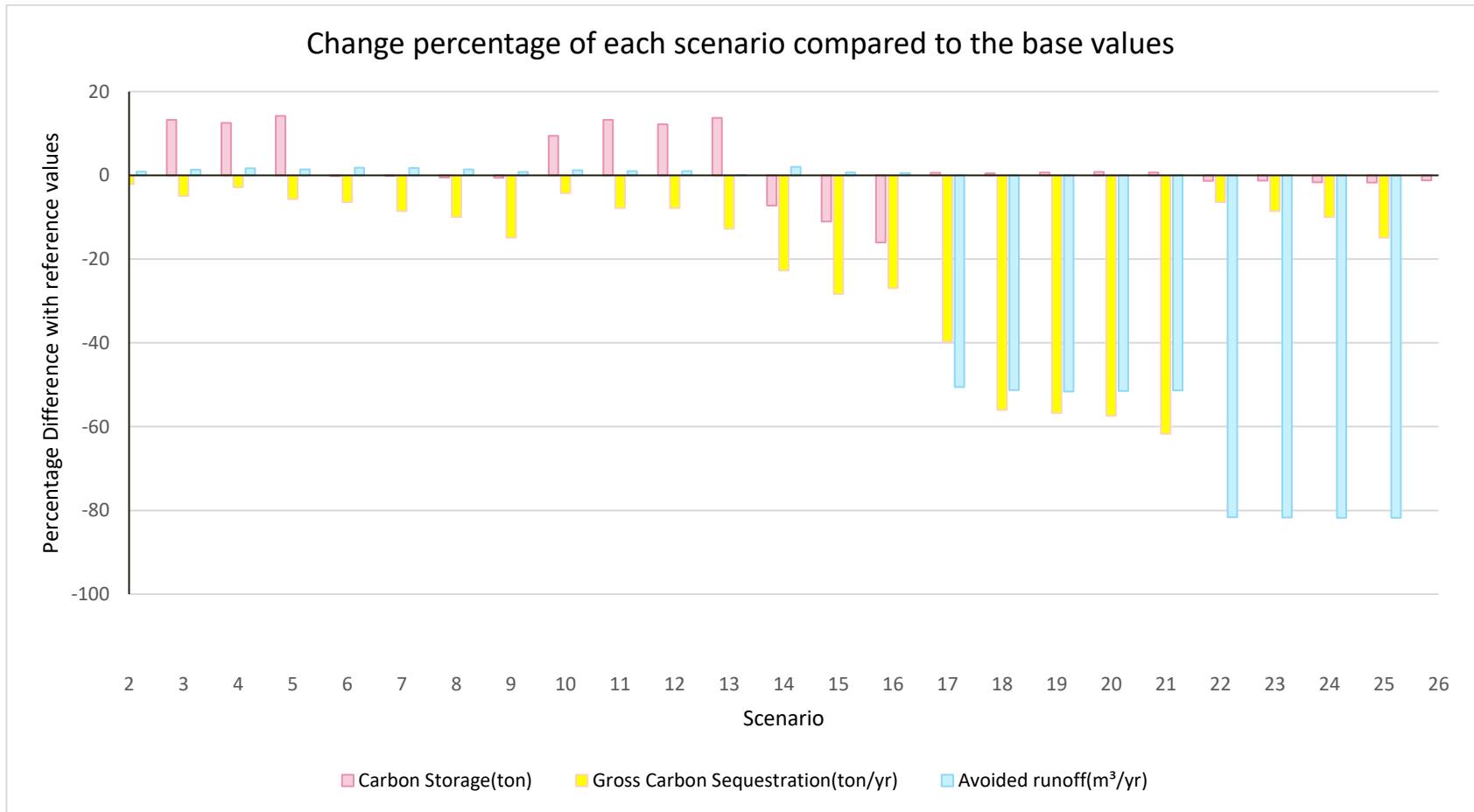


Figure 10. Visualization of the percentage difference with the reference values in each scenario.

## 5 Discussion

### 5.1 Field work

Using GNSS equipment can always be challenging under tree canopies due to multiple bounces of the satellite signals. In the field work phase of this study, control point establishment for plot centres was successfully conducted and the orientation of the total station was possible to achieve the required 3D accuracy. After completing the measurements in each plot, a backsight was measured again to ensure that the accuracy was preserved. Consistent results were observed in all four plots, with the coordinates remaining unchanged from the start of the survey.

In total 192 trees were measured in the field and the most common species were *Betula pendula* Roth (29 trees), *Pinus resinosa* Aiton (25 trees), *Pinus sylvestris* L. (24 trees), and *Pinus ponderosa* Douglas ex C. Lawson (23 trees), where other species count were less than 12 trees. The species in this study were identified using photographs collected in the field, analyzed through the Pl@ntNet app. Therefore, the accuracy of species detection is inherently tied to the strength and comprehensiveness of this app's existing database. This reliance on technology introduces the possibility of incorrect identification of species, as the app's accuracy may vary based on its available data for northern European tree species. While the ideal approach would have been to seek the expertise of a botanist specialized in the identification of northern European tree species, such an expert was unfortunately not available at the time of the study. Therefore, it is important to recognize the potential limitations in species identification resulting from this reliance on the Pl@ntNet app. Future studies in this area may benefit from collaboration with botanical experts to ensure more accurate and reliable identification.

When measuring tree locations, the prism was held at the closest point to the total station touching the tree bark. This is not the exact location of the tree. One suggestion could be to add a correction by adding the radius of the tree bark assuming that it is taking a circular shape.

One specific challenge was the use of the non-prism measurement option for measuring tree heights with an uncertainty of a 2 mm + 2 ppm. The dynamic movement of treetops, due to wind, made it exceptionally difficult to accurately measure their top. A more convenient and perhaps accurate method would have involved measuring the angle to the treetop using the total station, then applying simple trigonometry to calculate the tree height. This approach would leverage the known coordinates of the tree bottom and the instrument station, potentially offering a more stable and precise measurement.

## 5.2 Individual tree crown delineation and tree detection

When performing watershed delineation, noise in the CHM can create spurious peaks or valleys that interfere with the delineation process, leading to over-segmentation or misidentification of tree centers. In this study, the main reason for applying Gaussian and median filters to the CHM prior to the delineation is to help prevent the algorithm from detecting false peaks. To prevent from over or under segmentation of trees, the algorithm was run several times for the same CHM to tune the threshold values of the algorithm.

In Figure 5 (CHM), though the minimum value of the raster should be zero, it goes down to -0.41 m. For ideal conditions, the difference between the raster datasets created from the first and last returns of the ALS data should represent the canopy height, with the first return representing the top of the canopy and the last return representing the ground surface. However, negative values can occur in practice due to several potential reasons such as noise and outliers, multiple returns within the canopy before reaching the ground, which can lead to incorrect identification of true ground return, ground surface complexity such as when the ground is highly undulated or covered with understory vegetation, data processing errors such as filtering or classification, instrument calibration errors, etc. (Duan et al., 2015; Douss and Farah, 2010).

Smoothing the CHM may result in the disappearance of small crowns in proximity to larger crowns. Therefore, utilizing an adaptive or localized filter (Lisiewicz et al., 2022) could be a more suitable approach. A better approach would have been to use an adaptive filter (Jaafar et al., 2018) as adaptive filters can adjust to variable canopy structures, preserve edge information by adjusting to the local variance of the data, handling data gaps locally etc.

When working with raster data for canopy height model delineation, the edge effect is a common problem, which can be clearly seen in Figure 8(a). Due to abrupt cropping, the canopy shape looks quite unnatural in Figure 8(b). At the boundaries of the study area are where the ALS dataset was cut off. Due to inconsistencies and artificial edges, artifacts were generated in the CHM. Also, at the boundaries, some tree crowns were cut through the middle. Hence, the resulting CHM contains only portions of those tree crowns which may contribute to misinterpretation of tree heights and locations. A solution to this issue could have been the extension of the CHM delineation area beyond the boundaries of the actual study area by a certain buffer distance. The analysis can then be performed within this extended area, and thereafter, the results can be clipped based on the original study area (Picos et al., 2020). This can help alleviate boundary artifacts and ensure that the trees on the edges are fully captured. Furthermore, the results from the CHM delineated canopies could

have been validated with auxiliary data such as high-resolution imagery or field data. But in this study, the tree dimensions were not measured in the field.

When the trees are clustered very close to each other the watershed delineation technique tends to merge the tree canopies as a single canopy, though in reality multiple treetops exist. This is also true for multiple crowns, which may be delineated though only a single tree exists. This mainly happened in this study for deciduous trees as there are multiple local maxima. As a solution to these issues, post-processing techniques can be applied to merge or split delineated areas based on size, shape, or other characteristics (Wang et al., 2011). Using ancillary data, such as spectral or textural information, might also aid in resolving complex canopy structures (OZDARICI-OK and OK, 2023). The understory canopy cannot be delineated using this technique unless the ALS point cloud is sliced, and individual voxels are assessed.

### **5.3 Extraction of dendrometric parameters**

#### **5.3.1 Tree heights**

When compared to the field measured tree heights, the ALS derived tree heights have considerable differences. The results given by the scatter plot (see Figure 9) and the paired T-test done between the field measured tree heights and the ALS derived tree heights also confirmed this difference. The major reason for this difference is due to the technical error made in the fieldwork which was described in section 5.1. Besides, there can be several other reasons for this issue such as accuracy of measurements, tree structure and leaf density, ground surface errors, and differences in measurement protocols. This last reason can be due to how field measurements define tree height, which is the vertical distance to the highest live branch, whereas ALS might measure to the highest point regardless of whether it is a live branch or not.

When extracting tree heights from the delineated crowns (in the case of field measured tree locations and ALS data derived trees), there can always be a deviation, as seeds from watershed delineation technique are based on local maximum points of the CHM whilst in field measurements the tree trunk location is measured. One of the reasons, for applying smoothing and filtering to the CHM before identifying the maximum point is to reduce the effect of noise and the insufficient resolution in the CHM that can cause the maximum height point to be misplaced, especially if the difference in height within the crown is subtle (ALS point density was 0.5-1.0 point/m<sup>2</sup>). In practice, some tree crowns have multiple peaks and branches that reach similar heights, leading to ambiguity in defining the maximum height point. Inaccuracies in the delineated crowns due to over or under segmentation can lead to the effect that the maximum height point within the delineated area may not correspond to the true center of the tree crown.

### 5.3.2 DBH estimation

When attempting to estimate DBH directly from ALS data, there were some challenges due to the low point density of the data. This is a common obstacle in the field, given the limitations in the resolution of ALS data, particularly in environments characterized by dense forest cover. In an effort to overcome this issue, the focus was turned to allometric linear regression models with the aim of establishing relationships between different dendrometric parameters on a species-specific level. Unfortunately, this approach failed to yield substantial correlations. Addressing this lack of species-level correlations, an alternative strategy was introduced, i.e. to consider the dendrometric parameters at the level of tree families. Here, the parameters were averaged by family, and subsequently, a relationship between DBH and CM derived tree heights can be uncovered. It is important to note that relationships derived in this way are likely to be more consistent within a tree family than between distinct species. However, such relationships may be specific to the particular ecological conditions and tree species under scrutiny.

The subsequent statistics from the scatter plot provided confidence in this family-based model. With an R-squared value of 71.3%, it can be inferred that the model can explain over 70% of the variability in DBH, based on the CHM derived tree height. The closely related adjusted R-squared value, at 68.5%, validates this finding and affirms the validity of tree height as a useful predictor within our model. The standard error of estimate, captured by an S value of 6.3686, indicates that the model's predicted DBH values deviated from the actual values by this amount on average. Whilst these statistics suggest that the model is robust, it is better to exercise caution when interpreting these results. Given that the model is based on averaged values grouped by tree families, it may not yield equally accurate predictions for individual trees.

Moreover, inaccuracies inherent to the ALS derived tree heights could introduce further errors in the DBH estimates. A drawback of using linear regression allometric equations to predict the DBH is that trees with heights outside the range of the values to generate the model must be excluded. The reason is the predictions are limited to interpolation and cannot extrapolate beyond the available data range (Bruce and Bruce, 2017).

### 5.3.3 CLE calculation

The calculation of CLE was based on two significant contributing factors: the individual tree height and the distance to the nearest neighboring tree. In order to make these measures commensurable and to provide a consistent base for analysis, a linear normalization technique was adopted to stretch both values between 1 and 100. This method has certain advantages: it is relatively straightforward, and it aligns well

with the understanding that both tree height and proximity to neighboring trees can impact a tree's access to sunlight, a primary determinant of CLE. However, by linearly stretching both factors, we assume that their impacts on light exposure are equivalent and linearly related. In nature, this may not be the case. On the other hand, due to the sparse nature of the ALS point cloud, errors can occur in this approximation. Specifically, the third return may or may not have hit the bottom-most branch of a particular tree, leading to potential inaccuracies in the data interpretation. The method used to derive the CLE in this study was not validated since no ground truth data was collected regarding the CLE.

#### **5.3.4 CBH calculation**

In this study, the third return was utilized to calculate the height to the canopy base, or the Crown Base Height (CBH). This choice was determined due to a couple of key considerations. Firstly, the selection of the third return helped avoid the issue of negative values encountered when using the second return, which is crucial to ensure the validity of the data for subsequent analysis.

Secondly, the choice of the third return over later returns (like the 4th, 5th, and 6th) was likely based on the trade-off between capturing the desired information and maintaining a sufficient point density. As the return number increases, the point density tends to decrease, since not all laser pulses will have that many interactions before reaching the ground. In forested areas, the third return often provides a reasonable balance by representing points beneath the top of the canopy but not so low that the point density becomes too sparse for reliable analysis (Popescu et al., 2011; Sumnall et al., 2012). Hence the third return was used for the CBH derivation.

Additionally, later returns might increasingly represent the understory vegetation or ground surface rather than the main tree canopy, which could potentially introduce more inaccuracies into the derived CBH. Lastly, considering the insufficiency of the ALS point cloud density for voxel-based methods, using the third return for the DEM generation is a practical choice that allows for a reasonable approximation of the CBH. However, there were no field measured data that were gathered that can validate the CBH derived using the method applied in this study.

### **5.4 Species identification**

The approach employed for species prediction using MLP neural networks incorporated multiple aspects of tree information, derived from both field collected and ALS data. A range of variables, including tree height, DBH, CBH, crown area, and NDVI, provided a comprehensive set of inputs to predict tree species. It was found out that only by predicting the family can the results be acceptable. For this study, only two families were predicted by the model, which is Betulacea and

Pinaceas. Hence, the data were trained again by using only these two families, with the assumption that the study area consists only of these two. A major reason for this is the training samples being too small as in most cases at least 5000 samples must be taken in each tree species for an artificial neural network to provide reliable results (Walde et al., 2004). In this study, only 154 tree samples were used.

When using NDVI as an input, there can be several potential challenges such as saturation where NDVI values become saturated in areas with high vegetation density, lighting, and atmospheric conditions such as sunlight angle, cloud cover, and atmospheric particles. At this stage, since the locations of the treetops were already determined negative NDVI values were not removed but were taken to support the decision as negative values also existed on the locations of field measured trees as well. This is due to the poor quality of the orthophoto as it was clearly visible to the naked eye that a section of the orthophoto was too brownish, and the branches of trees were visible. This can be because of merging two datasets acquired in two seasons or non-green vegetation such as dead trees and branches that can affect the accuracy of the NDVI values. The orthophoto used in this study was taken in late spring. Hence some of the deciduous trees may not have started to regain their leaves. Suggestions to avoid these drawbacks could have been to use an enhanced vegetation index, integrating other spectral indices or other types that can differentiate non-green vegetation.

The MLP model was trained on a sizable portion of the data (74%), which is a good practice as it allows the model to learn from many examples and better generalize its prediction capability to unseen data. But it only left 26% for testing. While this might have helped achieve a lower error rate, it could also potentially lead to overfitting, where the model is too finely tuned to the training data and may perform poorly on unseen data. According to López et al. (2022), a more balanced train-test split or employing cross-validation techniques, which rotate the dataset used for training and testing, could be used to address this issue.

However, the model demonstrated relatively high accuracy, with only 12.3% incorrect predictions for the training set and an even better performance on the testing set with 7.5% incorrect predictions. The neural network used here is comprised of an input layer, one hidden layer, and an output layer. The choice of a hyperbolic tangent activation function in the hidden layer is suitable for its range of outputs (-1 to 1), which can lead to more efficient learning during backpropagation. Additionally, the softmax function in the output layer is an excellent choice for multi-class classification problems (Alzubaidi et al., 2021), which is the case here with tree family prediction.

The use of cross-entropy error as the metric for model performance is appropriate for classification tasks. Lower cross-entropy values indicate that the model's predicted

probabilities are closer to the true class labels, hence better performance. The cross-entropy error values for the training and testing sets were quite low (34.186% and 7.795%, respectively), further indicating the model's robust performance.

According to the estimated importance of each predictor variable on the model's output, CBH emerged as the most critical variable, contributing 100%. Other significant contributors were NDVI (51.2%), Crown area (55.7%), CHM derived tree heights (44.4%), and DBH (39.2%). This information is vital, not only for interpreting our model's decision-making but also for guiding future research through feature selection.

Lastly, the model may not work well in other regions with different climates, soil types, or tree species. The model is, in essence, a product of the environment from which the data was gathered. This could be improved by training the model on data collected from different geographic regions, environments, and tree species.

## **5.5 i-Tree Eco model sensitivity testing with field acquired and remotely sensed data estimated inputs**

According to analysis presented in Table 12 and Figure 10, scenarios II to V show a relatively higher percentage of change in carbon storage compared to the reference values, but the change remains within 15%. Similarly, scenario VI to IX indicates the highest change percentage in gross carbon sequestration, but it does not exceed 15% change as well. Moving on to scenarios X to XIII, the most significant change is observed in carbon storage, reaching 13.74%, while the smallest change is in avoided runoff, which shows 0.06% variation at the family level. Further, scenarios XIV to XVI demonstrate that gross carbon sequestration exhibits the highest percentage of change, amounting to 28.37. This is nearly twice the values obtained with average DBH scenarios, suggesting that the i-Tree eco model is more sensitive to species rather than DBH.

In the i-Tree eco model, there is an option to provide inputs with fewer inputs and let the model estimate the other parameters such as canopy dimensions and CBH. In scenarios XVII to XXI gross carbon sequestration and avoided runoff indicate deviations around 55% from the reference values. For scenarios XXII to XXVI, the highest errors are found in avoided runoff, indicating approximately 81% difference, emphasizing the importance of providing accurate tree structure parameters as inputs rather than letting the model estimate them. This is because the avoided runoff is influenced by how much water is intercepted by the tree's canopy and transpiration which is directly related to canopy dimensions and CLE. However, the change percentages in carbon storage and gross carbon sequestration remain relatively small and do not exceed 15%. This is due to both carbon storage and gross carbon

sequestration primarily depending on the amount of biomass present in the tree. The amount of biomass present in the tree is mostly governed by the diameter at breast height (DBH) and species of the tree. The DBH and species of a tree can be good predictors of its age and, thus, its carbon content. Given this, the model may still produce reasonably accurate predictions for carbon metrics even with few inputs, as long as the DBH and species information are available.

In scenario XXVII, gross carbon sequestration shows the highest relative change percentage of 21.99%, while carbon storage and avoided runoff have a change of 5.79% and 8.57%, respectively. These findings demonstrate the suitability of the methodology employed. Importantly, there is no specific threshold to determine whether a change above a certain percentage is favorable or unfavorable, as the appropriateness of the model's performance depends on the nature of the project and its specific requirements.

## **5.6 Future aspects**

In reflecting on this research, several areas for future exploration and improvements can be illustrated. A fundamental area requiring further examination involves the collection of ground truth data for canopy characteristics, such as crown length and width, as well as the CBH. The reliability of artificial neural network predictions could be enhanced by enlarging the ground truth data sample size (Sumayli, 2022). This study highlighted the limitation of small sample sizes for species prediction and DBH estimation via allometric equations, marking the need for a more substantial dataset.

Additionally, this research overlooked a critical parameter: the age of the trees, which could be included in future studies. The tree age could potentially offer a more nuanced understanding of urban forests and the ecological services they provide (Jonsson et al., 2020). Furthermore, carbon estimation in this study was confined to above-ground elements, leaving room for below-ground carbon estimation to provide a more comprehensive picture (Kho and Jepsen, 2015). In terms of spatial considerations, the study did not address understory vegetation, which is another component that future research could explore.

Multiple tree crown delineation techniques could be tested beyond watershed segmentation, such as seeded region growing, valley-following, edge detection, morphological reconstruction, and template matching methods. These alternative methods could offer valuable insights depending on the specific conditions of the terrain and tree canopy. As for the available ALS point cloud, it was quite sparse in this study. It is recommended to use a personal drone to collect data to match with a good resolution. According to Yoshii et al. (2022), other data collection methods like

full waveform and photon counting techniques could enhance the quality of remote sensing data in future studies.

Future research should also consider integrating additional vegetation indices like ratio vegetation index (RVI), green chlorophyll index (cIgreen), and enhanced vegetation index (EVI) into the species prediction process alongside MLP ANN (Glenn et al., 2008). Moreover, the exploration of alternative machine learning models, such as convolution neural networks (CNN), support vector machine, random forest, and gradient boosting machines, may yield improved species determination outcomes.

## 6 Conclusions

Urban trees offer significant benefits to the urban environment, providing a suite of services often referred to as ecological services. Quantifying these services is crucial, providing valuable insights for urban planning and environmental conservation efforts. However, this process typically requires substantial field work, which can be time-consuming and resource intensive.

In response to this challenge, this study has explored the potential of remotely sensed data such as ALS and RGB-NIR orthophotos as a viable alternative source of dendrometric parameters and species identification for urban trees in Sweden. It has made significant strides towards addressing three primary research questions concerning the feasibility of replacing field-gathers inputs for the i-Tree Eco model with remotely sensed data in Sweden, extraction techniques for these inputs, and the implications of averaging the i-Tree Eco model's outputs to various taxonomy levels. The key findings will be described in the following paragraphs.

In assessing the viability of replacing field-gathered dendrometric parameters and species data for the i-Tree Eco model with remotely sensed data, this research demonstrated that such an approach is indeed feasible. The parameters for tree location, diameter at breast height (DBH), canopy base height (CBH), crown light exposure (CLE), and species, up to the family taxonomy level, can be extracted from readily available airborne laser scanning (ALS) and orthophoto data provided by Lantmäteriet. The DBH estimation, derived from field-collected data, showed a promising performance with an R-squared value of 71.3% up to the family taxonomy level. In addition, the species prediction using orthophotos also achieved commendable results, with an overall correct identification of 87.7% during the training phase and 92.5% during the testing phase, again at the family taxonomy level. These results underscore the potential for remote sensing data to effectively contribute to the determination of species and dendrometric parameters in the Swedish urban tree landscape.

Nevertheless, we also encountered challenges and limitations. The correlation between field-measured tree heights and ALS-derived tree heights was weaker than anticipated, underscoring the need for caution when substituting field measurements with remotely sensed data. The Multilayer Perceptron (MLP) model used for tree species prediction demonstrated a certain level of misclassification, highlighting the need for continued refinement and exploration of machine learning models for this application.

Diving deep into the i-Tree Eco model's adaptability to inputs, it was revealed that while integrating ALS-derived inputs and averaging them to different taxonomy ranks

is plausible, there's variability in accuracy. A significant observation was that predictions at the family level emerged as the most reliable. However, when the model was entrusted with estimating tree structure parameters based solely on species and DBH, there were marked deviations, especially in services like carbon storage, gross carbon sequestration, and avoided runoff.

In conclusion, while this study has laid a potential for the use of remotely sensed data in urban tree management, future research is needed to refine these methodologies and expand our findings. This work could include improving the methods used to derive dendrometric parameters from remotely sensed data and enhancing the machine learning models for tree species prediction. Ultimately, the goal is to develop more effective and scalable practices for managing urban forestry and its ecological services to enrich our urban environments avoiding time-consuming and expensive practices.

## References

- August, T. A., Pescott, O. L., Joly, A., & Bonnet, P. (2020). AI Naturalists Might Hold the Key to Unlocking Biodiversity Data in Social Media Imagery. *Patterns*, 1(7), 100116. Doi: <https://doi.org/10.1016/j.patter.2020.100116>
- Alzubaidi, L., Zhang, J., Humaidi, A. J., Al-Dujaili, A., Duan, Y., Al-Shamma, O., Santamaría, J., Fadhe, I. M. A., Al-Amidie, M., & Farhan L. (2021). Review of deep learning: concepts, CNN architectures, challenges, applications, future directions. *Journal of Big Data*, 8(1), 53. Doi:10.1186/s40537-021-00444-8
- Billenberg, M. (2023). Investigation of above-ground biomass with terrestrial laser: A case study of Valls Hage in Gävle. Retrieved from <https://hig.diva-portal.org/smash/get/diva2:1768636/FULLTEXT02.pdf>
- Birdsey, R. A. (1992). Carbon storage and accumulation in United States forest ecosystems. General Technology Report WO-GTR-59, Northeastern Forest Experiment Station, Forest Service, US Department of Agriculture.
- Bodhwani, V., Acharjya, D. P., & Bodhwani, U. (2019). Deep residual networks for plant identification. *Procedia Computer Science*, 152, 186–194. Doi: <https://doi.org/10.1016/j.procs.2019.05.042>
- Bodnaruk, E. W., Kroll, C. N., Yang, Y., Hirabayashi, S., & Nowak, D. J. (2020). Assessing the ecosystem services of various types of urban green spaces based on i-Tree Eco. *Sustainability*, 12(4), 1630.
- Bruce, P., & Bruce, A. (2017). *Practical statistics for data scientists*. Reilly Media, Inc.
- Cabo, C., Ordóñez, C., López-Sánchez, C. A., & Armesto, J. (2018). Automatic dendrometry: Tree detection, tree height and diameter estimation using terrestrial laser scanning. *International Journal of Applied Earth Observation and Geoinformation*, 69, 164–174. Doi: <https://doi.org/10.1016/j.jag.2018.01.011>
- Cetin, Z., & Yastikli, N. (2022). The use of machine learning algorithms in urban tree species classification. *ISPRS International Journal of Geo-Information*, 11(4), 226. Doi: <https://doi.org/10.3390/ijgi11040226>
- Chameides, W.L., Lindsay, R.W. Richardson, J., & Kiang, C.S. (1988). The role of biogenic hydrocarbons in urban photochemical smog: Atlanta as a case study. *Science*, 241, 1473.
- Chen, J. M., Rich, P. M., Gower, S. T., Norman, J. M., & Plummer, S. (1997). Leaf area index of boreal forests: Theory, techniques, and measurements. *Journal of Geophysical Research: Atmospheres*, 102(D24), 29429–29443. Doi:10.1029/97jd01107
- Chen, Q., Baldocchi, D., Gong, P., Kelly, M. (2006). Isolating individual trees in savanna woodland using small footprint Lidar data. *Photogrammetric Engineering and Remote Sensing*, 72 (8), 923–932.

- Chen, J., Chen, Y., & Liu, Z. (2021). Classification of typical tree species in laser point cloud based on deep learning. *Remote Sensing*, 13(23), 4750. Doi: <https://doi.org/10.3390/rs13234750>
- Chojnacky, D.C., Jenkins, J. (2010). Literature Synthesis and Meta-analysis of Tree and Shrub Biomass Equations in North America. Final Report: JFSP Project Number 07-3-1-05. Virginia Polytechnic Institute & State University: 23.
- Cimburowa, Z., & Barton, D. N. (2020). The potential of geospatial analysis and Bayesian networks to enable I-tree eco assessment of existing tree inventories. *Urban Forestry & Urban Greening*, 55, 126801. Doi: 10.1016/j.ufug.2020.126801
- Corrao, M. V., Sparks, A. M., & Smith, A. M. S. (2022). A conventional cruise and felled-tree validation of individual tree diameter, height and volume derived from airborne laser scanning data of a loblolly pine (*P. taeda*) stand in Eastern Texas. *Remote Sensing*, 14(11), 2567. Doi:<https://doi.org/10.3390/rs14112567>
- Corte, A. P. D., Rex, F. E., de Almeida, D. R. A., Sanquetta, C. R., Silva, C. A., Moura, M. M., & Broadbent, E. N. (2020). Measuring individual tree diameter and height using gatereye high-density UAV-lidar in an integrated crop-livestock-forest system. *Remote Sensing*, 12(5). Doi: <https://doi.org/10.3390/rs12050863>
- Cristea, C., & Jocea, A. F. (2015). Applications of terrestrial laser scanning and GIS in forest inventory. *Journal of Applied Engineering Sciences*, 5(2), 13–20. Doi:10.1515/jaes-2015-0016
- Das, N. (2014). Modeling develops to Estimate leaf area and Leaf biomass Of *Lagerstroemia speciosa* in West vanugach Reserve Forest of Bangladesh. *ISRN Forestry*, 1–9. Doi:10.1155/2014/486478
- Davies, H., Doick, K., Handley, P., O'Brien, L., & Wilson, J. (2017). Delivery of ecosystem services by urban forests, forestry commission research report, forestry commission. *Edinburgh*, 4, 1–28. Retrieved from <https://cdn.forestresearch.gov.uk/2017/02/fcrp026.pdf>.
- Degericks, J., Roberts, D., McFadden, J., Hermy, M., & Somers, B. (2018). Urban tree health assessment using airborne hyperspectral and lidar imagery. *International Journal of Applied Earth Observation and Geoinformation*, 73, 26–38. Doi: 10.1016/j.jag.2018.05.021
- De Petris, S., Sarvia, F., & Borgogno-Mondino, E. (2020). Rpas-based photogrammetry to support tree stability assessment: Longing for precision arboriculture. *Urban Forestry & Urban Greening*, 55, 126862. Doi: 10.1016/j.ufug.2020.126862
- Dobbs, C., Kendal, D., and Nitschke, C.R. (2014). Multiple ecosystem services and disservices of the urban forest establishing their connections with landscape structure and sociodemographic. *Ecological Indicators*, 43, 44–55.

- Doick, K., Davies, H., Handley, P., Vaz Monteiro, M., O'Brien, L., & Ashwood, F. (2016). *Introducing England's Urban Forests*.
- Douss, R., & Farah, I.R. (2010). Extraction of individual trees based on canopy height model to monitor the state of the forest. *Trees, Forest and People*, 8, 100257. Doi: <https://doi.org/10.1016/j.tfp.2022.100257>
- Duan, Z., Zhao, D., Zeng, Y., Zhao, Y., Wu, B., & Zhu, J. (2015). Assessing and correcting topographic effects on forest canopy height retrieval using airborne LiDAR data. *Sensors (Basel)*, 15(6), 12133–12155. Doi: <https://doi.org/10.3390/s150612133>
- ESRI. (2011). ArcGIS Desktop: Release 10. Redlands, CA: Environmental Systems Research Institute.
- Fan, J., Zeng, G., Body, M., & Hacid, M. S. (2005). Seeded region growing: an extensive and comparative study. *Pattern Recognition Letters*, 26(8), 1139–1156. Doi: <https://doi.org/10.1016/j.patrec.2004.10.010>
- Fonseca, W., Alice, F. E., & Rey-Benayas, J. M. (2011). Carbon accumulation in aboveground and belowground biomass and soil of different age native forest plantations in the humid tropical lowlands of Costa Rica. *New Forests*, 43(2), 197–211. Doi: <https://doi.org/10.1007/s11056-011-9273-9>
- Glenn, E. P., Huete, A. R., Nagler, P. L., & Nelson, S. G. (2008). Relationship between remotely-sensed vegetation indices, canopy attributes and plant physiological processes: What vegetation indices can and cannot tell us about the landscape. *Sensors*, 8(4), 2136–2160. Doi: <https://doi.org/10.3390/s8042136>
- Goldbergs, G., Maier, S., Levick, S., & Edwards, A. (2018). Efficiency of individual Tree detection approaches based on lightweight and low-cost Uas imagery in Australian Savannas. *Remote Sensing*, 10(2), 161. Doi: [10.3390/rs10020161](https://doi.org/10.3390/rs10020161)
- Goodwin, N. R., & Coops, N. C. (2016). Assessment of sub-canopy structure in a complex coastal temperate rainforest using airborne laser scanning. *Remote Sensing*, 8(7), 558.
- Gougeon, F. A. (1995). A crown-following approach to the automatic delineation of individual tree crowns in high spatial resolution aerial images. *Canadian Journal of Remote Sensing*, 21(3), 274–284. Doi: <http://dx.doi.org/10.1080/07038992.1995.10874622>
- Gschwantner, T., Schadauer, K., Vidal, C., Lanz, A., Tomppo, E., Di Cosmo, L., Lawrence, M. (2009). Common tree definitions for national forest inventories in Europe. *Silva Fennica*, 43(2). Doi: [10.14214/sf.463](https://doi.org/10.14214/sf.463)
- Gunnarsson, A., & Lorentzon, K. (2017). Vård och utvecklingsplan för arboretet Valls Hage i Gävle Institutionen för Landskapsarkitektur, planering och förvaltning i samarbete med Samhällsbyggnad Gävle Sveriges lantbruksuniversitet Fakulteten för landskapsarkitektur, trädgårds-ochväxtproduktionsvetenskap.

- Guo, Q., Zhang, J., Guo, S., Ye, Z., Deng, H., Hou, X., & Zhang, H. (2022). Urban tree classification based on object-oriented approach and random forest algorithm using unmanned aerial vehicle (UAV) multispectral imagery. *Remote Sensing*, 14(16), 3885. Doi: <https://doi.org/10.3390/rs14163885>
- Guo, X., Li, H., Jing, L., & Wang, P. (2022). Individual tree species classification based on convolutional neural networks and multitemporal high-resolution remote sensing images. *Sensors*, 22(9), 3157, Doi: <https://doi.org/10.3390/s22093157>
- Hanapi, S. N. H. S., Shukor, S. A. A., & Johari, J. (2019). A review on remote sensing-based method for tree detection and delineation. *Man Machine Systems*, 705, 012024. Doi: 10.1088/1757-899X/705/1/012024
- Hangarge, L. M., Kulkarni, D. K., Gaikwad, V. B., Mahajan, D. M., & Chaudhari, N. (2012). Carbon Sequestration potential of tree species in Somjaichirai (Sacred grove) at Nandghur village, in Bhor region of Pune District, Maharashtra State, India. *Annals of Biological Research*, 7, 3426–3429.
- Hayes A. 2022. Systematic Sampling: What Is It, and How Is It Used in Research? Retrieved from <https://www.investopedia.com/terms/s/systematic-sampling.asp>
- Hirabayashi, S. (2013). I-Tree Eco Precipitation Interception Model Descriptions. HMK, (2021), Swedish handbook in surveying and mapping, HMK– Geodetisk infrastruktur 2021. Retrieved from <https://www.lantmateriet.se/hmk>
- Holmgren, J., & Persson, Å. (2004). Identifying species of individual trees using airborne laser scanner. *Remote Sensing of Environment*, 90(4), 415–423. Doi:10.1016/s0034-4257(03)00140-8
- Hu, B., Li, J., Jing, L., & Judah, A. (2014). Improving the efficiency and accuracy of individual tree crown delineation from high-density LiDAR data. *International Journal of Applied Earth Observation and Geoinformation*, 26, 145–155. Doi:<https://doi.org/10.1016/j.jag.2013.06.003>
- IBM Corp. (2021). IBM SPSS Statistics for Windows, Version 28.0. Armonk, NY: IBM Corp.
- i-Tree tools. (2006). i-Tree landscape methods, limitations, and uncertainties. Retrieved from [https://www.itreetools.org/documents/115/Landscape\\_Methods.pdf](https://www.itreetools.org/documents/115/Landscape_Methods.pdf)
- i-Tree Eco user's manual, (2017). Retrieved from [https://www.rrds.ca/sites/default/files/documents/Ecov6\\_UsersManual.pdf](https://www.rrds.ca/sites/default/files/documents/Ecov6_UsersManual.pdf)
- Jaafar W. S. W., Woodhouse, I.H., Silva, C. A., Omar, H., Maulud, K. N. A., Hudak, A.T., Klauberg, C., Cardil, A., & Mohan, M. (2018). Improving individual tree crown delineation and attributes estimation of tropical forests

using airborne LiDAR data. *Forests*, 9(12), 759. Doi:  
<https://doi.org/10.3390/f9120759>

- Jacobsson, M. (2012). Förstudie för byte till SWEREF 99 vid Forsmarks kärnkraftverk (Dissertation). Retrieved from  
<http://urn.kb.se/resolve?urn=urn:nbn:se:hig:diva-14277>.
- Jahan, I., Ahmed, M. F., Ali, m. O., & Jang, Y. M. (2023). Self-gated rectified linear unit for performance improvement of deep neural networks. *ICT Express*, 9 (3), 320–325, Doi: <https://doi.org/10.1016/j.ict.2021.12.012>.
- Jarabo-Amores, M.P., la Mata-Moya, D.d., Gil-Pita, R. & Rosa-Zurera, M. (2013). Radar detection with the Neyman–Pearson criterion using supervised-learning-machines trained with the cross-entropy error. *EURASIP Journal on Advances in Signal Processing*, 44. Doi:<https://doi.org/10.1186/1687-6180-2013-44>
- Jarron, L. R., Coops, N. C., MacKenzie, W. H., Tompalski, P., & Dykstra, P. (2020). Detection of sub-canopy forest structure using airborne lidar. *Remote Sensing of Environment*, 244, 111770. Doi: 10.1016/j.rse.2020.111770
- Jaskierniak, D., Lucieer, A., Kuczera, G., Turner, D., Lane, P., Benyon, R., & Haydon, S. (2021). Individual tree detection and CROWN delineation from unmanned aircraft System (UAS) lidar in structurally complex mixed species eucalypt forests. *ISPRS Journal of Photogrammetry and Remote Sensing*, 171, 171–187. Doi: 10.1016/j.isprsjprs.2020.10.016
- Jenkins, J. C., Chojnacky, D.C., Heath, L. S., Birdsey, R. A. (2003). National-scale biomass estimators for United States tree species. *Forest Science*, 49, 12–35.
- Jithila, P. J., & Prasad, P. K. (2018). Carbon sequestration by trees-A study in the Western Ghats, Wayanad region. *Indian Journal of Ecology*, 45(3), 479–482.
- Jonsson, M., Bengtsson, J., Moen, J., Gamfeldt, L., & Snäll, T. (2020). Stand age and climate influence forest ecosystem service delivery and multifunctionality. *Environmental Research Letters*, 15(9),0940a8. Doi:  
<https://doi.org/10.1088/1748-9326/abaf1c>
- Kaartinen, H., Hyypä, J., Yu, X., Vastaranta, M., Hyypä, H., Kukko, A., Holopainen, M., Heipke, C., Hirschmugl, M., Morsdorf, F., Erik, N., Juho, P., Sorin, P., Svein, S., Michael, W. B., & Cheng, W. J. (2012). An international comparison of individual tree detection and extraction using airborne laser scanning. *Remote Sensing*, 4(4), 950–974. Doi:  
<https://doi.org/10.3390/rs4040950>
- Karna, Y. K., Penman, T. D., Aponte, C., Hinko-Najera, N., & Bennett, L. T. (2020). Persistent changes in the horizontal and vertical canopy structure of fire-tolerant forests after severe fire as quantified using multi-temporal airborne lidar data. *Forest Ecology and Management*, 472, 118255. Doi:  
10.1016/j.foreco.2020.118255

- Kho, L. K., & Jepsen, M. R. (2015). Carbon stock of oil palm plantations and tropical forests in Malaysia: A review. *Singapore Journal of Tropical Geography*, 36(2), 249–266. Doi:10.1111/sjtg.12100
- Khosravipour, A., Skidmore, A. K., Isenburg, M., Wang, T., & Hussin, Y. A. (2013). Development of an algorithm to generate a Lidar pit-free canopy height model. *SilviLaser*, 30, 125–128.
- Kindermann, G., Kristöfel, F., Neumann, M., Rössler, G., Ledermann, T., & Schueler, S. (2018). 109 years of forest growth measurements from individual Norway spruce trees. *Sci Data* 5, 180077. Doi: <https://doi.org/10.1038/sdata.2018.77>
- Kim, D., Kim, J., & Kim, J. (2020). Elastic exponential linear units for convolutional neural networks. *Neuro computing*, 406, 253–266, Doi:<https://doi.org/10.1016/j.neucom.2020.03.051>.
- King, K. L., & Locke, D. H. (2013). A comparison of three methods for measuring local urban tree canopy cover. *Arboriculture & Urban Forestry*, 39(2), 62–67.
- Knoke, T., Kindu, M., Schneider, T., & Gobakken, T. (2021). Inventory of forest attributes to support the integration of non-provisioning ecosystem services and biodiversity into forest planning—from collecting data to providing information. *Current Forestry Report*, 7, 38–58. Doi: <https://doi.org/10.1007/s40725-021-00138-7>
- Köhl, M., & Magnussen, S. (2016). Sampling in Forest Inventories BT – Tropical Forestry Handbook (L. Pancel & M. Köhl, eds.). Doi: [https://doi.org/10.1007/978-3-642-54601-3\\_72](https://doi.org/10.1007/978-3-642-54601-3_72)
- Koprivica, M. I. L. O. Š. (2017). Stratified sampling in forest inventory. Шлямарцтво/Forestry/Sylviculture/Forstwesen.
- Krooks, A., Kaasalainen, S., Kankare, V., Joensuu, M., Raunonen, P., & Kaasalainen, M. (2014). Tree structure vs. height from terrestrial laser scanning and quantitative structure models. *Silva Fennica*, 48(2). Doi:10.14214/sf.1125
- Kubiske, M. E. (2013). Tree height and diameter data from the Aspen FACE Experiment, 1997-2008. *Newtown Square, PA: USDA Forest Service, Northern Research Station*. Doi: <https://doi.org/10.2737/RDS-2013-0015>
- LAStools. (2021). Efficient LiDAR processing software (version 141017, academic). Retrieved from <http://rapidlasso.com/LAStools>.
- Leica geosystems. (2015). Leica TS15 user manual. Retrieved from:file:///C:/Users/chrpw.LANTM/Downloads/Leica-TS15-User-Manual.pdf
- Liang, X., Kankare, V., Hyypä, J., Wang, Y., Kukko, A., Haggrén, H., Yu, X., Kaartinen, H., Jaakkola, A., Guan, F., Holopainen, M., & Vastaranta, M.

- (2016). Terrestrial laser scanning in forest inventories. *ISPRS Journal of Photogrammetry and Remote Sensing*, 115, 63–77. Doi: 10.1016/j.isprsjprs.2016.01.006
- Lin, W. (2023). Forest aboveground biomass monitoring in southern Sweden using random forest model with Sentinel-1, Sentinel-2, and LiDAR data. Retrieved from <https://hig.diva-portal.org/smash/get/diva2:1771924/FULLTEXT01.pdf>
- Lines, E.R., Fischer, F.J., Owen, H.J.F., & Jucker, T. (2022). The shape of trees: Reimagining Forest ecology in three dimensions with remote sensing. *Journal of Ecology*, 10(8), 1730–1745. Doi: <https://doi.org/10.1111/1365-2745.13944>
- Lisiewicz, M., Kamińska, A., Kraszewski, B., & Stereńczak, K. (2022). Correcting the results of CHM-based individual tree detection algorithms to improve their accuracy and reliability. *Remote Sensing*, 14(8), 1822. Doi: <https://doi.org/10.3390/rs14081822>
- Lister, A. J., Andersen, H., Frescino, T., Gatzliolis, D., Healey, S., Heath, L. S., Liknes, G. C., McRoberts, R., Moisen, G. G., Nelson, M., Rachel, R., Karen, S., Todd A. S., James, W., & Tyler, W. B. (2020). Use of remote sensing data to improve the efficiency of national forest inventories: A case study from the United States national forest inventory. *Forests*, 11(12), 1364. Doi:<https://doi.org/10.3390/f11121364>
- López, O. A. M., López, A.M., & Crossa, J. (2022). Overfitting, model tuning, and evaluation of prediction performance. In *Multivariate Statistical Machine Learning Methods for Genomic Prediction*, 109–139. Doi:[https://doi.org/10.1007/978-3-030-89010-0\\_4](https://doi.org/10.1007/978-3-030-89010-0_4)
- Ma, K., Chen, Z., Fu, L., Tian, W., Jiang, F., Yi, J., Du, Z., & Sun, H. (2022). Performance and sensitivity of individual tree segmentation methods for UAV-LiDAR in multiple forest types. *Remote Sensing*, 14(2), 298. Doi: <https://doi.org/10.3390/rs14020298>
- Macdicken, K. G. (1997). A guide to monitoring carbon storage in forestry and agro forestry projects, Winrock International Institute for Agriculture Development, US, 13-14.
- Magalhaes, J., Polinko, A., Amoroso, M., Kohli, G. S., & Larson, B. C. (2022). The predicting tree growth app: an algorithmic approach to modelling individual tree growth. *Ecological Modelling*, 467, 109932, Doi:<https://doi.org/10.1016/j.ecolmodel.2022.109932>.
- Magarik, Y. A., Roman, L. A., & Henning, J. G. (2020). How should we measure the dbh of multi-stemmed urban trees? *Urban Forestry & Urban Greening*, 47, 126481. Doi: 10.1016/j.ufug.2019.126481
- Maki, S. C. (1994). U.S. Patent No. 5,323,163. Washington, DC: U.S. Patent and Trademark Office.

- Malabanan, M. V., Paringit, E. C., Zaragosa, G. P., Ibañez, C. A. G., Faelga, R. A. G., Argamosa, R. J. L., & Maralit, A. A. R. (2016). Extracting tree count and individual tree crown from LiDAR-derived Canopy Height Model using Object-based Image Analysis. *37<sup>th</sup> Asian Conference on Remote Sensing*, 1, 470–478.
- Maltamo, M., Bollandås, O. M., Næsset, E., Gobakken, T., & Packalén, P. (2011). Different plot selection strategies for field training data in ALS-assisted forest inventory. *Forestry: An International Journal of Forest Research*, 84(1), 23–31. Doi: <https://doi.org/10.1093/forestry/cpq039>
- Maltamo, M., Næsset, E., & Vauhkonen, J. (2014). *Forestry applications of airborne laser scanning: concepts and case studies* (Dordrecht: Springer Science & Business Media).
- McPherson, G., Simpson, J. R., & Peper, P. (2005). Municipal forest benefits and costs in five US cities. *Journal of Forestry*, 103(8), 411–416.
- Monumental trees, (2023). Retrieved from <https://www.monumentaltrees.com/en/heightrecords/swe/>
- Marrs, J., & Ni-Meister, W. (2019). Machine learning techniques for tree species classification using co-registered LiDAR and hyperspectral data. *Remote Sensing*, 11(7), 819. Doi:<https://doi.org/10.3390/rs11070819>
- McCoy, D. E., Goulet-Scott, B., Meng, W., Atahan, B. F., Kiros, H., Nishino, M., & Kartesz, J. (2022). Species clustering, climate effects, and introduced species in 5 million city trees across 63 US cities. *eLife*, 11, 77891. Doi: <https://doi.org/10.7554/eLife.77891>
- McRoberts, R. E., Wendt, D. G., Nelson, M. D., & Hansen, M. H. (2002). Using a land cover classification based on satellite imagery to improve the precision of forest inventory area estimates. *Remote Sensing of Environment*, 81(1), 36–44. Doi: [https://doi.org/10.1016/S0034-4257\(01\)00330-3](https://doi.org/10.1016/S0034-4257(01)00330-3)
- Michałowska, M., & Rapiński, J. (2021). A review of tree SPECIES classification based on airborne lidar data and Applied Classifiers. *Remote Sensing*, 13(3), 353. Doi:10.3390/rs13030353
- Mielcarek, M., Stereńczak, K., & Khosravipour, A. (2018). Testing and evaluating different lidar-derived canopy height model generation methods for tree height estimation. *International Journal of Applied Earth Observation and Geoinformation*, 71, 132–143. Doi: 10.1016/j.jag.2018.05.002
- Minitab, LLC. (2021). Minitab. Retrieved from <https://www.minitab.com>.
- Moeller, G. H. (1977). The Pinchot institute: Toward managing our urban our urban forest resources. *Journal of Arboriculture*, 3(10), 181–186.

- Mohammed, S. I. (2021). Important methods measurements to exam the accuracy and reliability of reflector-less total station measurements. *Journal of Physics: Conference Series*, 1895(1), 012007. Doi:10.1088/1742-6596/1895/1/012007
- Mohammadi, Z., Limaie, S. M., & Lohmander, L. O. (2017). Estimating the aboveground carbon sequestration and its economic value (case study: Iranian Caspian forests). *Journal of Forest Science*, 63(11),511–518.
- Morales, Y., & Tsubouchi, T. (2007). DGPS, RTK-GPS and StarFire DGPS performance under tree shading environments. *2007 IEEE International Conference on Integration Technology*. Doi:10.1109/icitechnology.2007.4290370
- Morgenroth, J., & Gomez, C. (2014). Assessment of tree structure using a 3D image analysis technique—A proof of concept. *Urban Forestry & Urban Greening*, 13(1), 198–203, Doi: <https://doi.org/10.1016/j.ufug.2013.10.005>.
- Næsset, E. (2004). Practical large-scale forest stand inventory using a small-footprint airborne scanning laser. *Scandinavian Journal of Forest Research*, 19(2), 164–179. Doi:10.1080/02827580310019257
- Negash, M., Starr, M. & Kanninen, M. (2013). Allometric equations for biomass estimation of Enset (*Ensete ventricosum*) Grown in indigenous agroforestry systems in the Rift Valley Escarpment of Southern-Eastern Ethiopia. *Agroforestry System*, 87, 571–581. Do: <http://dx.doi.org/10.1007/s10457-012-9577-6>
- Nowak, D. J. (1996). Estimating leaf area and leaf biomass of open-grown deciduous urban trees. *Forest Scienc.*, 42(4), 504–507.
- Nowak, D. J., Crane, D. E., & Stevens, J. C. (2006). Air pollution removal by urban trees and shrubs in the United States. *Urban Forestry & Urban Greening*, 4(3–4), 115–123. Doi: 10.1016/j.ufug.2006.01.007
- Nowak, D.J., Crane, D.E., Stevens, J.C., Hoehn, R.E., Walton, J.T., & Bond, J. (2008). A ground-based method of assessing urban forest structure and ecosystem services, 34, 347–58.
- Nowak, D. J., Greenfield, E. J., Hoehn, R. E., & Lapoint, E. (2013). Carbon storage and sequestration by trees in urban and community areas of the United States. *Environmental Pollution*, 178, 229–236. Doi: 10.1016/j.envpol.2013.03.019
- Nowak, D. J., & Greenfield, E. J. (2020). The increase of impervious cover and decrease of tree cover within urban areas globally (2012–2017). *Urban Forestry & Urban Greening*, 49, 126638. Doi: <https://doi.org/10.1016/j.ufug.2020.126638>
- Osada, N. (2012). Crown exposure to light and tree allometry of 11 tree species in a SNOWY cool-temperate forest in Japan. *Plant Ecology*, 213(5), 783–794. Doi:10.1007/s11258-012-0041-5

- Ostadhashemi, R., Rostami Shahraji, T., Roehle, H., & Mohammadi Limaiei, S. (2014). Estimation of biomass and carbon storage of tree plantations in northern Iran. *Journal of Forest Science*, 60(9), 363–371. Doi: <https://doi.org/10.17221/55/2014-jfs>
- OZDARICI-OK, A., & OK, A. O. (2023). Using remote sensing to identify individual tree species in orchards: A review. *Scientia Horticulturae*, 321, 112333. Doi:<https://doi.org/10.1016/j.scienta.2023.112333>
- Pace, R., Masini, E., Giuliarelli, D., Biagiola, L., Tomao, A., Guidolotti, G., Agrimi, M., Portoghesi, L., De Angelis, P. & Calfapietra, C. (2022). Tree measurements in the urban environment: insights from traditional and digital field instruments to smartphone applications. *Arboriculture & Urban Forestry*.
- Pascual, C., Mauro, F., Garcia-Abril, A., & Manzanera, J.A. (2018). Applications of ALS (Airborne Laser Scanning) data to forest inventory. Experiences with pine stands from mountainous environments in Spain. *Earth and Environmental Science*, 226, 012001, Doi:10.1088/1755-1315/226/1/012001.
- Paudel, P., & Mandal, R. (2019). Comparing growing stock using circular, square and rectangular plots shape in inventory (A study from Community Forests in Chitwan District, Nepal). *Canadian Journal of Soil Science*, 4(11), 448–454. <https://doi.org/10.32474/OAJESS.2019.04.000177>
- Pelc-Mieczkowska, R., Tomaszewski, D., & Jurgielewicz, K. (2018). Application of ALS data for Gns terrain obstacles inventory. *E3S Web of Conferences*, 63, 00014. Doi:10.1051/e3sconf/20186300014
- Picos, J., Bastos, G., Míguez, D., Alonso, L., & Armesto, J. (2020). Individual tree detection in a eucalyptus plantation using unmanned aerial vehicle (UAV)-LiDAR. *Remote Sensing*, 12(5), 885. Doi: <https://doi.org/10.3390/rs12050885>
- Popescu, S. C., Zhao, K., Neuenschwander, A., & Lin, C. (2011). Satellite lidar vs. small footprint airborne lidar: Comparing the accuracy of aboveground biomass estimates and forest structure metrics at footprint level. *Remote Sensing Environment*, 115(11), 2786–2797. Doi:10.1016/j.rse.2011.01.026
- QGIS Development Team. (2021). QGIS Geographic Information System. Open-source geospatial foundation project. Retrieved from <http://qgis.osgeo.org>
- Ramezan, C. A., Warner T. A., & Maxwell A. E. (2019). Evaluation of Sampling and Cross-Validation Tuning Strategies for Regional-Scale Machine Learning Classification. *Remote Sensing*, 11(2), 185. Doi: <https://doi.org/10.3390/rs11020185>
- Roberge, C. (2022). The Swedish national forest inventory. Retrieved from <https://www.slu.se/en/Collaborative-Centres-and-Projects/the-swedish-national-forest-inventory/about-the-nfi/>

- Roberts, B. R. (1987). Methods for measuring water status and reducing transpirational water loss in trees. *Journal of Arboriculture*, 13(2), 57.
- Saarela, S., Wästlund, A., Holmström, E., Mensah, A. A., Holm, S., Nilsson, M., & Ståhl, G. (2020). Mapping aboveground biomass and its prediction uncertainty using lidar and field data, accounting for tree-level allometric and lidar model errors. *Forest Ecosystems*, 7(1). Doi:10.1186/s40663-020-00245-0
- Sačkov, I., Kulla, L., & Bucha, T. (2019). A comparison of two tree detection methods for estimation of forest stand and ecological variables from airborne lidar data in Central European forests. *Remote Sensing*, 11(12), 1431. Doi:10.3390/rs11121431
- Sumnall, M. J., Hill, R. A., & Hinsley, S. A. (2012). The estimation of forest inventory parameters from small-footprint waveform and discrete return airborne LiDAR data. *SilviLaser*, SL2012–020.
- Schardt, M., Ziegler, M., Wimmer, A., Wack, R., & Hyypäe, J. (2002). Assessment of forest parameters by means of laser scanning. *International Archives of Photogrammetry and Remote Sensing*, 34, 302–309.
- Schettini, B. L., Jacovine, L. A. G., Torres, C. M. M. E., Carneiro, A. de C. O., Castro, R. V. O., Villanova, P. H., da Rocha, S. J. S. S., Rufino, M. P. M. X., Neto, S. N. de O., & Júnior, V. T. M. de M. (2022). Use of destructive and non-destructive methodologies to estimate stem biomass accumulation and carbon stock in a Eucalyptus Forest. *Scientific Article*, Doi: <http://dx.doi.org/10.1590/1806-908820220000011>
- Schreuder, H. T., Gregoire, T. G., & Wood, G. B. (1993). Sampling methods for multiresource forest inventory. New York, New Jersey: J. Wiley.
- Seidel, D., Annighöfer, P., Thielman, A., Seifert, Q. E., Thauer, J., Glatthorn, J., Ehbrech, M., Kneib, T. & Ammer, C. (2021). Predicting tree species from 3D laser scanning point clouds using deep learning. *Technical Advances in Plant Science*, 12, Doi: <https://doi.org/10.3389/fpls.2021.635440>
- Sharma, M., Garg, R. D., Badenko, V., Fedotov, A., Min, L., & Yao, A. (2021). Potential of airborne lidar data for terrain parameters extraction. *Quaternary International*, 317–327. Doi: 10.1016/j.quaint.2020.07.039
- Sheikh, M. A., Kumar, M., Bussman, R. W., & Todaria, N. P. (2011). Forest carbon stocks and fluxes in physiographic zones of India. *Carbon Balance Management*, 6(15).
- Skovsgaard, J.P. (2004). MENSURATION | Forest Measurements. *Encyclopedia of Forest Sciences*, 550-566. Doi:10.1016/b0-12-145160-7/00142-3
- Stoew, B., Jarlemark, P., Johansson, J., & Elgered, G. (2001). Real-time processing of gps data delivered by swepos. *Physics and Chemistry of the Earth, Part*

*A: Solid Earth and Geodesy*, 26(6–8), 493–496. Doi: 10.1016/s1464-1895(01)00090-4

- Sumayli, A. (2022). Modeling and prediction of biodiesel production by using different artificial intelligence methods: Multi-layer perceptron (MLP), Gradient boosting (GB), and Gaussian process regression (GPR). *Arabian Journal of Chemistry*, 16, 104801. Doi: <https://doi.org/10.1016/j.arabjc.2023.104801>
- Sumsion, G. R., Bradshaw, M. S., Hill, K. T., Pinto, L. D., & Piccolo, S. R. (2019). Remote sensing tree classification with a multilayer perceptron. *PeerJ*, 7. Doi:10.7717/peerj.6101
- Tanhuanpää, T., Saarinen, N., Kankare, V., Nurminen, K., Vastaranta, M., Honkavaara, E., Karjalainen, M., Yu, X., Holopainen, M., & Hyyppä, J. (2016). Evaluating the performance of High-Altitude AERIAL image-based digital Surface models in Detecting individual Tree Crowns in mature boreal forests. *Forests*, 7(12), 143. Doi:10.3390/f7070143
- Taubert, F., Fischer, R., Knapp, N., & Huth, A. (2021). Deriving tree size distributions of tropical forests from lidar. *Remote Sensing*, 13(1), 131. Doi:10.3390/rs13010131
- Tiede, D., Hochleitner, G., & Blaschke, T. (2005). A full GIS-based workflow for tree identification and tree crown delineation using laser scanning. *In ISPRS Workshop CMRT*, 5.
- Udayakumar, M., Manikandan, S., Selvan, B. T., & Sekar, T. (2016). Density, Species Richness and Aboveground Biomass of Trees in 10 Hectare Permanent Study Plot, Pachaimalai, Tamil Nadu. *Scholars Academic Journal of Bioscience*, 4(4), 342–347.
- United States Department of Agriculture, forest service. (2019). Urban tree canopy assessment: a community's path to understanding and managing the urban forest. FS–1121. Washington, DC.
- Ventura, J., Honsberger, M., Gonsalves, C., Rice, J., Pawlak, C., Love, N. L. R., Han, S., Nguyen, V., Sugano, K., Doremus, J., Fricker, A., Yost, J. & Ritter, M. (2022). Individual tree detection in large-scale urban environments using high-resolution multispectral imagery. *ISPRS Journal of Photogrammetry and Remote Sensing*, Doi: 10.48550/arXiv.2208.10607
- Vishnu, P. R., & Patil, S. S. (2016). Carbon storage and sequestration by trees in and around university campus of Aurangabad City, Maharashtra. *International Journal of Innovative Research in Science, Engineering and Technology*, 5(4), 5459–5468.
- Vorster, A.G., Evangelista, P.H., Stovall, A.E.L., & Ex, S. (2020). Variability and uncertainty in forest biomass estimates from the tree to landscape scale: the role

of allometric equations. *Carbon Balance Manage*, 15 (1), 8.

<https://doi.org/10.1186/s13021-020-00143-6>

- Walde, J. F., Tappeiner, G., Tappeiner, U., Tasser, E., & Holub, H. W. (2004). Statistical aspects of multilayer perceptrons under data limitations. *Computational Statistics & Data Analysis*, 46(1), 173–188. Doi:10.1016/s0167-9473(03)00140-3
- Wang, H., Moss, R. H., Chen, X., Stanley, R. J., Stoecker, W. V., MCelebi, M. E., Malters, J. M., Grichnik, J. M., Marghoob J. M., Rabinovitz, H. S., Menzies, S. W., & Szalapski, T. M. (2011). Modified watershed technique and post-processing for segmentation of skin lesions in dermoscopy images. *Computerized Medical Imaging and Graphics*, 35(2), 116–120. Doi: 10.1016/j.compmedimag.2010.09.006
- Wang, Y., & Fang, H. (2020). Estimation of LAI with the LiDAR technology: A review. *Remote Sensing*, 12(20), 3457. Doi:10.3390/rs12203457
- White, J. (1998). Estimating the age of large and veteran trees in Britain. Forestry Commission Information Note. Forestry Commission, Edinburgh.
- Wiman, M., & Larsson, F. H. (2023), En jämförelse av noggrannhet och tidseffektivitet mellan olika gångmönster med handhållen laserskanner BLK2GO i tallskog. Retrieved from <https://hig.diva-portal.org/smash/get/diva2:1776991/FULLTEXT01.pdf>
- Woodget, A. S., Donoghue, D. N. M., & Carbonneau, P. (2007). An assessment of airborne LiDAR for forest growth studies. *Ekscentar*, 10, 47– 52.
- Wulder, M., Niemann, K. O., & Goodenough, D. G. (2000). Local maximum filtering for the extraction of tree locations and basal area from high spatial resolution imagery. *Remote Sensing of Environment*, 73(1), 103–114. Doi: [https://doi.org/10.1016/S0034-4257\(00\)00101-2](https://doi.org/10.1016/S0034-4257(00)00101-2)
- Wu, X., Shen, X., Cao, L., Wang, G., & Cao, F. (2019). Assessment of individual tree detection and canopy cover estimation using unmanned aerial vehicle based light detection and ranging (UAV-LiDAR) data in planted forests. *Remote Sensing*, 11(8), 908. Doi: <https://doi.org/10.3390/rs11080908>
- Yan, F., Ullah, M. R., Gong, Y., Feng, Z., Chowdury, Y., & Wu, L. (2012). Use of a no prism total station for field measurements in Pinus Tabulaeformis carr, stands in China. *Biosystems Engineering*, 113(3), 259–265. Doi: 10.1016/j.biosystemseng.2012.08.007
- Yang, J., Kang, Z., Cheng, S., Yang, Z., & Akwensi, P. (2020). An individual tree segmentation method based on watershed algorithm and 3D spatial distribution analysis from airborne LiDAR point clouds. *Applied Earth Observations and Remote Sensing*, 13(1), 1055–1067. Doi: <http://dx.doi.org/10.1109/JSTARS.2020.2979369>

- Yilmaz, A., & Poli, R. (2022). Successfully and efficiently training deep multi-layer perceptrons with logistic activation function simply requires initializing the weights with an appropriate negative mean. *Neural Networks*, 153, 87–103, Doi: <https://doi.org/10.1016/j.neunet.2022.05.030>
- Yoon, T. K., Park, C., Lee, S. J., Suin Ko, Kim, K. N., Son, Y., Lee, K. H., Oh, S., Lee, W., Son, Y. (2013). Allometric equations for estimating the aboveground volume of five common urban street tree species in Daegu, Korea. *Urban Forestry & Urban Greening*, 12(3), 344–349. Doi: <https://doi.org/10.1016/j.ufug.2013.03.006>
- Yoshii, T., Matsumura, N., & Lin, C. (2022). Integrating UAV-SfM and airborne lidar point cloud data to plantation forest feature extraction. *Remote Sensing*. 14(7),1713. Doi: <https://doi.org/10.3390/rs14071713>
- Zhan, Q., Liang, Y., Cai, Y., & Xiao, Y. (2011). Pattern detection in airborne LiDAR data using Laplacian of Gaussian filter. *Geo-spatial Information Science*, 14(3), 184–189. Doi:10.1007/s11806-011-0540-x
- Zhang, H., Yang, Q., Zhou, D., Xu, W., Gao, J., & Wang, Z. (2021). How evergreen and deciduous trees coexist during secondary forest succession: Insights into forest restoration mechanisms in Chinese subtropical forest. *Global Ecology and Conservation*, 25. Doi: 10.1016/j.gecco. 2020.e01418
- Zhao, H., Morgenroth, J., Pearse, G., & Schindler, J. (2023). A systematic review of individual tree crown detection and delineation with convolutional neural networks (CNN). *Current Forestry Reports*, 9, 149-170. Doi:<https://doi.org/10.1007/s40725-023-00184-3>
- Zhao, P., Gao, L., & Gao, T. (2020). Extracting forest parameters based on Stand Automatic segmentation algorithm. *Scientific Reports*, 10(1). Doi:10.1038/s41598-020-58494-6
- Zolkos, S. G., Goetz, S. J., & Dubayah, R. (2013). A meta-analysis of terrestrial aboveground biomass estimation using LiDAR remote sensing. *Remote Sensing of Environment*, 128, 289–298. Doi: <https://doi.org/10.1016/j.rse.2012.10.017>

## Appendix A. Species, genus, family, and order of field measured trees

Table A1. Species, genus, family, and order of field measured trees

Species	Number of trees per species	Genus	Family	Order
Acer saccharinum L.	1	Acer	Sapindaceae	Sapindales
Alnus glutinosa (L.) Gaertn.	1	Alnus	Betulaceae	Fagales
Betula pendula Roth	29	Betula		
Betula pubescens Ehrh.	6			
Carya illinoensis (Wangenh.) K.Koch	1	Carya	Juglandaceae	
Cedrus libani A.Rich.	1	Cedrus	Pinaceae	Pinales
Celtis laevigata Willd.	1	Celtis	Cannabaceae	Rosales
Fraxinus americana L.	2	Fraxinus	Oleaceae	Lamiales
Gleditsia triacanthos L.	1	Gleditsia	Fabaceae	Fabales
Koelreuteria paniculata Laxm.	1	Koelreuteria	Sapindaceae	Sapindales
Larix decidua Mill.	12	Larix	Pinaceae	Pinales
Nothofagus alpina (Poepp. & Endl.) Oerst	3	Nothofagus	Nothofagaceae	Fagales
Nothofagus obliqua (Mirb.) Oerst.	1			
Pinus banksiana Lamb.	1	Pinus	Pinaceae	Pinales
Pinus halepensis Mill.	1			
Pinus pinaster Aiton	7			
Pinus pinea L.	7			

Pinus ponderosa Douglas ex C.Lawson	23			
Pinus resinosa Aiton	25			
Pinus strobus L.	10			
Pinus sylvestris L.	24			
Populus alba L.	4	Populus	Salicaceae	Malpighiales
Populus tremula L.	1			
Populus tremuloides Michx.	1			
Prunus avium (L.) L.	6	Prunus	Rosaceae	Rosales
Prunus dulcis (Mill.) D.A.Webb	1			
Prunus serotina Ehrh.	2			
Prunus serrulata Lindl.	1			
Pseudotsuga menziesii (Mirb.) Franco	5	Pseudotsuga	Pinaceae	Pinales
Quercus castaneifolia C.A.Mey.	1	Quercus	Fagaceae	Fagales
Quercus pubescens Willd.	1			
Quercus robur L.	1			
Quercus rubra L.	1			
Quercus suber L.	2			
Sterculia africana (Lour.) Fiori	1	Sterculia	Malvaceae	Malvales
Ulmus americana L.	1	Ulmus	Ulmaceae	Rosales
Ulmus pumila L.	1	Ulmaceae	Rosales	Rosids
Vachellia gerrardii (Benth.) P.J.H. Hurter	1	Acacia	Fabaceae	Fabales

## Appendix B. Results from MLP model

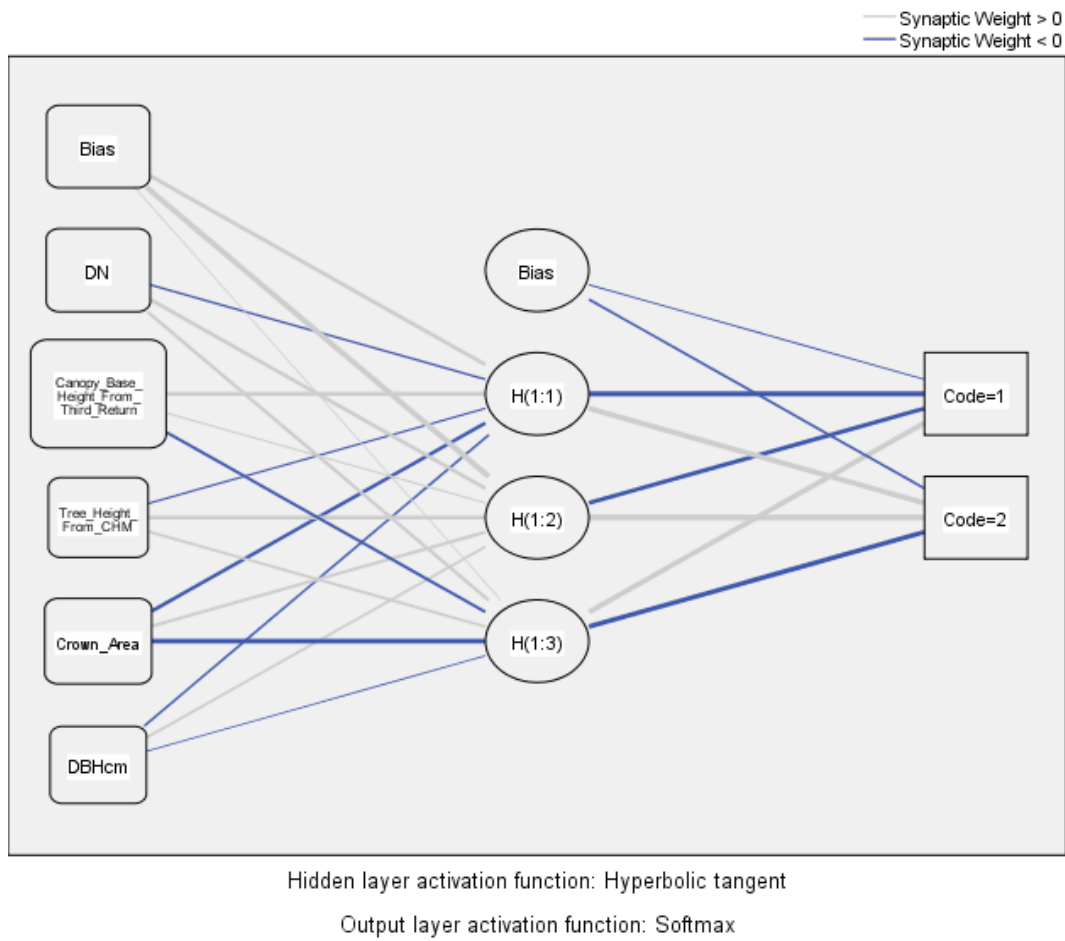
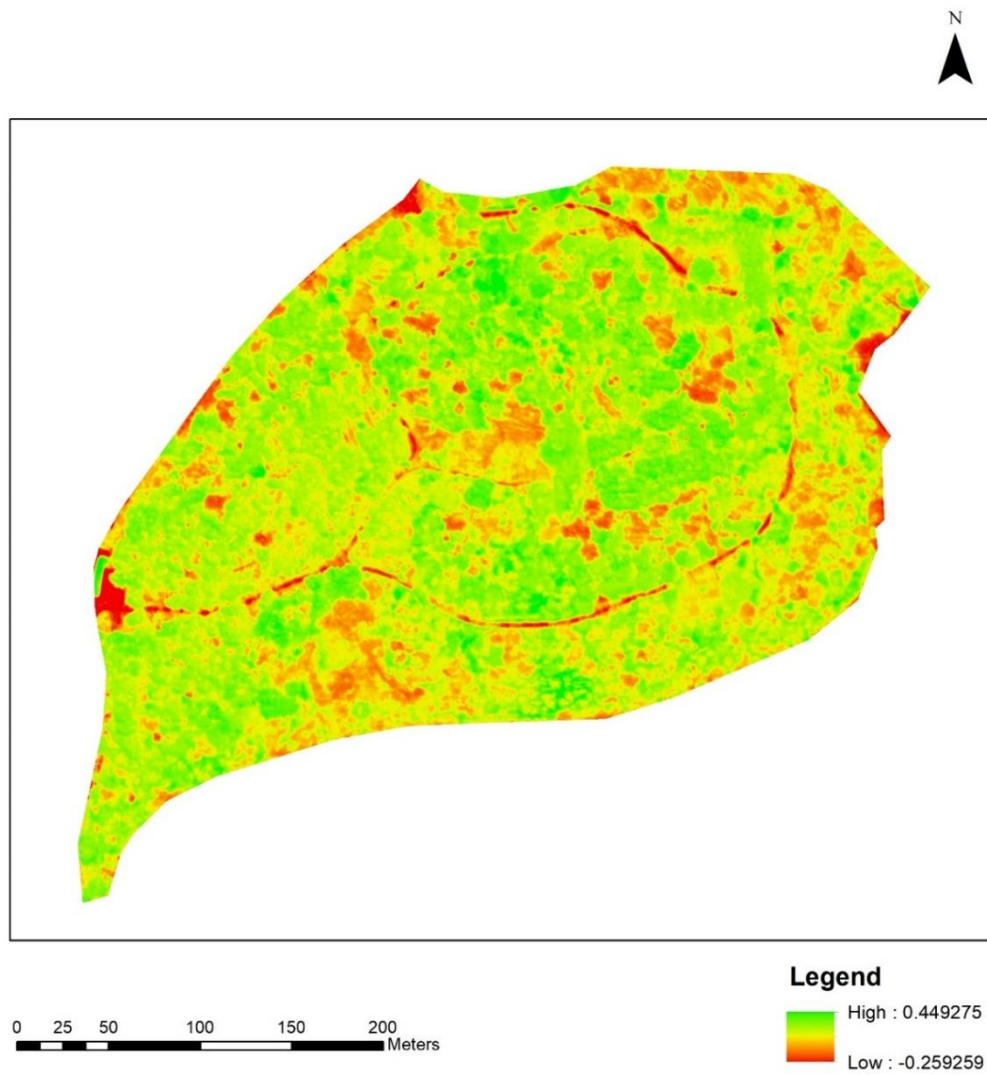


Figure B1. Hidden layer activation function and output layer function of MLP model.

Table B1. Parameter estimate of MPL model

Predictor		Predicted				
		Hidden Layer 1			Output Layer	
		H(1:1)	H(1:2)	H(1:3)	[Code=1]	[Code=2]
Input Layer	(Bias)	.904	1.694	.237		
	NDVI	-.476	.863	.655		
	Canopy_Base_Height_From _Third_Return	1.027	.298	-.625		
	Tree_Height_From_CHM	-.423	.910	.624		
	Crown_Area	-.833	.652	-1.087		
	DBHcm	-.477	.525	-.276		
Hidden Layer 1	(Bias)				-.280	-.491
	H(1:1)				-1.336	1.664
	H(1:2)				-.980	1.791
	H(1:3)				1.528	-1.303

## Appendix C. NDVI map



*Figure C1. NDVI map of the study area.*

## Appendix D. Inputs for i-Tree Eco model

Table D1. Inputs for i-Tree Eco model that derived from field data.

ID	Tree height	DBH (cm)	Number of Crowns	Species	Crown area	CLE	Tree height from CHM	CBH	Lat	Lon
1	13.25	33.12	1	Prunus dulcis (Mill.) D.A.Webb	29.37	2	22.38	2.44	60.67696	17.10944
2	25.96	59.24	1	Fraxinus americana L.	50.39	5	21.54	5.00	60.67677	17.10955
3	5.66	20.70	2	Fraxinus americana L.	62.13	2	9.77	2.05	60.67671	17.10942
4	14.94	24.84	1	Populus tremuloides Michx.	18.68	3	18.73	2.75	60.67694	17.10962
5	8.43	47.45	3	Ulmus americana L.	70.68	2	13.93	6.00	60.67846	17.11413
6	4.65	19.43	1	Cedrus libani A.Rich.	6.19	2	15.57	8.30	60.67688	17.10807
7	13.91	65.92	1	Quercus castaneifolia C.A.Mey.	27.01	3	30.33	2.93	60.67672	17.10958
8	12.33	65.29	3	Pinus pinaster Aiton	59.24	3	14.75	6.99	60.67678	17.10787
9	14.54	65.61	1	Pinus pinaster Aiton	141.16	4	16.73	13.52	60.67689	17.10756
10	10.48	48.73	1	Pinus pinaster Aiton	68.54	2	16.87	2.02	60.67698	17.10889
11	13.04	22.93	1	Pinus pinaster Aiton	19.83	3	17.13	14.47	60.6777	17.11022
12	13.19	28.66	1	Pinus pinaster Aiton	8.10	3	20.70	17.48	60.67774	17.11026
13	15.14	41.40	1	Pinus pinaster Aiton	17.26	4	24.40	22.43	60.6777	17.10997
14	18.24	38.22	2	Pinus pinaster Aiton	33.38	4	20.02	5.00	60.67781	17.11017
15	13.54	37.26	1	Quercus suber L.	7.73	2	20.18	2.05	60.67682	17.10939
16	26.81	35.99	1	Quercus suber L.	7.73	4	20.11	4.33	60.67683	17.10941
17	14.44	12.42	1	Pseudotsuga menziesii (Mirb.) Franco	33.31	3	22.91	7.31	60.67684	17.10795
18	15.61	27.07	1	Pseudotsuga menziesii (Mirb.) Franco	31.75	3	17.13	5.06	60.67679	17.10766
19	15.03	35.67	1	Pseudotsuga menziesii (Mirb.) Franco	13.55	3	19.84	15.40	60.67681	17.10762

20	10.48	29.94	1	Pseudotsuga menziesii (Mirb.) Franco	13.55	2	17.30	13.27	60.67683	17.10763
21	16.06	42.68	1	Pseudotsuga menziesii (Mirb.) Franco	94.53	4	18.66	3.71	60.67694	17.10902
22	9.95	41.40	1	Quercus pubescens Willd.	61.68	2	22.33	1.68	60.67681	17.10926
23	9.41	62.10	7	Alnus glutinosa (L.) Gaertn.	66.05	3	12.48	1.90	60.67823	17.11391
24	8.48	19.75	2	Populus tremula L.	32.18	2	9.29	1.69	60.67663	17.10758
25	12.49	21.02	1	Larix decidua Mill.	33.31	3	24.50	6.43	60.67685	17.10797
26	15.71	31.85	1	Larix decidua Mill.	35.29	4	20.52	15.87	60.6768	17.108
27	9.22	12.74	1	Larix decidua Mill.	31.14	3	11.20	4.81	60.67667	17.10787
28	12.19	33.12	1	Larix decidua Mill.	48.96	3	16.03	5.57	60.67829	17.11392
29	12.61	39.49	1	Larix decidua Mill.	35.31	3	23.52	12.57	60.67756	17.10973
30	13.71	29.62	1	Larix decidua Mill.	67.95	3	20.20	16.45	60.67772	17.11028
31	17.35	35.35	1	Larix decidua Mill.	17.09	4	9.28	15.83	60.67771	17.11013
32	8.98	32.48	1	Larix decidua Mill.	15.58	2	22.14	6.98	60.67769	17.11006
33	20.67	33.12	1	Larix decidua Mill.	17.26	5	22.09	8.87	60.67771	17.11003
34	8.47	46.18	2	Larix decidua Mill.	28.36	2	22.91	16.21	60.67776	17.11008
35	18.73	37.58	1	Larix decidua Mill.	62.70	4	20.51	6.29	60.6778	17.11011
36	10.82	31.21	1	Larix decidua Mill.	26.00	2	16.33	3.83	60.67831	17.11366
37	10.91	38.22	1	Betula pendula Roth	31.14	3	19.86	3.51	60.67669	17.10779
38	4.46	11.46	1	Betula pendula Roth	31.14	2	4.52	0.73	60.67669	17.10769
39	19.61	92.04	2	Betula pendula Roth	238.81	4	25.46	21.00	60.67851	17.11333
40	15.12	32.48	1	Betula pendula Roth	38.30	3	21.75	5.91	60.67679	17.1074
41	16.88	35.35	1	Betula pendula Roth	38.30	4	22.69	17.32	60.6768	17.10744
42	22.18	47.13	1	Betula pendula Roth	83.67	4	23.41	4.40	60.67683	17.10885
43	20.68	42.36	1	Betula pendula Roth	51.21	4	23.26	4.03	60.67687	17.10891
44	8.65	32.80	1	Betula pendula Roth	45.40	3	13.04	1.56	60.67697	17.1092
45	15.27	29.62	1	Betula pendula Roth	22.22	2	13.88	2.49	60.67698	17.10925

46	18.49	36.94	1	Betula pendula Roth	60.68	3	22.48	3.12	60.67704	17.10938
47	16.48	43.63	1	Betula pendula Roth	48.81	3	25.64	2.77	60.67702	17.1094
48	16.32	27.71	1	Betula pendula Roth	15.84	3	23.64	2.78	60.67706	17.10951
49	22.21	38.85	1	Betula pendula Roth	63.10	4	21.18	3.79	60.67707	17.10956
50	15.84	28.34	1	Betula pendula Roth	10.89	3	24.40	2.86	60.67706	17.10961
51	17.57	28.34	1	Betula pendula Roth	8.97	3	22.96	2.98	60.67697	17.10957
52	21.92	27.39	1	Betula pendula Roth	8.97	4	26.92	3.70	60.67699	17.1096
53	24.73	30.57	1	Betula pendula Roth	13.88	4	25.69	4.19	60.67701	17.10959
54	18.22	29.94	1	Betula pendula Roth	18.68	3	27.08	3.19	60.67694	17.10953
55	9.94	32.80	1	Betula pendula Roth	20.80	2	25.81	1.68	60.6769	17.10951
56	12.03	42.36	1	Betula pendula Roth	21.95	2	22.82	2.13	60.67684	17.10929
57	17.11	42.04	1	Betula pendula Roth	26.35	3	23.62	2.91	60.67681	17.1093
58	14.39	44.27	1	Betula pendula Roth	45.10	3	21.03	2.61	60.67683	17.10921
59	17.24	38.22	1	Betula pendula Roth	21.62	3	23.51	3.00	60.67681	17.10903
60	10.67	35.35	2	Betula pendula Roth	23.63	3	21.38	4.67	60.67747	17.11015
61	9.39	30.57	1	Betula pendula Roth	24.09	2	20.33	1.32	60.67746	17.1102
62	10.54	39.17	3	Betula pendula Roth	7.65	3	22.23	5.40	60.67745	17.11025
63	12.15	32.17	1	Betula pendula Roth	23.53	3	8.13	0.05	60.67739	17.1103
64	18.24	37.90	1	Betula pendula Roth	23.51	4	22.80	2.41	60.67741	17.11025
65	14.37	23.25	1	Betula pendula Roth	27.72	4	13.97	9.63	60.6776	17.11029
66	20.67	41.08	1	Koelreuteria paniculata Laxm.	20.80	4	28.44	3.54	60.67692	17.1095
67	17.84	35.99	1	Vachellia gerrardii (Benth.) P.J.H. Hurter	68.80	4	20.15	3.90	60.67752	17.11033
68	11.97	17.52	1	Pinus banksiana Lamb.	35.71	3	8.08	1.29	60.67766	17.11046
69	14.53	36.62	1	Prunus serrulata Lindl.	6.87	3	21.25	6.47	60.6775	17.11026
70	12.48	32.80	2	Prunus serrulata Lindl.	23.32	3	21.54	15.04	60.67751	17.11021
71	13.78	75.16	2	Pinus halepensis Mill.	136.73	5	18.94	13.27	60.67757	17.1101

72	20.84	37.58	1	Prunus avium (L.) L.	52.94	4	23.43	4.04	60.67685	17.10899
73	14.36	29.94	1	Prunus avium (L.) L.	35.31	3	13.56	1.57	60.67755	17.11031
74	12.45	30.57	1	Prunus avium (L.) L.	38.89	3	20.69	14.11	60.67743	17.11029
75	8.96	36.62	1	Prunus avium (L.) L.	22.49	2	20.22	4.05	60.67743	17.11017
76	6.38	36.94	1	Prunus avium (L.) L.	36.44	2	19.19	3.37	60.67745	17.11012
77	6.83	37.90	1	Prunus avium (L.) L.	33.97	2	23.47	15.04	60.67741	17.11014
78	8.59	28.98	1	Carya illinoensis (Wangenh.) K.Koch	9.89	1	11.20	1.46	60.67678	17.10914
79	13.11	76.43	4	Quercus rubra L.	27.95	3	27.81	3.07	60.6769	17.10973
80	10.65	41.40	4	Nothofagus obliqua (Mirb.) Oerst.	43.14	3	12.21	2.52	60.67671	17.10919
81	27.72	70.70	2	Quercus robur L.	17.19	5	29.20	4.98	60.67685	17.1096
82	10.61	79.30	3	Pinus ponderosa Douglas ex C.Lawson	137.63	2	14.12	8.74	60.67701	17.10756
83	10.69	29.62	1	Pinus ponderosa Douglas ex C.Lawson	27.53	2	16.46	11.39	60.67678	17.10774
84	12.30	28.66	1	Pinus ponderosa Douglas ex C.Lawson	18.55	3	17.58	9.95	60.67767	17.11009
85	9.23	29.30	1	Pinus ponderosa Douglas ex C.Lawson	18.29	2	21.10	18.64	60.67769	17.11016
86	7.82	36.31	1	Pinus ponderosa Douglas ex C.Lawson	18.41	2	20.63	3.68	60.67777	17.11022
87	11.00	34.08	1	Pinus ponderosa Douglas ex C.Lawson	32.62	3	21.66	4.81	60.67779	17.1102
88	15.43	29.94	1	Pinus ponderosa Douglas ex C.Lawson	62.70	4	18.66	13.74	60.67777	17.11014
89	7.78	32.17	1	Pinus ponderosa Douglas ex C.Lawson	8.51	2	22.08	1.10	60.67774	17.11
90	15.02	39.81	1	Pinus ponderosa Douglas ex C.Lawson	36.72	4	22.65	20.00	60.67772	17.10995
91	16.65	47.77	1	Pinus ponderosa Douglas ex C.Lawson	48.98	4	23.30	16.71	60.67775	17.10992
92	17.04	29.62	1	Pinus ponderosa Douglas ex C.Lawson	24.05	4	20.83	14.56	60.67776	17.10998
93	10.51	50.00	1	Pinus ponderosa Douglas ex C.Lawson	67.41	2	18.32	13.21	60.6786	17.11378
94	17.96	39.49	1	Pinus ponderosa Douglas ex C.Lawson	18.90	4	20.92	8.79	60.67859	17.11393
95	6.07	37.90	1	Pinus ponderosa Douglas ex C.Lawson	17.53	1	21.23	15.44	60.67859	17.11383
96	11.05	41.08	1	Pinus ponderosa Douglas ex C.Lawson	34.04	2	20.76	17.20	60.67853	17.11393
97	14.60	24.20	1	Pinus ponderosa Douglas ex C.Lawson	7.56	3	20.27	8.43	60.67854	17.11388

98	7.38	30.25	1	Pinus ponderosa Douglas ex C.Lawson	25.28	1	18.27	17.32	60.67849	17.11392
99	11.92	36.62	1	Pinus ponderosa Douglas ex C.Lawson	47.23	2	17.27	9.67	60.67835	17.11367
100	14.74	35.03	1	Pinus ponderosa Douglas ex C.Lawson	39.60	3	17.51	15.46	60.67829	17.11363
101	12.47	42.04	1	Pinus ponderosa Douglas ex C.Lawson	34.80	3	20.49	18.37	60.67829	17.11343
102	14.57	30.57	1	Pinus ponderosa Douglas ex C.Lawson	14.24	3	19.67	17.50	60.67834	17.11343
103	18.39	58.92	1	Pinus ponderosa Douglas ex C.Lawson	68.87	4	19.68	6.55	60.67836	17.11342
104	14.37	40.13	1	Pinus ponderosa Douglas ex C.Lawson	50.57	3	21.13	18.12	60.67829	17.11338
105	14.39	24.84	1	Nothofagus alpina (Poepp. & Endl.) Oerst	21.62	2	18.32	2.46	60.67679	17.109
106	7.97	12.42	1	Nothofagus alpina (Poepp. & Endl.) Oerst.	22.22	1	13.26	1.13	60.67697	17.10928
107	7.20	18.79	1	Nothofagus alpina (Poepp. & Endl.) Oerst.	22.22	1	10.53	1.00	60.67697	17.1093
108	10.66	33.76	1	Pinus resinosa Aiton	29.34	3	19.85	13.69	60.6783	17.11329
109	11.07	24.20	1	Pinus resinosa Aiton	48.56	2	19.43	17.18	60.67832	17.11327
110	14.01	35.67	1	Pinus resinosa Aiton	20.65	3	18.65	2.41	60.67835	17.11325
111	15.95	19.11	1	Pinus resinosa Aiton	26.07	3	15.54	11.12	60.67679	17.10776
112	14.20	35.03	1	Pinus resinosa Aiton	26.04	3	19.11	15.84	60.67765	17.11003
113	17.04	31.85	1	Pinus resinosa Aiton	40.50	4	21.64	9.00	60.67768	17.10974
114	17.03	36.31	1	Pinus resinosa Aiton	34.79	4	23.78	19.64	60.67765	17.10969
115	12.42	24.84	1	Pinus resinosa Aiton	29.18	3	17.35	12.46	60.67778	17.11036
116	7.92	12.10	1	Pinus resinosa Aiton	29.18	2	9.56	3.78	60.67778	17.1104
117	13.81	33.12	1	Pinus resinosa Aiton	18.90	3	21.63	1.44	60.6786	17.11389
118	18.02	38.22	1	Pinus resinosa Aiton	18.90	4	20.06	5.34	60.67861	17.11392
119	17.09	29.94	1	Pinus resinosa Aiton	9.72	4	19.43	10.59	60.67855	17.11384
120	9.64	32.17	1	Pinus resinosa Aiton	19.89	2	19.94	12.09	60.67855	17.11393
121	10.57	39.81	1	Pinus resinosa Aiton	51.58	2	23.19	18.42	60.67846	17.11383
122	9.36	38.54	1	Pinus resinosa Aiton	25.28	2	22.67	17.09	60.67848	17.11388
123	13.03	36.62	1	Pinus resinosa Aiton	51.58	3	18.83	15.15	60.67842	17.11383

124	9.91	41.08	1	Pinus resinosa Aiton	33.34	2	16.94	10.98	60.67836	17.11392
125	12.25	34.39	1	Pinus resinosa Aiton	22.28	2	17.57	2.62	60.67835	17.11388
126	13.09	32.17	1	Pinus resinosa Aiton	19.39	3	17.98	3.56	60.67835	17.11379
127	9.93	33.44	1	Pinus resinosa Aiton	53.78	3	17.17	11.90	60.67827	17.11383
128	7.69	33.44	1	Pinus resinosa Aiton	23.01	1	17.77	4.24	60.67833	17.11369
129	14.64	36.31	1	Pinus resinosa Aiton	39.60	3	19.04	14.96	60.67829	17.11354
130	17.34	27.07	1	Pinus resinosa Aiton	22.35	4	19.37	15.17	60.67831	17.11353
131	15.38	33.44	1	Pinus resinosa Aiton	39.03	3	19.69	16.70	60.67833	17.11356
132	15.45	32.48	1	Pinus resinosa Aiton	23.12	3	19.13	5.51	60.67834	17.11351
133	10.10	13.69	1	Prunus serotina Ehrh.	45.84	3	11.16	0.03	60.67773	17.11046
134	11.74	26.11	1	Prunus serotina Ehrh.	14.24	2	19.29	14.49	60.67831	17.11341
135	10.75	31.53	1	Pinus sylvestris L.	35.31	3	21.74	19.16	60.67758	17.10979
136	14.81	33.12	1	Pinus sylvestris L.	17.26	4	20.40	15.02	60.67768	17.11
137	16.21	27.71	1	Pinus sylvestris L.	55.47	4	20.99	15.64	60.67763	17.10987
138	14.65	34.08	1	Pinus sylvestris L.	20.21	4	24.07	21.22	60.67762	17.10981
139	15.38	28.66	1	Pinus sylvestris L.	17.63	4	23.38	19.92	60.6776	17.10976
140	9.91	33.44	1	Pinus sylvestris L.	32.72	2	23.39	19.07	60.67757	17.10965
141	11.12	29.62	1	Pinus sylvestris L.	9.77	3	21.93	15.58	60.67763	17.10973
142	14.55	25.16	1	Pinus sylvestris L.	7.52	4	20.68	17.55	60.67765	17.10978
143	17.49	33.44	1	Pinus sylvestris L.	47.63	4	21.83	17.48	60.67766	17.10984
144	17.13	27.07	1	Pinus sylvestris L.	28.36	4	19.78	5.96	60.67773	17.11009
145	4.37	14.65	1	Pinus sylvestris L.	19.05	1	7.94	5.09	60.67776	17.11043
146	4.03	11.46	1	Pinus sylvestris L.	3.59	1	5.78	2.69	60.67765	17.11051
147	8.42	13.06	1	Pinus sylvestris L.	35.71	2	7.49	3.73	60.67764	17.11047
148	13.92	45.86	1	Pinus sylvestris L.	80.48	3	19.63	1.31	60.67861	17.11383
149	15.26	37.58	1	Pinus sylvestris L.	41.19	3	18.56	16.24	60.67854	17.11378

150	16.42	24.84	1	Pinus sylvestris L.	7.90	3	20.10	17.64	60.67853	17.11383
151	13.94	49.68	1	Pinus sylvestris L.	89.67	3	21.88	12.74	60.67847	17.11378
152	18.42	30.57	1	Pinus sylvestris L.	25.28	4	21.61	3.93	60.67846	17.11392
153	16.10	33.76	1	Pinus sylvestris L.	25.20	3	17.27	13.50	60.67842	17.11392
154	8.64	32.48	1	Pinus sylvestris L.	25.20	2	19.57	16.39	60.67841	17.11388
155	11.08	35.67	1	Pinus sylvestris L.	20.04	2	18.57	12.33	60.6784	17.11383
156	10.50	35.03	1	Pinus sylvestris L.	18.59	2	18.08	8.01	60.67836	17.11383
157	14.96	29.94	1	Pinus sylvestris L.	15.64	3	19.22	9.22	60.67829	17.1135
158	5.63	30.57	1	Pinus sylvestris L.	98.39	3	17.20	13.50	60.6775	17.10998
159	18.02	52.23	1	Ulmus pumila L.	49.31	3	27.52	3.07	60.67689	17.10947
160	6.12	31.00	2	Populus alba L.	29.67	1	19.96	18.37	60.67669	17.10739
161	10.09	54.78	1	Populus alba L.	105.45	3	23.35	11.14	60.67676	17.10749
162	11.66	24.52	1	Populus alba L.	38.30	2	21.17	11.92	60.6768	17.10738
163	15.91	23.57	1	Populus alba L.	17.19	3	15.98	2.89	60.67702	17.10954
164	22.02	57.32	1	Acer saccharinum L.	17.19	4	13.16	4.00	60.67683	17.10966
165	8.85	17.83	1	Celtis laevigata Willd.	9.89	2	9.61	1.50	60.67676	17.10914
166	4.45	17.20	1	Gleditsia triacanthos L.	30.88	1	18.48	11.35	60.6768	17.10813
167	8.90	23.57	1	Sterculia africana (Lour.) Fiori	51.21	2	6.56	2.09	60.67688	17.1088
168	12.43	53.82	1	Pinus pinea L.	30.88	3	20.54	13.51	60.67681	17.10811
169	13.50	47.77	1	Pinus pinea L.	40.11	4	21.22	5.36	60.67671	17.108
170	18.39	33.44	1	Pinus pinea L.	33.25	4	21.59	18.86	60.67754	17.10968
171	16.37	30.57	1	Pinus pinea L.	55.47	4	18.51	11.10	60.67761	17.1099
172	19.67	72.61	2	Pinus pinea L.	67.95	5	21.51	5.32	60.67767	17.11026
173	10.32	79.30	2	Pinus pinea L.	61.03	3	12.46	0.67	60.67841	17.11407
174	17.26	89.49	1	Pinus pinea L.	73.90	5	18.46	12.10	60.6786	17.11408
175	16.00	53.50	1	Pinus strobus L.	32.18	4	16.94	12.30	60.67665	17.10754

176	11.69	31.85	1	Pinus strobus L.	72.13	4	12.32	1.32	60.67688	17.10779
177	17.60	43.95	1	Pinus strobus L.	28.60	4	18.78	13.93	60.67666	17.10744
178	11.43	70.38	1	Pinus strobus L.	29.67	2	21.00	13.65	60.67671	17.1074
179	11.30	30.89	1	Pinus strobus L.	50.34	3	15.51	12.20	60.67698	17.10793
180	11.76	33.12	1	Pinus strobus L.	31.97	3	16.41	11.85	60.67698	17.10798
181	10.44	31.21	1	Pinus strobus L.	31.75	2	19.70	16.67	60.67682	17.10772
182	13.01	30.57	1	Pinus strobus L.	31.75	3	19.44	16.14	60.67681	17.1077
183	10.63	49.36	1	Pinus strobus L.	60.05	2	17.31	2.04	60.67695	17.10886
184	10.97	33.12	1	Pinus strobus L.	19.83	3	22.00	9.43	60.67773	17.11019
185	22.24	28.66	1	Betula pubescens Ehrh.	25.70	5	21.62	16.99	60.67683	17.10788
186	17.89	26.43	1	Betula pubescens Ehrh.	5.23	3	22.52	3.13	60.67698	17.10948
187	12.52	31.85	1	Betula pubescens Ehrh.	8.97	2	5.56	2.11	60.67697	17.10952
188	23.10	34.39	1	Betula pubescens Ehrh.	15.96	4	26.57	4.15	60.67697	17.10966
189	15.22	34.39	1	Betula pubescens Ehrh.	66.05	3	22.06	2.60	60.67678	17.10904
190	10.74	13.06	1	Betula pubescens Ehrh.	37.97	4	8.42	1.89	60.67756	17.11052
191	21.50	31.53	2	Betula pubescens Ehrh.	26.82	4	9.67	3.78	60.67695	17.10923

Table D2. Inputs for i-Tree Eco model that derived from ALS data.

	CHM height	CBH	Crown Area	NDVI	DBH	MLP prediction	CLE	Lat	Lon
0	20.17	14.080	28.602	0.2357	40.741	2	4	60.67666	17.10746
1	20.02	14.540	64.359	0.1333	40.520	2	4	60.67667	17.10756
2	17.73	1.160	27.221	0.2159	37.139	1	3	60.67669	17.10796
3	23.59	17.100	93.408	0.1433	45.789	2	5	60.6767	17.1078
4	21.08	17.010	59.341	0.1580	42.084	2	4	60.67671	17.10741
5	21.88	8.110	40.107	0.1445	43.265	2	4	60.67671	17.10801
6	22.13	12.300	11.226	0.2561	43.634	2	4	60.67675	17.10745
7	16.73	11.940	27.528	0.1878	35.663	2	2	60.67678	17.10774
8	18.85	14.750	59.241	0.1829	38.793	2	3	60.67674	17.10791
9	20.30	15.510	35.288	0.1963	40.933	2	3	60.6768	17.108
10	26.73	21.520	105.449	0.2557	50.423	2	5	60.67677	17.10752
11	18.46	15.320	26.072	0.1404	38.217	2	3	60.67679	17.1078
12	22.63	18.840	25.701	0.2364	44.372	2	4	60.67682	17.10789
13	23.50	0.590	21.750	0.2007	45.656	1	4	60.67683	17.10798
14	20.08	16.460	27.106	0.1772	40.608	2	3	60.67681	17.10764
15	22.93	20.140	61.759	0.1018	44.815	2	4	60.67682	17.10812
16	19.55	13.070	15.119	0.1264	39.826	2	2	60.67682	17.10765
17	20.13	16.080	63.501	0.2635	40.682	2	3	60.67682	17.10772
18	25.37	16.310	114.899	0.2676	48.416	2	5	60.6768	17.10745
19	11.46	0.510	9.310	0.0785	27.885	2	2	60.67685	17.10745
20	15.56	10.920	6.190	0.1574	33.937	2	3	60.67687	17.10808
21	21.50	15.130	33.645	0.2132	42.704	2	3	60.67685	17.1079
22	25.29	4.060	66.612	0.1400	48.298	1	4	60.67686	17.10797
23	16.79	13.240	141.157	0.1619	35.752	2	3	60.6769	17.10757
24	13.19	1.000	72.134	0.0296	30.438	2	2	60.6769	17.10779
25	15.10	11.750	50.343	0.1915	33.258	2	2	60.67697	17.10794
26	16.75	9.740	25.077	0.0890	35.693	2	2	60.67699	17.10771
27	16.33	11.920	31.971	0.1886	35.073	2	2	60.67698	17.10798
28	18.05	10.700	42.682	0.0925	37.612	2	2	60.677	17.10767
29	14.98	5.870	137.629	0.1463	33.080	2	3	60.67701	17.10753
30	23.19	2.160	62.134	0.1231	45.198	2	4	60.67671	17.10951
31	12.59	4.750	43.140	0.0409	29.553	2	2	60.67671	17.10919
32	22.16	5.330	66.051	0.2065	43.678	1	3	60.67678	17.10904
33	12.73	2.570	19.787	0.2316	29.759	1	2	60.67678	17.10916
34	16.97	3.020	50.387	0.1094	36.018	2	3	60.67674	17.10942
35	26.05	17.110	50.387	0.0843	49.420	2	4	60.67678	17.1095
36	25.83	20.480	9.990	0.0394	49.095	2	4	60.67679	17.10955
37	23.18	12.990	26.354	0.2644	45.184	2	3	60.67681	17.1093
38	22.84	0.000	9.821	0.0642	44.682	1	4	60.67681	17.10948
39	21.09	15.270	22.155	0.1228	42.099	2	3	60.67681	17.10938
40	23.80	21.030	43.245	0.1589	46.099	2	4	60.6768	17.10904
41	22.94	17.060	61.676	0.2940	44.829	2	3	60.67681	17.10926

42	27.39	16.770	5.136	0.0101	51.398	2	4	60.67683	17.10956
43	27.31	20.790	10.065	0.0181	51.280	2	4	60.67683	17.10954
44	22.65	19.900	17.816	0.2827	44.401	2	4	60.67684	17.10885
45	21.63	15.860	15.463	0.0316	42.896	2	3	60.67683	17.10939
46	26.07	10.920	15.989	0.0126	49.449	2	5	60.67684	17.10968
47	23.84	7.910	21.949	0.1172	46.158	2	4	60.67683	17.1093
48	20.07	18.070	3.570	0.0071	40.593	2	3	60.67687	17.10969
49	23.97	15.800	3.668	0.0169	46.350	2	4	60.67687	17.10972
50	26.38	17.660	18.587	0.0169	49.907	2	4	60.67684	17.10949
51	23.15	14.850	45.104	0.1894	45.139	2	4	60.67684	17.10917
52	23.70	22.000	52.943	0.2012	45.951	2	4	60.67685	17.109
53	26.88	20.880	29.495	0.0629	50.645	2	5	60.67688	17.10945
54	19.48	13.140	11.288	0.1266	39.722	2	2	60.67688	17.10922
55	19.54	12.220	24.972	0.1948	39.811	2	2	60.67688	17.10922
56	23.77	18.420	102.418	0.2831	46.055	2	4	60.67687	17.10892
57	26.87	16.720	16.368	0.0065	50.630	2	4	60.67689	17.10967
58	9.03	0.310	5.988	0.2710	24.298	1	1	60.67694	17.10932
59	11.94	2.400	20.590	0.0755	28.593	2	1	60.67693	17.10913
60	12.64	4.530	26.825	0.0984	29.627	2	1	60.67695	17.1092
61	17.49	13.900	60.048	0.2618	36.785	2	3	60.67694	17.10887
62	25.26	16.600	29.372	0.1945	48.254	2	4	60.67696	17.10941
63	24.52	20.280	5.232	0.2651	47.162	2	4	60.67698	17.10948
64	26.55	20.790	15.956	0.2557	50.158	2	4	60.67698	17.10965
65	21.94	12.940	9.064	0.2298	43.353	2	3	60.67699	17.10945
66	26.84	16.230	26.902	0.2804	50.586	2	4	60.67699	17.10961
67	16.83	14.650	45.402	0.2224	35.811	2	2	60.67698	17.10918
68	20.13	15.270	94.525	0.2281	40.682	2	4	60.67694	17.109
69	17.31	14.590	68.542	0.0870	36.520	2	3	60.67698	17.10889
70	16.95	10.230	66.668	0.1999	35.988	2	2	60.67699	17.10923
71	24.13	13.230	17.192	0.2708	46.586	2	4	60.67704	17.1095
72	26.51	3.690	13.876	0.2829	50.099	1	5	60.67702	17.10959
73	25.73	19.830	48.808	0.2169	48.947	2	4	60.67703	17.1094
74	24.55	4.660	15.835	0.2762	47.206	1	4	60.67707	17.10952
75	25.43	16.500	10.894	0.2661	48.505	2	4	60.67706	17.10961
76	26.41	19.840	60.681	0.2028	49.951	2	4	60.67705	17.10938
77	26.72	23.120	63.099	0.2728	50.409	2	4	60.67708	17.10956
78	23.65	15.820	33.971	0.1432	45.877	2	4	60.67741	17.11014
79	23.03	0.510	23.526	0.1318	44.962	1	4	60.67739	17.11032
80	23.95	7.630	23.515	0.1557	46.320	2	4	60.67741	17.11026
81	26.33	19.330	22.491	0.1858	49.833	2	5	60.67744	17.11018
82	22.48	3.630	7.646	0.0492	44.150	1	4	60.67745	17.11025
83	23.55	19.480	38.891	0.1732	45.730	2	4	60.67744	17.11031
84	23.70	18.960	36.442	0.1575	45.951	2	4	60.67745	17.11009
85	22.36	0.930	15.128	0.2021	43.973	1	3	60.67747	17.11029
86	23.25	12.020	23.632	0.1807	45.287	2	4	60.67748	17.11013
87	22.15	0.000	24.087	0.1849	43.663	1	3	60.67748	17.11019

88	22.32	11.340	6.871	0.1198	43.914	2	3	60.6775	17.11027
89	20.33	5.940	17.070	0.1167	40.977	2	3	60.67751	17.11032
90	21.47	18.060	33.249	0.1707	42.660	2	3	60.67755	17.10968
91	17.09	13.450	98.389	0.1527	36.195	2	4	60.6775	17.10997
92	19.88	11.500	11.444	0.1108	40.313	2	3	60.67752	17.11026
93	21.03	15.860	23.322	0.1166	42.010	2	3	60.67752	17.11021
94	23.48	19.450	70.630	0.1546	45.626	2	4	60.67756	17.10975
95	20.85	3.780	68.798	0.1448	41.745	2	3	60.67753	17.11035
96	19.25	4.620	35.315	0.1097	39.383	2	3	60.67757	17.1103
97	23.24	20.230	32.722	0.1685	45.272	2	4	60.67757	17.10965
98	8.79	3.690	37.968	0.1891	23.944	2	2	60.67757	17.11052
99	23.38	17.510	17.631	0.1724	45.479	2	4	60.6776	17.10977
100	19.22	10.070	136.728	0.1466	39.339	2	4	60.67758	17.1101
101	14.28	3.350	27.725	0.0888	32.047	2	2	60.67761	17.1103
102	23.68	21.170	20.215	0.1679	45.922	2	4	60.67762	17.10981
103	22.19	16.590	9.766	0.1627	43.722	2	3	60.67763	17.10974
104	21.05	14.320	55.472	0.1637	42.040	2	3	60.67763	17.10987
105	19.20	16.060	26.039	0.2006	39.309	2	3	60.67765	17.11003
106	21.65	14.720	7.517	0.1869	42.925	2	3	60.67765	17.10979
107	18.85	12.500	18.553	0.1989	38.793	2	3	60.67767	17.11011
108	8.22	0.620	35.707	0.1514	23.103	2	2	60.67766	17.11046
109	24.22	21.250	34.791	0.2130	46.719	2	4	60.67766	17.1097
110	20.84	18.650	18.291	0.1396	41.730	2	3	60.67769	17.11016
111	21.90	0.270	15.580	0.1552	43.294	1	3	60.67769	17.11007
112	21.83	17.930	47.626	0.1158	43.191	2	3	60.67766	17.10984
113	22.10	12.460	40.501	0.1801	43.590	2	4	60.67768	17.10974
114	24.15	22.080	51.790	0.1767	46.615	2	4	60.6777	17.10998
115	24.14	21.660	36.718	0.1636	46.601	2	4	60.67773	17.10994
116	21.86	14.060	17.085	0.1518	43.235	2	3	60.67772	17.11016
117	22.08	4.940	19.830	0.1315	43.560	2	3	60.67773	17.1102
118	22.08	6.170	8.514	0.1841	43.560	2	3	60.67774	17.11001
119	23.90	18.490	135.903	0.0481	46.246	2	5	60.67769	17.11029
120	20.86	14.850	8.098	0.1135	41.759	2	3	60.67774	17.11024
121	20.61	3.040	18.413	0.1311	41.390	2	3	60.67777	17.11023
122	23.41	16.520	28.362	0.1780	45.523	2	4	60.67776	17.11008
123	21.23	15.290	24.046	0.2095	42.305	2	3	60.67777	17.10998
124	23.45	19.120	48.980	0.1964	45.582	2	4	60.67775	17.10992
125	21.82	15.370	32.619	0.1578	43.176	2	3	60.67779	17.11021
126	17.25	12.050	29.181	0.0079	36.431	2	3	60.67778	17.11036
127	21.53	10.750	62.698	0.2148	42.748	2	4	60.67778	17.1101
128	20.99	10.690	33.384	0.1091	41.951	2	3	60.67782	17.11018
129	13.23	6.730	66.051	0.2736	30.497	2	2	60.67822	17.11388
130	20.42	16.780	79.197	0.1791	41.110	2	3	60.67829	17.11357
131	19.10	9.290	15.645	0.2042	39.162	2	3	60.67829	17.11351
132	20.59	15.720	34.801	0.1824	41.361	2	3	60.67829	17.11343
133	17.43	12.330	53.782	0.2657	36.697	2	3	60.67827	17.11382

134	22.30	18.650	48.559	0.2394	43.885	2	3	60.67831	17.11325
135	16.05	10.200	48.959	0.1395	34.660	2	3	60.6783	17.11393
136	17.02	7.190	25.997	0.1573	36.092	2	2	60.67831	17.11368
137	21.01	18.310	22.347	0.1924	41.981	2	3	60.67831	17.11354
138	21.21	17.840	50.572	0.2221	42.276	2	3	60.67829	17.11337
139	20.71	17.920	29.342	0.2266	41.538	2	3	60.6783	17.1133
140	20.43	16.230	28.489	0.2340	41.125	2	3	60.67832	17.11343
141	17.38	5.360	22.278	0.2173	36.623	2	2	60.67835	17.11389
142	17.94	3.450	23.015	0.1866	37.449	2	2	60.67833	17.1137
143	20.73	1.080	20.646	0.1760	41.567	1	3	60.67835	17.11327
144	18.15	10.400	19.389	0.2436	37.759	2	2	60.67835	17.1138
145	18.15	12.030	18.588	0.2424	37.759	2	2	60.67836	17.11383
146	17.16	9.420	33.335	0.1658	36.298	2	2	60.67836	17.11393
147	20.03	11.570	39.418	0.2148	40.534	2	3	60.67837	17.11326
148	20.78	1.050	23.116	0.1991	41.641	1	3	60.67834	17.11353
149	19.66	16.880	39.029	0.1969	39.988	2	3	60.67833	17.11355
150	17.56	14.310	47.232	0.2126	36.889	2	2	60.67835	17.11367
151	18.95	10.810	68.866	0.2203	38.940	2	3	60.67837	17.11342
152	19.55	11.880	20.037	0.2317	39.826	2	3	60.6784	17.11381
153	19.87	17.650	50.398	0.2172	40.298	2	3	60.67841	17.11388
154	14.03	5.310	61.034	0.2976	31.678	1	3	60.6784	17.11411
155	23.15	14.960	51.582	0.2163	45.139	2	4	60.67846	17.11383
156	22.94	18.440	75.836	0.1929	44.829	2	4	60.67848	17.11389
157	22.53	20.290	89.674	0.2385	44.224	2	4	60.67848	17.11378
158	14.86	3.270	70.683	0.1675	32.903	2	3	60.67848	17.11414
159	19.51	15.140	7.903	0.2278	39.767	2	3	60.67853	17.11385
160	21.09	12.660	34.038	0.0925	42.099	2	3	60.67852	17.11393
161	20.11	8.260	7.556	0.1378	40.652	2	3	60.67854	17.11388
162	20.25	10.930	9.717	0.2488	40.859	2	3	60.67855	17.11383
163	19.15	16.490	41.192	0.2384	39.235	2	3	60.67854	17.11378
164	20.40	18.370	19.886	0.1676	41.080	2	3	60.67855	17.11394
165	13.61	4.550	39.635	0.2378	31.058	2	1	60.67854	17.11411
166	12.28	2.040	3.459	0.2980	29.095	1	1	60.67856	17.11409
167	26.37	18.420	238.808	0.2659	49.892	2	5	60.6785	17.11336
168	26.11	22.120	93.500	0.2599	49.508	2	4	60.67852	17.11332
169	21.18	16.980	17.527	0.2698	42.232	2	3	60.67859	17.11384
170	19.59	15.290	73.902	0.1469	39.885	2	3	60.67861	17.1141
171	22.15	2.140	56.696	0.1778	43.663	1	3	60.67861	17.11388
172	20.24	14.830	67.411	0.2316	40.844	2	3	60.67861	17.11378
173	20.79	12.880	35.948	0.1239	41.656	2	3	60.67862	17.11393
174	21.84	0.010	80.485	0.2320	43.206	1	3	60.67862	17.11384